UNIVERSITÉ DU QUÉBEC À MONTRÉAL

SCANNING ELECTROCHEMICAL MICROSCOPY AND ITS APPLICATION TO BIOLOGICAL SYSTEMS

MÉMOIRE

PRÉSENTÉ

COMME EXIGENCE PARTIELLE

DE LA MAÎTRISE EN CHIMIE (OPTION BIOCHIMIE)

PAR

SABINE KUSS

JANVIER 2011

To my mother

Uta Hübner

and to my husband and my son

Christian Kuss

Theodor C. Kuss

ACKNOWLEDGMENTS

The author thanks Prof. Janine Mauzeroll, Prof. Borhane Annabi and Dr. Matthias Geissler for their help and supervision during the presented projects. Janine, I thank you for giving me the opportunity not only to work in your laboratory but also for letting me follow my own ideas and to discover to me unknown areas in natural science. Borhane and Matthias, I thank you for your guidance and collaboration in the past months.

I would like to thank the team of the Mauzeroll lab for their support, especially Isabelle Beaulieu for making the start as easy as possible and for her translational skills. The techniqual assistance of Michel Marion as well as the supply of material of the department of chemistry at UQAM is also acknowledged. Thanks are due to Denis Flipo for his help and assistance during the confocal microscopy as well as Dr. Renaud Cornut for helpful discussions and comments. Finally I thank my husband Christian Kuss for supporting me all the way through encouragement, knowledgeable discussion and excellent cooking.

CONTENTS

LIST OF FIGURES

LIST OF ABBREVIATIONS AND ACRONYMS

ABCC1	ATP-binding cassette, sub-family C (CFTR/MRP), member 1
ATP	Adenosine 5'-triphosphate
a.u.	Arbitrary units
Bio-SECM	Biological Scanning Electrochemical Microscopy
BSA	Bovine Serum Albumin
CE	Counter Electrode
CL	Confidence level
CMFDA	5-chloromethylfluorescein diacetate
DI	Deionized
DMEM	Dulbecco's Modified Eagle's Medium
DMSO	Dimethyl sulfoxide
EDTA	Ethylenediaminetetraacetic acid
$FcCH_2OH$	Ferrocenemethanol
FL1-H	Fluorescence intensity at the CMFDA fluorescence wave length
FSC-H	Forward Scattering
GAPDH	Glyceraldehyde-3-phosphate dehydrogenase
Gm	Geometric mean
GSH	Reduced Glutathione

GSSG	Oxidized Glutathione
GST	GSH s-transferase
HeLa	Adenocarcinoma cervical cancer cells
HeLa-R	Adenocarcinoma cervical cancer cells overexpressing MRP1
HEPES	4-(2-Hydroxyethyl)piperazine-1-ethanesulfonic acid
MDR1	Multi-drug resistance gene, encoding for P-gp
MEM	Minimum Essential Medium
MRP1	Multidrug Resistance Associated Protein
NSOM	Near Field Scanning Optical Microscopy
O	Redox mediator in oxidized form
PBS	Phosphate buffered saline
PDMS	Poly (dimethylsiloxane)
P-gp	P-glycoprotein
PI	Propidium iodide
Pt	Platinum
PVDF	Polyvinylidene fluoride
R	Redox mediator in reduced form
RE	Reference Electrode
RG	Dimensionless radius of glass
ROS	Reactive Oxygen Species
$[Ru(NH_3)_6]^{3+}$	Hexaammineruthenium(III) chloride
SDS	Sodium dodecyl sulphate
SEBS	Styrenic ethylene butylene block copolymer

SECM	Scanning Electrochemical Microscopy
SSC-H	Side Scattering
WE	Working Electrode

LIST OF SYMBOLS

a(Substance)	Activity of Substance
c	Concentration (mol/l)
D	Diffusion coefficient (m^2/s)
E	Electrode Potential (V)
E^0	Electrode Potential at standard conditions (V)
F	Faraday constant (F = 96 485.34 C/mol)
I	Current (A)
J	Flux ($mol/(m^2\ s)$)
n	Number of independent experiments
n_e	Number of electrons exchanged during redox reaction
p	Pressure (atm)
r	Radius of active material (m)
R	Universal Gas Constant (R = 8.314472 J / (K mol))
t	Time (s)
T	Temperature (K)
x	Length (m)
α	Significance level
ν(Substance)	Stoichiometric factor of Substance
Π	Product of values

SUMMARY

The phenomenon of multidrug resistance leaves cancer patients with a disadvantageous prognosis and limits their treatment options. Therefore growing interest in the search for new antitumor compounds or other strategies to battle multidrug resistance emerged. Scanning Electrochemical Microscopy (SECM) is one promising candidate for a new approach to study living cells. This method employs nanoscale electrodes that can be used to detect metabolites in single cell studies. One major objective in the present work is to demonstrate the influence of ferrocenemethanol ($FcCH_2OH$) on two different human cervix cancer cell lines. The potential of Biological Scanning Electrochemical Microscopy (Bio-SECM) studies is demonstrated by showing the differential response to $FcCH_2OH$ in multidrug-resistant cells in part due to the unspecific efflux pump of the Multidrug Resistant Associated Protein (MRP1). The newly established triangulation between $FcCH_2OH/[FcCH_2OH]^+$, reduced and oxidized Glutathione (GSH/GSSG) and multidrug resistance in human cancer cells might impact future applications that require adequate assessment of the metabolic response to anti-cancer drugs in chemotherapy resistant cells. As a second goal of the presented work, to improve future Bio-SECM studies on cells, a new cell patterning procedure is established using elastomeric through-hole membranes allowing patterning of single cell types as well as co-cultures. As a third objective the technique of Bio-SECM is furthermore improved by introducing a constant distance mode allowing coupling of information about topography and reactivity depending of the nature of the substrate. The presented work is a major first step towards the establishment of a quantifiable indicator for multidrug resistance activity that could be used over cell life and across cell lines thereby enabling targeted drug screening and improving existing cancer analysis for chemotherapy treatment.

The presented thesis is structured into three chapters, two of which have the format of a manuscript of a scientific article. The first chapter focuses on the application of the electrochemical technique of Scanning Electrochemical Microscopy (SECM) to biological living cells. Using this technique the authors are approaching the phenomenon of multidrug resistance in human cancer cells and outline its impact on future medical research. A new cell patterning procedure is presented in chapter two of this thesis in order to improve working conditions during Bio-SECM studies whereas the closing chapter outlines prospects and long term goals to be achieved during the continuation of the described projects.

Keywords: Scanning Electrochemical Microscopy, Multidrug Resistance, Cell Patterning, Electrochemical Imaging, Cancer

RÉSUMÉ

Le phénomène de multirésistance aux médicaments laisse les patients atteints de cancer avec un pronostic défavorable et leurs options de traitement sont limitées. Par conséquent, des intérêts croissants dans la recherche de nouveaux composés antitumoraux ou d'autres stratégies pour combattre la multirésistance se sont manifestés. La microscopie électrochimique à balayage (SECM) est dans ce domaine une candidate prometteuse pour l'étude de cellules vivantes. Cette méthode emploie des électrodes nanométriques qui peuvent être utilisées pour détecter des métabolites dans les études portant sur une cellule unique. Le présent travail montre l'influence du ferrocèneméthanol ($FcCH_2OH$) sur deux lignées différentes de cellules humaines cancéreuses du col utérin. Le potentiel de la microscopie électrochimique à balayage biologique (Bio-SECM) est démontré par le fait que la réponse différentielle au $FcCH_2OH$ des cellules résistantes aux médicaments provient en partie de l'efflux non spécifique d'uneprotéine associée cette résistance, la MRP1. Le liennouvellement établi entre $FcCH_2OH$ / $[FcCH_2OH]^+$, GSH / GSSG et la multirésistance dans les cellules cancéreuses humaines pourrait avoir un impact sur de futures applications qui nécessitent une évaluation adéquate de la réponse métabolique à des médicaments anticancéreux chez les cellules résistantes à la chimiothérapie. Pour améliorer les futures études de Bio-SECM sur les cellules, une nouvelle procédure d'adhésion cellulaire est établie. Grâce à des membranes élastomériques comprenant despores à des endroits précis, il est possible de créer des motifs contenant un seul type de cellules, ainsi que de co-cultures. En outre, la technique de Bio-SECM est améliorée par l'introduction d'un mode particulier de balayage de la sonde. Ce mode, appelé distance constante, permetde découpler les'informations sur la topographie et sur la réactivité. Le travail présenté est une première étape importante vers l'établissement d'un indicateur quantifiant les activités reliées à la résistance aux médicaments des cellules. Cela pourrait être utilisé tout au long de la vie des cellules et sur différentes lignées, ce qui permettrait de faire un dépistage de médicaments ciblés. Cela améliorerait l'analyse actuelle du cancer, ce qui conduirait finalement à avoir un meilleur traitement chimiothérapeutique.

La présente thèse est structurée en trois chapitres, dont deux ont le format d'un manuscrit d'un article scientifique. Le premier chapitre se concentre sur l'utilisation de la microscopie électrochimique à balayage (SECM) pour étudier les cellules vivantes. Grâce à cette technique, les auteurs abordent le phénomène de multirésistance chez les cellules cancéreuses humaines et son impact sur la recherche médicale future. Une nouvelle procédure de structuration de l'adhésion cellulaire sur des motifs définis est présentée dans le chapitre deux de cette thèse. Elle vise à améliorer les conditions de travail pendant les études de Bio-SECM. Le dernier chapitre décrit les perspectives et les objectifs à long terme à atteindre au cours qu'offrent ce travail.

Mots-clés: Microscopie Électrochimique à Balayage, Multirésistance aux médicaments, Formation de motif cellulaire, Imagerie électrochimique, Cancer

INTRODUCTION

I.1 Theme of the Thesis

As the second most common cause of death in the United States, cancer accounts for almost 1 of every 4 deaths. That means, more than 1,500 people per day are estimated to die from cancer in 2010, whereas about 1.5 Mio new cancer cases are estimated to be diagnosed. (American Cancer Society, 2010) Multidrug resistance is a phenomenon that enables cancer cells to defend themselves actively against chemotherapeutic treatment. This leads to a devastating prognosis for cancer patients. Multidrug resistance occurs in a variety of cancer types, such as lung cancer, kidney or colon cancer, or acute leukemia. (Goldstein, Pastan and Gottesman, 1992) In 2007, 70% of ovarian cancer patients exhibited multidrug resistance in Canada and the United States, which lowered their survival rate to 10-30%. (Persidis, 1999)

Multidrug resistance is due to the overexpression of proteins belonging to the family of multidrug resistance related proteins, a subgroup of Adenosine 5'-triphosphate (ATP) - binding cassette-transporters or ABC transporters. P-glycoprotein (P-gp) as well as the multidrug resistance protein 1 (MRP1, Figure I.1) are two proteins of this group. P-gp overexpression can be triggered by a widely investigated mechanism involving the glucosaminoglycan hyaluronan, which will be described in the following. It is known that hyaluronan, playing an important role in wound repair as well as in cancer metastasis, binds to the cell surface glycoprotein CD44. This interaction leads to a variety of different reactions that are specific to tumor cells, among which it triggers the up-regulation of the transcriptional cofactor p300 expression and its activity. p300 is responsible for the acetylation of histones and other transcriptional factors and thereby plays a role in regulating transcriptional activity of the involved gene. Among the acetylated factors are beta-catenin and NFkappaB-p65, leading to an NFkappaB-specific transcriptional up-regulation. This

specifically is the case for the multi-drug resistance gene (MDR1) leading to the production of P-gp and with that chemoresistance in cells. (Bourguignon, Xia and Wong, 2009) Although the mechanism that causes the expression of P-gp is roughly understood, the development of multidrug resistance caused by MRP1 remains unclear. Therefore, in our studies we are focusing on human cancer cells that are not overexpressing P-gp, but MRP1. The MRP1 structure is similar to P-gp, except for an amino-terminal extension that contains five-membrane-spanning domains attached to a Pgp-like core. (Gottesman and Bates, 2002)

As an active transporter, MRP1 relies on the availability of ATP as energy source. Drugs can be transported by MRP1 directly or they need to be conjugated to glutathione. These drugs' transport by MRP1 is therefore also dependent on the continued synthesis of GSH. Other substrates are also known to be conjugated to glucuronate, sulfate or are organic anions that do not require conjugation. (Borst *et al.*, 2000) Chemoresistant cells expressing the MRP1 efflux pump that is primarily located in the plasma membrane (Zaman *et al.*, 1994), are therefore enabled to expel chemotherapeutic agents, such as anthracyclines and cisplatin or other drugs. (Morrow and Cowan, 1990) (Figure I.2). This allows the unhindered growth of tumour tissue despite chemotherapeutic treatment.

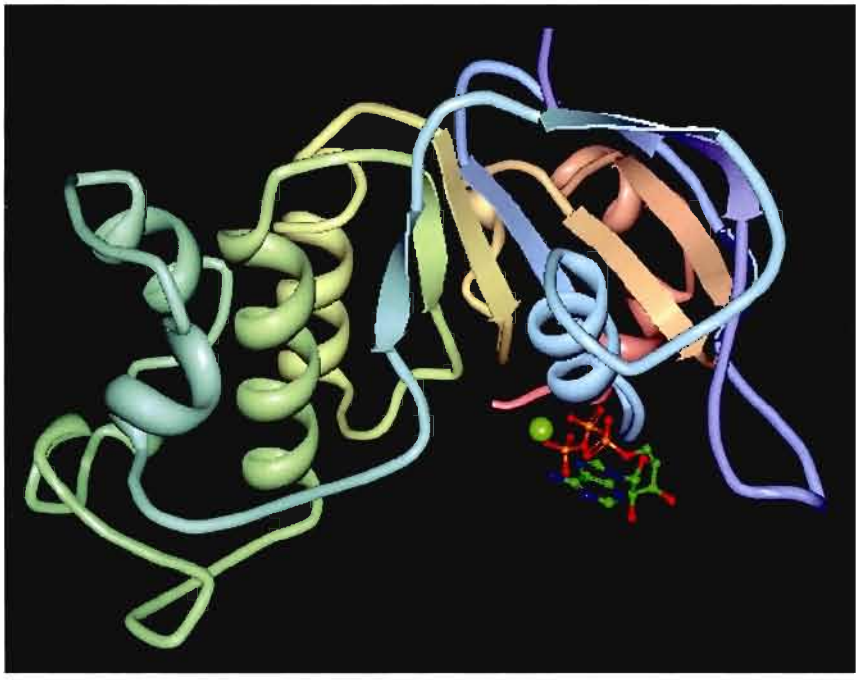

Figure I.1 Structure of the human multidrug resistance protein 1 nucleotide binding domain 1 (Research Collaboratory for Structural Bioinformatics Protein Database).

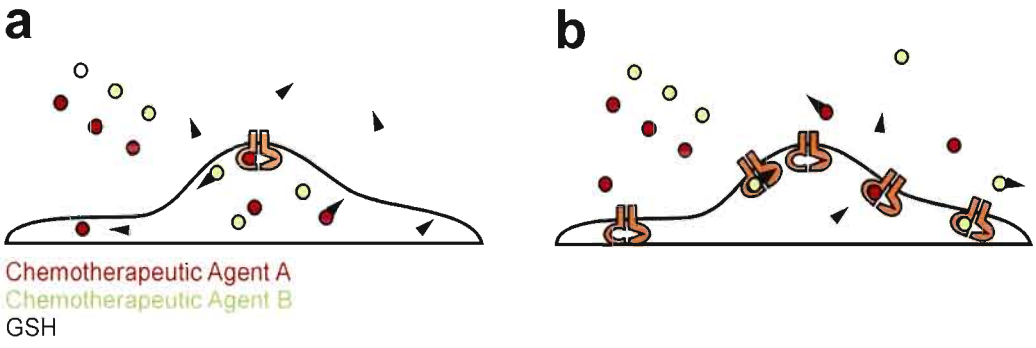

Figure I.2 Principle of multidrug resistance due to overexpression of MRP1. (a) Chemotherapeutics entering a non-resistant cell to cause cell death. (b) Pristine chemotherapeutics or in conjugation with GSH transported out of the cell by MRP1.

To approach the phenomenon of multidrug resistance it would be an enormous advantage to have a tool that allows monitoring the development of multidrug resistance in single cells and observing its effect on metabolic changes. In treatment this tool could be used to quantify the extent of multidrug resistance in a patient's sample in order to adjust the treatment to the cancer. To develop such a tool, we made use of different techniques that will now be briefly introduced.

I.2 Fundamentals of Electrochemistry

The basis of the capability of living organisms to convert and use energy from nutrition is redox reactions – reactions with transfer of electrons. (Alberts *et al.*, 2004, p. 908-922) After digestion, energy can be stored in the body by creating carbon compounds with low carbon oxidation numbers, such as fats or glycogen. Through respiration these compounds are oxidized and the delivered energy is used to contract muscles, heat the organism, move and think. The processes connected with these energy transformations are very complex and many different chemical reactions and equilibria ensure that the organism functions properly. Therefore many cellular dysfunctions change the redox behavior of an organism. An excellent way to probe these changes is analytical electrochemistry. All reactions that can be directly observed electrochemically are redox reactions, however, different from biological redox reactions, in electroanalytical chemistry oxidation and reduction are locally separated and take place on two different electrodes. (Atkins, 2001, p. 304-305) At the cathode reduction occurs, while at the anode oxidation takes place. The fact that oxidation and reduction are separated implies also that there has to be an electric and an ionic current between the electrodes. By measuring between cathode and anode one can observe and follow the reactions in detail.

While taking up or releasing electrons the energy of a substance changes. This change in energy is different from one substance to the other and is characterized in electrochemistry by the electrode potential.

$$\nu(Red)\,\mathrm{Red} \longrightarrow \nu(Ox)\,\mathrm{Ox} + \mathrm{n_e\ e^-}$$

$$E = E^0 + \frac{R \cdot T}{n_e \cdot F} \ln \frac{\prod a(Ox)^{\nu(Ox)}}{\prod a(Red)^{\nu(Red)}} \tag{1}$$

Equation (1), the Nernst equation, shows the dependency of the electrode potential E on the activities of participating substances *a(Ox)* and *a(Red)* as well as the temperature. (Atkins, 2001, p. 311-321) The standard potential E^0 is the potential of a redox pair under standard conditions (T = 25 °C, p = 1 bar, *a(Ox)* = *a(Red)* = 1), F is the Faraday constant and R is the universal gas constant. By having an electric and ionic contact between two electrodes with two different potentials a potential difference can be measured as voltage. The dependency of the electrode potential on redox pair and concentration can be interpreted in open circuit measurements. Another possible measure in electrochemistry is the electric current as a function of the electrode potential. The current is defined by the charge flow at the active surface of the electrodes, which is limited by the charge transfer kinetics, by the diffusion of the consumed substance to the electrode surface or by both. (Atkins, 2001, p. 955-961) For different systems, individual models are available to describe current behavior and evaluate experimental results. In many cases, such as SECM, it is beneficial to set up experiments so that diffusion is determining the current. Therefore Fick's laws play an important role in electroanalytical chemistry:

$$J = -D\nabla c \tag{2}$$

$$\frac{\partial c}{\partial t} = D\nabla^2 c \tag{3}$$

with J as the flux of substance, D as the diffusion coefficient, c as the concentration and t as the time.

I.3 Methods

I.3.1 Bio-SECM. A self-evident possibility to monitor MRP1 activity is to observe substances pumped out of the cell by MRP1. Scanning Electrochemical Microscopy (SECM) is one of the few tools that are able to perform those measurements on a microscopic scale. So far SECM has mainly been used in the field of electrochemical surface science, *e.g.* in corrosion studies. (Bard and Mirkin, 2001) This microscopic technique allows imaging of the electrochemical reactivity of surfaces by scanning in close proximity over a surface using nano- or micro-scale electrodes. The size of these nano-scale electrodes ranges from 10-100 nm. First applications of SECM to biological samples emerged in 2001. (Bard, Li and Zhan, 2006) By combining SECM and inverted microscopes the technique of Biological Scanning Electrochemical Microscopy (Bio-SECM) was introduced in 2004. (Mauzeroll and Bard, 2004; Mauzeroll *et al.*, 2004; Bauermann, Schuhmann and Schulte, 2004) This tool is developed further in the laboratory of Prof. Janine Mauzeroll by applying the technique of SECM to detect molecules, released or received by a biological living cell.

In SECM the current is defined by the diffusion of a redox active substance to the electrode surface. Given that the electrode is far away from any substrate, the current is solely influenced by the active area of the electrode, the diffusion coefficient of the reacting species and the concentration of the reacting species. The solution of Fick's second law (3) for this case gives the following relation:

$$I = 4n_e FDcr \tag{4}$$

where I is the current at steady state, n_e is the number of electrons exchanged per formula unit of reactant, F is the Faraday constant, D is the diffusion coefficient, c is the bulk concentration of the reactant and r is the radius of the surface of active material at the tip of the electrode. When approaching an insulating surface with the tip of the electrode, the diffusion gets hindered by the presence of the substrate, resulting in a decrease of current. This behavior is called negative feedback (Figure I.3 a). When approaching an electrochemically reactive surface, the substance, transformed at the tip, can be regenerated by the surface, thus increasing the flux of redox active substance to the electrode and increasing the current. If this regeneration process is not limited by interfacial kinetics this behavior is called positive feedback (Figure I.3 b). For both feedback modes well established mathematical models can reproduce experimental results. In many cases mixed behavior can

be observed, when the electrochemically reactive substrate is not able to regenerate the redox substance fast enough to compensate for the decrease in diffusion due to space limitation.

The Bio-SECM (Figure I.4) consists of an optical microscope with a fluorescence module and a camera to allow also the optical imaging of cells. A working electrode (WE) is positioned in z axis and the electrochemical cell, which includes counter (CE) and reference electrode (RE), is positioned in x and y axis. The positioning is achieved by a stepper-piezo/motor combination. Closed loop step motors allow highest precision and avoid motor hysteresis during long distance imaging. The Bio-SECM is placed inside a Faraday cage in addition to a vibration isolation table to avoid noise caused by vibrations and electromagnetic interference and is connected to a computer unit and a low current bi-potentiostat.

The bi-potentiostat allows the control and measurement of potentials and currents in the fA-μA scale. In principle, the potentiostat measures the electrochemical potential difference between RE and WE and compares it to the chosen potential difference given by the computer. It then regulates the voltage source between WE and CE accordingly (Figure I.5 a). If a stable Chloride ion (Cl^-) concentration is given during the experimental work, a silver/silverchloride (Ag/AgCl) wire can be used as RE, whereas a platinum wire functions as CE to retransfer the collected electrons from the WE (Figure I.5 b). In the presented work the SECM is used in feedback mode, whereby the potential, applied at the WE, is chosen, so that after a very short time the concentration of untransformed mediator at the active surface of the microelectrode decreases to zero. At that time the measured current is determined by the diffusion of the mediator to the electrode's active surface due to its depletion by oxidation or reduction.

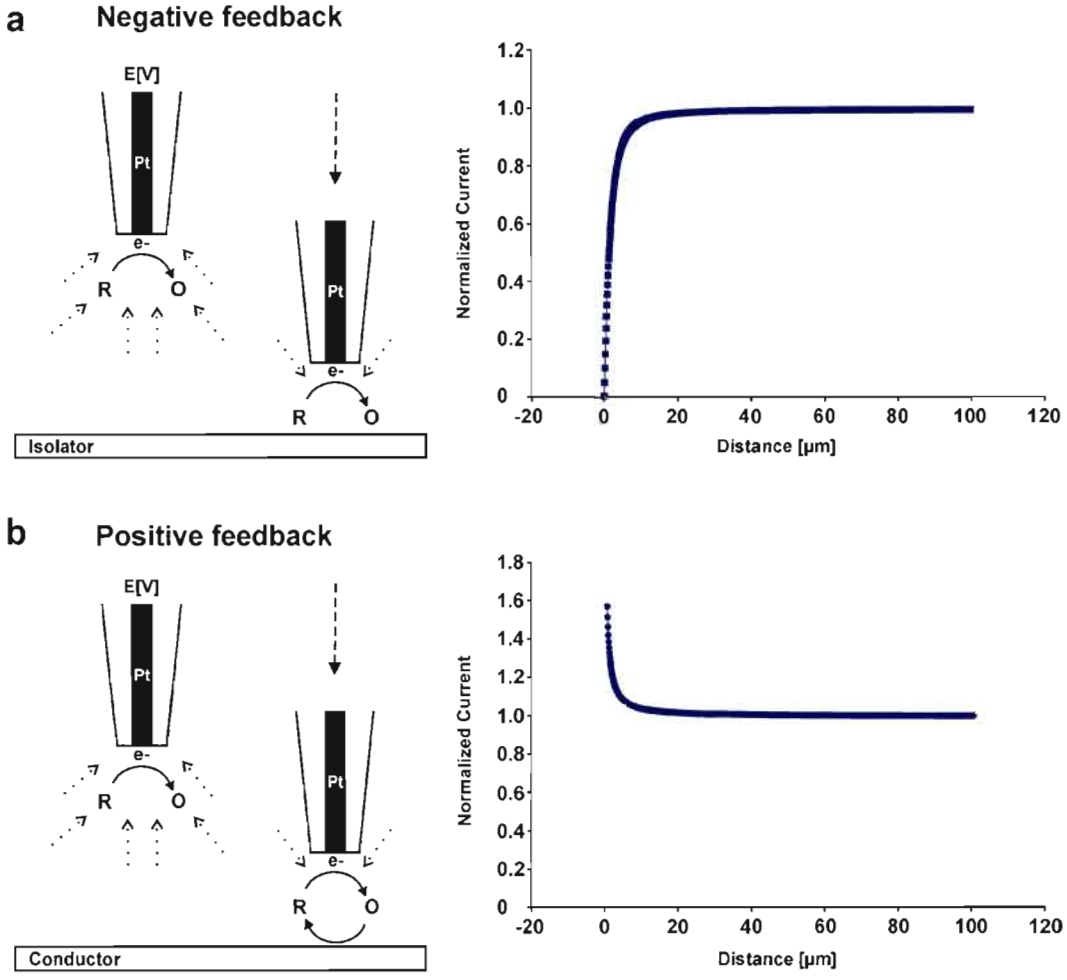

Figure I.3 Schematic representation of the feedback mode. (a) Negative feedback is observed while approaching an isolator whereas (b) positive feedback is recorded while approaching a conductor. The normalized current is the current at a certain point divided by the current far away from the substrate.

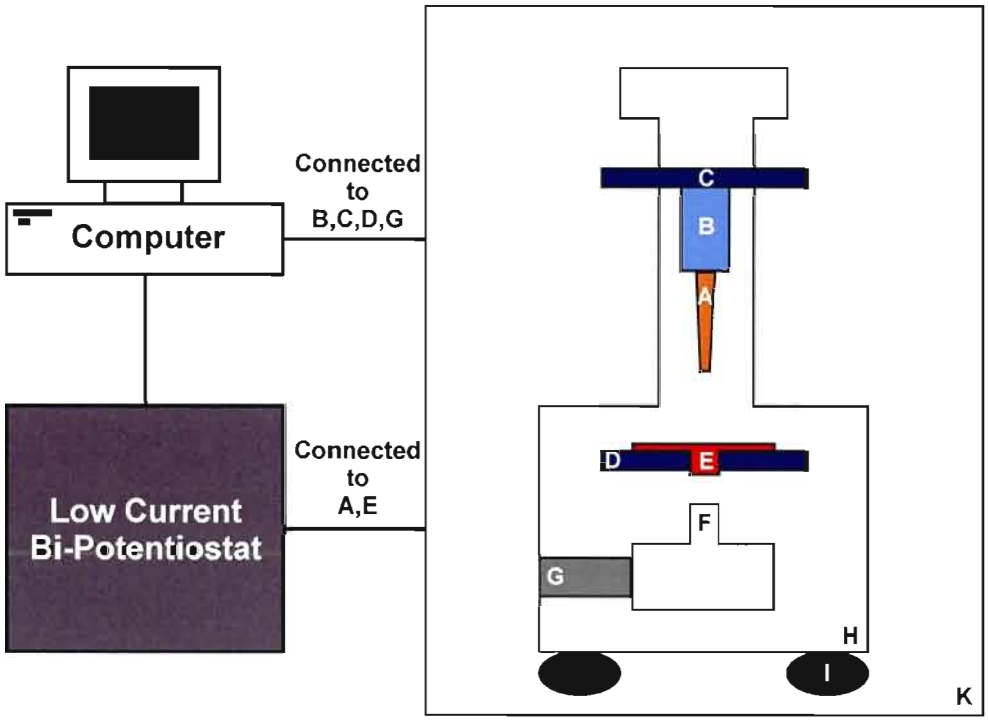

A Microelectrode
B Constant Distance Controller
C Z Axis Positioner
D X and Y Axis Positioner
E Electrochemical Cell
F Fluorescence Module
G Camera
H Optical Microscope
I X-Y Translation Stage
K Faraday Cage Vibration Isolation Table

Figure I.4 Schematic representation of the instrumental design of a Bio-SECM.

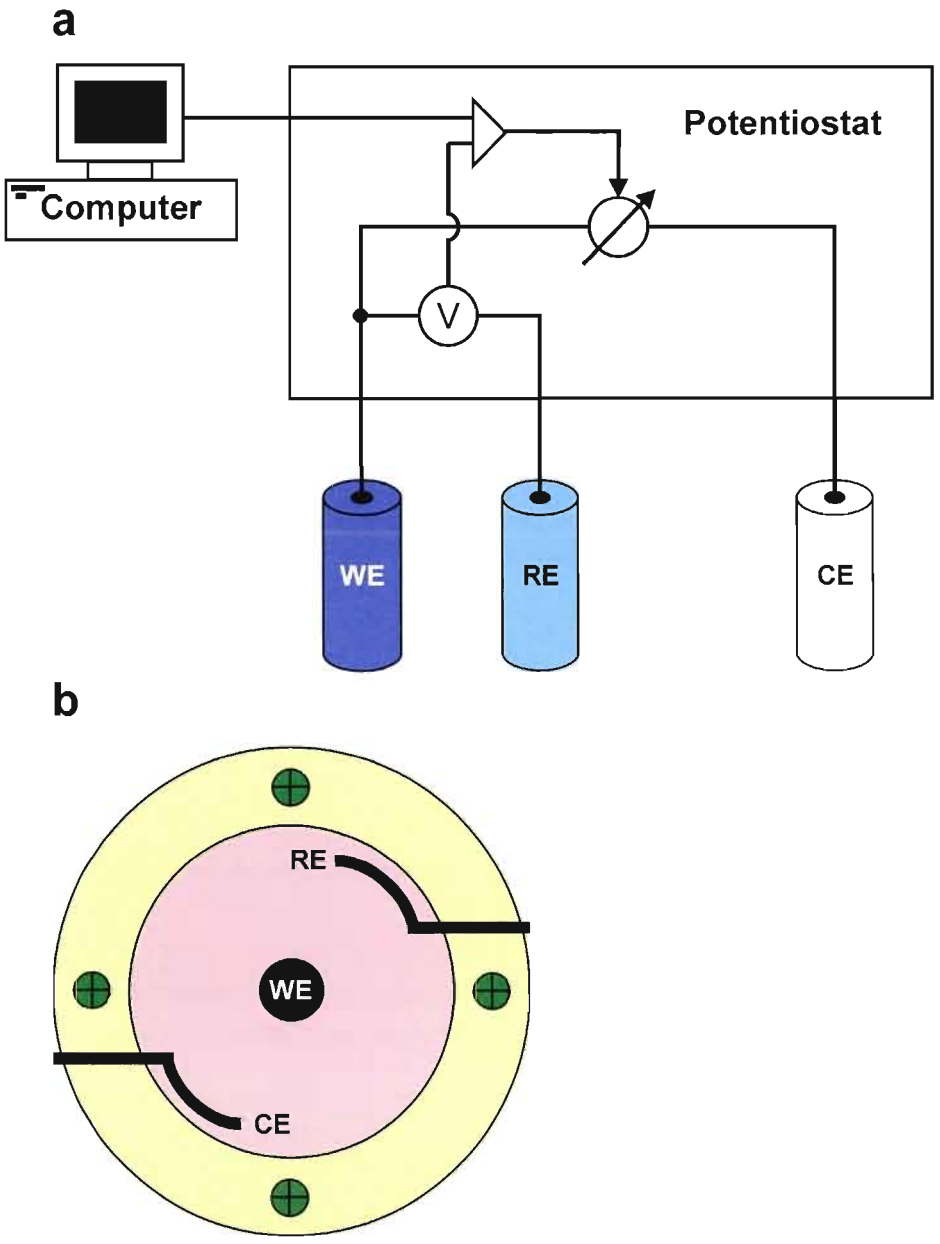

Figure I.5 (a) Simplified representation of the low current bi-potentiostat connected to the computer, working (WE), counter (CE) and reference electrode (RE). (b) Schematic representation of the electrochemical cell used in Bio-SECM studies.

Two imaging modes are available in SECM. In constant height mode the electrode is rastered lateral across an area always keeping the same height above a surface. Therefore, the tip to substrate distance changes depending on the topology of the sample analyzed (Figure I.6 a). By scanning over a surface of constant reactivity the tip current is a measure for the tip to substrate distance and therefore delivers topological information. Only by scanning over very smooth but heterogeneous surfaces, the tip current represents the electrochemical reactivity of the surface. For complex samples, such as biological cells, in constant height mode the current is altered by effects of electrochemical reactivity and topology. To decouple these two sources of information strategies for constant distance measurements have to be used. In constant distance mode the microelectrode always keeps the same distance from the surface when rastered across a sample (Figure I.6 b). Detailed information about the realization of the constant distance mode is given in chapter 3. Both techniques have been used for successful analyses of biological samples, such as yeast cells, hepatocytes and breast cancer cells. (Mauzeroll and Bard, 2004; Mauzeroll *et al.*, 2004; Bauermann, Schuhmann and Schulte, 2004; Liu, Rotenberg and Mirkin, 2000; Kaya *et al.*, 2003; Li and Bard, 2009; Saito *et al.*, 2006; Kurulugama *et al.*, 2005) Although successful imaging techniques have been developed (Kurulugama *et al.*, 2005) and analytical strategies have been proposed (Kuss *et al.*, 2011), no routine applications for medical purposes using Bio-SECM are available so far.

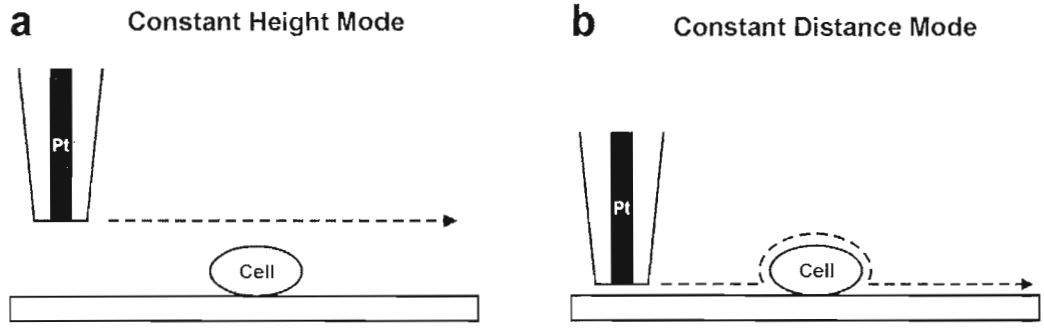

Figure I.6 Schematic representation of Constant Height and Constant Distance Mode. (a) At Constant Height Mode the electrode is rastered across an area keeping the same height above the substrate. Hence the distance between electrode and surface changes depending on the sample during scanning process. (b) At Constant Distance Mode the electrode keeps the same distance from the surface when rastered across a sample.

I.3.2 Flow Cytometry. For preliminary evaluation of the effect of $FcCH_2OH$ on intracellular levels of Glutathione we made use of Flow Cytometry, a technique that is well developed and enables the determination of properties of single cells.

As many other promising and auspicious inventions, the idea of a flowing system to count cells was born in Montreal in 1934 by Andrew Moldavan. His idea to guide stained yeast cells or red blood cells through a capillary on a microscope stage was further developed by Louis Kamentsky in the mid 1960s in order to approach the problem of automated cervical cytology screening. During this decade the development of flow cytometry took major steps forward: The development of a sorting machine in 1967 and the first fluorescence-detection cytometer in 1969 are great examples of the interest in the method of flow cytometry all around the world. Until now flow cytometry has developed into one of the most useful multi-purpose tools in analytical science and therefore became essential equipment in countless laboratories. (Longobardi Givan, 2004)

This method allows counting, examining and even sorting cells in suspension and it is an excellent way to measure several intracellular parameters cell by cell. Size, shape or pigments of the cell, proliferation (Haberkorn *et al.*, 1991), cell cycle (Boquest, Day and Prather, 1999) and chromosome analysis (Carrano *et al.*, 1979), protein expression (Leith *et al.*, 1995), enzyme activity (Watson, 1980) or concentration of reactive oxygen species (Marchetti *et al.*, 2002) demonstrate only a fraction the possibilities of what flow cytometry can determine. The characteristics of every single cell are established by looking at the cell's physical characteristics. The sample is injected into a liquid flow, also known as stealth liquid that focuses the cells hydrodynamically, wherefore they pass through a tube one by one. Passing a laser beam, up to 200,000 cells per second can be analyzed by different detectors for fluorescence and forward as well as side scattering. Therefore the laser emits light at a particular wavelength and one or more detectors are registering the light's modulation in presence of the cells. Light gets scattered by the cell due to refraction and reflection at the different cell compartments. Forward scattering is the signal of light detected in small angles around 180° to the excitation beam, while side scattering is the signal of light detected around 90° to the excitation beam. (Longobardi Givan, 2004) In the case of light scattering the responsible detectors will capture light with the same wavelength as emitted by the laser. The laser can also excite fluorophores inside the cell. Therefore the fluorophore is electronically

excited when absorbing light in a wavelength range specific to the fluorophore. The release of the absorbed energy takes place in two steps: first, the fluorophore transfers some of its vibrational energy to its environment, and second, the fluorophore releases the remaining energy by relaxing to its electronic ground state and emitting a phonon of the corresponding remaining energy (Figure I.7) Usually, fluorophores are added in fluorescence labeling steps (see section I.4). (Atkins, 2001, p. 565) Because of the lower energy, released in fluorescence, fluorescence detectors always detect at higher wavelengths then the laser, in contrast to the scattering detectors. These wavelengths can be adjusted to the different substances that need to be analyzed. Thereby cell parameters like size, shape and surface can be measured by light scattering, other cell contents in contrast by fluorescence. This way, for every cell forward scattering signal, side scattering signal and fluorescence signal are recorded (Figure I.8).

To graphically present the collected data, histograms or dot plots can be used. Using linear or logarithmic scaling in histograms it is difficult to see two different connected parameters at the same time. So most commonly a two-dimensional dot plot shows multiple characteristics and connections between several parameters, whereas one dot represents one cell passed through the instrument. If needed there is also software available to analyze and present data even in a three dimensional way or to analyze only a specific type of the cells by selecting them on a dot plot this is called gating.

The option of cell sorting will not be explained at this point, since it is not relevant for the performed studies mentioned in this work.

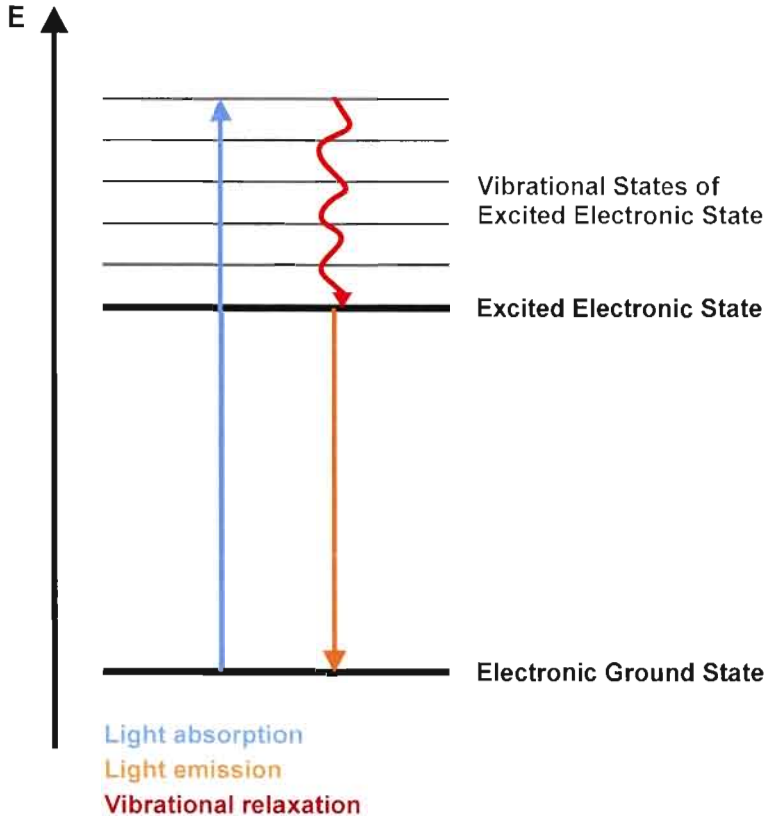

Figure I.7 Energy scheme of fluorescence process. The fluorophore first absorbs a phonon and is thereby excited to a higher electronic state (blue arrow). Some of the absorbed energy is transferred through vibrational relaxation to neighboring molecules (red arrow). During fluorescence, the fluorophore emits a phonon of the remaining energy while relaxing to the electronic ground state (orange arrow).

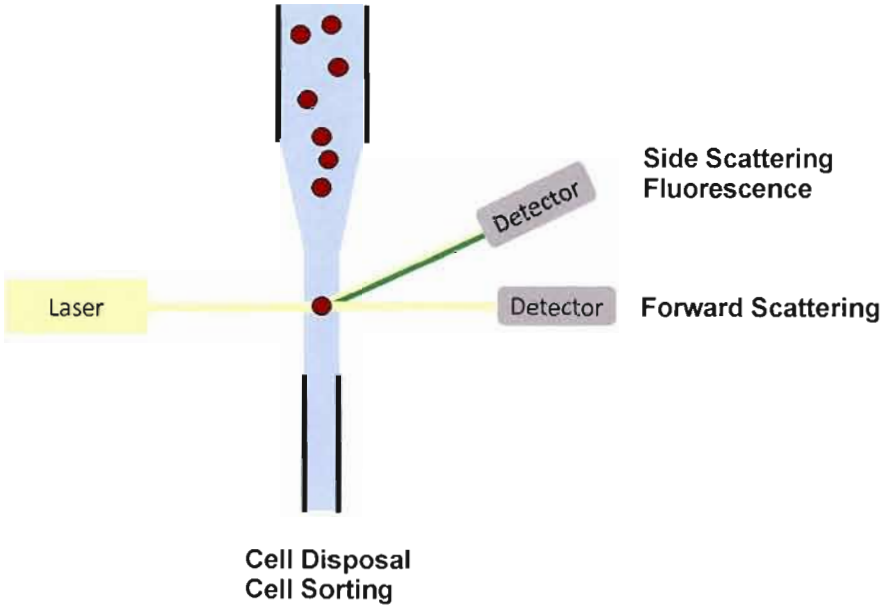

Figure I.8 Schematic representation of the principle of flow cytometry. Inside the flow cytometer cells are hydrodynamically lined up passing a laser beam. The laser light is scattered and captured by detectors collecting information about cell morphology, granularity and fluorescence.

I.3.3 Fluorescent Labeling. Fluorescence labeling is a technique of enormous importance to modern life science. Its applications include localization of cell organelles or specific molecules in microscopic imaging techniques (Müller, 2006), or monitoring of dynamic processes such as DNA damage following exposure to mutagenes. (Cosa, 2002) Advantageous to fluorescent labeling are the simplicity of equipment to detect the labels, well devcloped microscopic techniques for localization, non-invasive detection, and very low detection limits. Fluorescein, Green fluorescent protein and their variants are often used in combination with recognition sites as highly specific fluorescent labels. Lately also nano-size semiconductors, so called quantum dots, are developed as fluorophores for life science application. (Goldys *et al.*, 2006) The remaining main problems of fluorescent labeling are chemical stability, degradation after prolonged excitation (photobleaching) and wide emission ranges, making it hard to avoid spectral spillover from one fluorophore to the other. (Goldys *et al.*, 2006; Waggoner, 2006)

Intracellular levels of glutathione were detected by flow cytometry using 5-chloromethylfluorescein diacetate (CMFDA) as fluorescent label. CMFDA binds to thiol groups and allows monitoring of intracellular glutathione homeostasis. (Hedley and Chow, 1993; Voehringer *et al.*, 1998)

For fluorescence microscopy, the markers PKH2 and PKH26 were also used for fluorescent staining of Adenocarcinoma cervical cancer cells (HeLa) and a variant overexpressing MRP1 (HeLa-R) cells. Those fluorescent dyes with long aliphatic tails are incorporated into lipid regions of the cell membrane (Figure I.9). (Horan and Slezak, 1989)

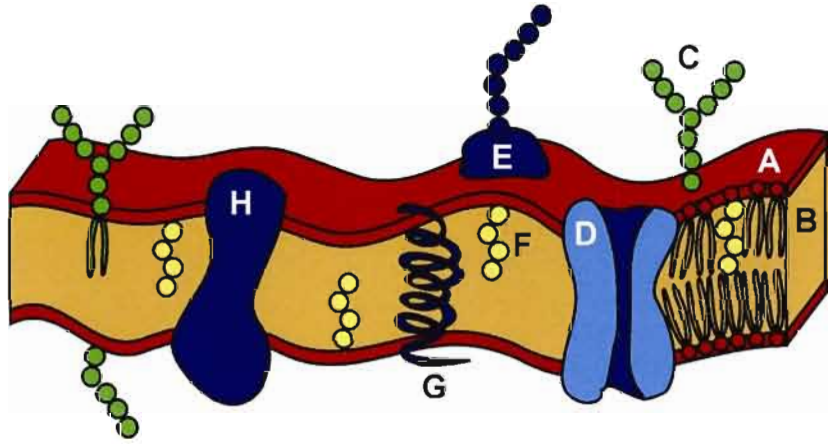

A Hydrophilic Head
B Hydrophobic Tail } **Phospholipid bilayer**
C Glycolipid
D Protein Channel (Transport Protein)
E Glycoprotein
F Cholesterol
G Alpha-Helix (Integral) Protein
H Globular (Integral) Protein

Figure I.9 Structure of a cell membrane.

The presented work shows the enormous potential of Bio-SECM in pharmaceutical research. The manuscript will be presented in 3 chapters: the first chapter describes the chemical relationship between the redox mediator ferrocenemethanol and multidrug resistance in form of a submitted article. The second chapter shows the progress the authors made on the field of cell patterning to improve Bio-SECM studies. The third chapter provides insight into ongoing studies to improve the constant distance mode for Bio-SECM measurements. In these chapters, the author hopes to convince the reader of the ability of Bio-SECM to serve as a tool for future chemotherapeutic research and development by coupling this electrochemical technique with fluorescence analyses in order to assess multidrug resistance in a new way.

CHAPTER I

SCIENTIFIC ARTICLE: MULTIDRUG RESISTANCE ASSESSMENT USING BIOLOGICAL SCANNING ELECTROCHEMICAL MICROSCOPY

The following chapter presents an application of the electrochemical technique of Scanning Electrochemical Microscopy (SECM) to biological living cells. Human adenocarcinoma cervical cancer cells HeLa (HeLa) and a multidrug resistant variant (HeLa-R) overexpressing the multidrug resistance protein 1 (MRP1) are used as targets. In order to develop a tool being able to quantify multidrug resistance in human cancer cells, the following objectives are approached: First, the influence of the cell's environment is evaluated during Biological Scanning Electrochemical Microscopy (Bio-SECM) measurements in order to enable the precise measurement of cell metabolites. Second, the response of HeLa and HeLa-R in the presence of the redox mediator ferrocenemethanol ($FcCH_2OH$) is observed. Third, the differential response of those cell lines during Bio-SECM studies is monitored.

The presented results in the following chapter demonstrate the relation between $FcCH_2OH/[FcCH_2OH]^+$, GSH/GSSG and multidrug resistance in human cancer cells and the impact of Bio-SECM analysis on future medical research and applications are outlined.

Article submitted to Bioelectrochemistry 2010

Multidrug Resistance Assessment Using Biological Scanning Electrochemical Microscopy

Sabine Kuss[1,2], Isabelle Beaulieu[1], Mohamed A. Mezour[1], Renaud Cornut[1] Borhane Annabi[2], Janine Mauzeroll[1]*

[1]Laboratory for Electrochemical Reactive Imaging and Detection for Biological Systems, Department of Chemistry, NanoQAM Research Centre, Université du Québec à Montréal, C.P. 8888, Succ. Centre-ville, Montréal, QC, Canada, H3C 3P8.

[2]Molecular Oncology Laboratory, Department of Chemistry, BioMED Research Centre, Université du Québec à Montréal, C.P. 8888, Succ. Centre-ville, Montréal, QC, Canada, H3C 3P8.

* Corresponding author. E-mail: Mauzeroll.janine@uqam.ca.

Sabine Kuss performed all experiments with exception of Figure 1.5 a-c and 1.6, treated all data and wrote the manuscript. Isabelle Beaulieu contributed by experimentation and data treatment to Figures 1.5 a-c and 1.6 and participated in writing the manuscript. Mohamed Amine Mezour assisted experiments and data treatment for Figure 1.5. Dr. Renaud Cornut advised during data treatment and interpretation and participated in writing the manuscript. Prof. Borhane Annabi and Prof. Janine Mauzeroll directed the research and wrote the manuscript.

Abstract

Background: Cancer cell multidrug resistance is a molecular signature that highly influences the outcome of chemotherapy treatment. There currently is no robust method to monitor *in vitro* multidrug resistance activity. Herein, we describe the transport and interaction of ferrocenemethanol ($FcCH_2OH$) in human adenocarcinoma cervical cancer cells HeLa and in a multidrug resistant variant overexpressing the multidrug resistant protein 1 (MRP1). **Result:** We demonstrate that the $FcCH_2OH/[FcCH_2OH]^+$ couple can be used to evaluate the redox state of the cell since both can interact with reduced and oxidized glutathione (GSH/GSSG). We demonstrate that the differential response to $FcCH_2OH$ in multidrug-resistant cells is in part due to MRP1's unspecific efflux. **Method:** This newly established relation between $FcCH_2OH/[FcCH_2OH]^+$, GSH/GSSG and multidrug resistance in human cancer cells has then been used in a Biological Scanning Electrochemical Microscopy (Bio-SECM) configuration, illustrating the possibility of a local quantification of GSH/GSSG amount in cells. **Conclusion:** Bio-SECM could enable efficient and robust assessment of the extent of multidrug resistance in human cancer cells prior to phase-I cancer clinical trials.

Keywords. Multidrug Resistance; Scanning Electrochemical Microscopy; Glutathione; Flow Cytometry

1.1 Introduction

Cancer cells actively defend themselves through multidrug resistance. Such cellular and molecular signature in many different cancer types, including acute leukemia, colon, kidney, pancreas, and carcinoid cancers, seriously undermines the success of chemotherapeutical treatments. (Goldstein, Pastan and Gottesman, 1992) For example, it is estimated that out of 7,000 new ovarian cancer patients annually in Canada and the US, 70% of them will exhibit resistance to treatment such as their survival rates decline to 10-30%. (Persidis, 1999)

The decrease in sensitivity against chemotherapeutic agents in resistant tumor cells is closely related to the action of non-selective transmembrane proteins that actively remove the agents from inside the cells. (Grant *et al.*, 1994) In the present study, the contribution of the multidrug resistance protein MRP1 is specifically evaluated through the action of two human cervical adenocarcinoma cancer cell lines: a HeLa cell line (HeLa) and a multidrug-resistant variant, overexpressing MRP1 (HeLa-R). MRP1 is known to transport, among others, glutathione (GSH) and drugs conjugated to GSH out of the cell. (Borst *et al.*, 2000) Alterations in the GSH levels, in GSH s-transferase (GST) levels and its activity, have been reported to affect cellular resistance to chemotherapeutic agents such as anthracyclines and cisplatin. (Morrow and Cowan, 1990) More recently, there has been a growing interest in the search for new antitumor compounds that do not interact with MDR1-Pgp and MRP1 drug transporters to circumvent the effect of these proteins conferring multidrug resistance and poor prognosis. (Ascione *et al.*, 2009)

As most of the current anticancer agents are subject to multidrug-resistance efflux and are currently irreplaceable in several chemotherapy regimens, an attractive solution for improving response to therapy can therefore be the development of new classes of agents that do not interact with the multidrug ABC transporters. Interestingly, antitumoral properties of the nitrobenzofurazane derivative 6-(7-nitro-2,1,3-benzoxadiazol-4-ylthio)hexanol, which is a strong inhibitor of the GST family, has recently been reported. (Ricci *et al.*, 2005) GST catalyzes the conjugation with GSH of many anticancer drugs that can be efficiently removed from the cell by specific export pumps. (Bakos and Homolya, 2007) To date, no efficient and

reliable cell-based methods have been designed to effectively monitor the cell's GSH/GSSG redox state and potential capacity as a target for a given chemotherapeutic drug.

Scanning Electrochemical Microscopy (SECM) is a well known technique that has been extensively used to study the topography and reactivity of surfaces in electrochemistry. (Bard and Mirkin, 2001) Biological Scanning Electrochemical Microscopy (Bio-SECM) is a promising technology to specifically study living cells. This method employs nanoscale electrodes that can be used to detect metabolites in single cell studies. In the last decade, several cell lines have been successfully analyzed by SECM. (Bard, Li and Zhan, 2006; Bauermann, Schuhmann and Schulte, 2004; Kaya *et al.*, 2003; Li and Bard, 2009; Liu, Rotenberg and Mirkin, 2000; Mauzeroll and Bard, 2004; Mauzeroll *et al.*, 2004; Saito *et al.*, 2006) To establish SECM as a general method enabling one to quantify the extent of multidrug resistance in cancer cells, it is mandatory to first identify a pair of mediators that are cell permeable/impermeable and that interact with a specific major cell constituent that is affected by multidrug resistance. The purpose of this study is therefore to assess whether the $FcCH_2OH/[FcCH_2OH]^+$ and $[Ru(NH_3)_6]^{2+}/[Ru(NH_3)_6]^{3+}$ redox couples are suitable redox probes that would allow accurate identification of interaction partners related to intracellular thiols present in all cells and intimately related to the multidrug resistance phenotype.

1.2 Experimental Section

1.2.1 Cell culture. All products were purchase from Sigma-Aldrich (ON, Canada) if not indicated differently. HeLa (CCL-2, American Type Culture Collection, VA, USA) were grown in Dulbecco's Modified Eagle's Medium (DMEM, high glucose, HyClone, UT, USA) completed with 10 % v/v heat inactivated fetal bovine serum (Gibco/Invitrogen, ON, Canada), 2 mM glutamine, penicillin and streptomycin (50 units/ml) (HYQ HyClone, UT, USA), which was used as basic medium ($DMEM^+$). HeLa-R overexpress the Multidrug Resistance Protein 1 (MRP1) and are resistant to actinomycin D, etoposide, adriamycin and vincristine. (Kast and Gros, 1998) Cells were maintained in tissue culture flasks (Sarstedt Inc, QC, Canada) at 37 °C and 5 % CO2 using an CO_2/Multi-gas incubator (Sanjo Scientific,

Japan). The culture medium for the HeLa-R contained Etoposide (VP-16, 250 ng/ml), which was removed prior to experiments. (Souslova and Averill-Bates, 2004) Both cell lines, ranging from 70 % to 90 % confluence, were washed with 37 °C phosphate-buffered saline (PBS) (pH 7.4 at 25 °C) and harvested with 37 °C 0.25 % v/v Trypsin-Ethylenediaminetetraacetic acid (EDTA) solution (10x, 2.0 g EDTA, in 0.9 wt% NaCl). Optical micrographs of platted cultured cells were acquired using an inverted microscope (Nikon Eclipse TS100) equipped with a camera (Olympus CAMEDIA C-500 ZOOM, using Gimp 2.4).

1.2.2 Membrane preparation and western blotting. MRP1 and Glyceraldehyde-3-phosphate dehydrogenase (GAPDH, Immuno Chemical, CA, USA) protein expression in HeLa and HeLa-R cells was detected by western blot analysis as described elsewhere. (Sina, Lord-Dufour and Annabi, 2009) The Bradford method was used for protein quantification of the cell lysates. (Bradford, 1976) Membranes were further washed and incubated for 1 h at room temperature with TBS-Tween 0.3 % v/v containing the MRP1 specific monoclonal antibody QCRL (1:100) (Abcam Inc, MA, USA) followed by an 1 h incubation period with horseradish peroxidase anti-mouse antibody (1:1,000) (Amersham Pharmacia Biotech, Rainham, UK) in 1.0 wt% skim milk in TBS-Tween 0.3 % v/v. The same membranes were used to detect GAPDH as control protein. The GAPDH specific monoclonal antibody (1:10,000) in TBS-Tween 0.1 % v/v + 3 wt% bovine serum albumin (BSA) + 0.02 wt% NaN3 was exposed to the membranes for 20 min and protein detection and analysis was performed as described before for MRP1-QCRL detection (Also see supporting information).

1.2.3 Flow cytometry. HeLa and HeLa-R cells were plated into 60-mm Petri dishes 24 hrs before experiment. Cells were washed with PBS and incubated in $DMEM^+$, $DMEM^-$ or PBS for different periods of time. To detect the intracellular GSH, cells were incubated 15 min in respective medium before CMFDA (Invitrogen, ON, Canada) was added in concentrations ranging from zero to 2.5 μM. CMFDA was dissolved and diluted in dimethyl sulfoxide (DMSO). Cells were incubated in respective medium containing CMFDA for another 15 minutes, washed with PBS and harvested with a 37 °C Trypsin solution. Trypsin

solution was removed by centrifugation at 1,000 g for 5 minutes. Cells were resuspended in 0.5 ml $DMEM^+$. Flow cytometric measurements were performed using FACSCalibur (BD Bioscience, USA) and data was analyzed with the software WinMDI (Windows Multiple Document Interface for Flow Cytometry, version 2.8). $FcCH_2OH$ and hexaammineruthenium(III) chloride ($[Ru(NH_3)_6]^{3+}$), both in 1 mM concentrations, were used respectively as cell permeable and impermeable electrochemical probes. Simultaneously, cell death was monitored using 0.02 mg/ml Propidium iodide (PI) solution (EMD Chemicals, NJ, USA).

1.2.4 Preparation of the control strain of HeLa cells before the electrochemical analysis. HeLa cells (ATCC, VA, USA) were seeded on 25-mm polymer disks (NUNC Brand Thermanox) or 23 mm Zeonor 1060R (Zeon Chemicals, KY, USA) oxygen plasma-treated (40 W/sccm) disks, 24 hrs prior to measurements. (Beaulieu, Geissler and Mauzeroll, 2009) The day of the analysis, the cells were washed with PBS and put in the corresponding redox solution.

1.2.5 Bulk electrolysis of $FcCH_2OH$ into $[FcCH_2OH]^+$ and exposure of HeLa cells to $[FcCH_2OH]^+$. Bulk electrolysis of $FcCH_2OH$ (1 mM dissolved in Minimum Essential Medium (MEM^-)) into its ferrocenium cation ($[FcCH_2OH]^+$) was achieved using a platinum sheet working electrode, an galvanized steel control electrode contained in a fritted glass tube and an Ag/AgCl reference electrode placed in a three-chamber electrolysis cell. Oxidation of $FcCH_2OH$ was performed by applying 0.4 V constant voltage for 3 hrs and resulted in a calculated faradic efficiency of 0.94.

The effect of $[FcCH_2OH]^+$ on HeLa cells was evaluated by CMFDA fluorescence intensity. Cells were washed with PBS and incubated for 15 min in MEM^- for the control group and MEM^- containing $[FcCH_2OH]^+$ for the tested group. Both groups were then stained with 2 μM CMFDA for 15 min, rinsed with PBS and then placed in MEM^- prior to acquisition. Fluorescence micrographs were acquired using a Nikon Eclipse TE2000-U inverted microscope equipped with a FITC/ RSGFP/ Bodipy/ Fluo 3/ DiO filter # 41001

(Chroma Technology, VT, USA) using a Retiga 2000R Fast 1394 Mono Cooled CCD camera (Qimaging, BC, Canada).

1.2.6 Biological-SECM measurements on HeLa cells.

1.2.6.1 Electrodes. A three-electrode setup was used for voltammetry and SECM experiments with 25 micrometer Platinum (Pt) diameter or laser pulled Pt working electrodes, a commercial Ag/AgCl reference and 0.5 mm Pt auxillary. The preparation of conventional 25 micrometer Pt microelectrodes followed a well established fabrication protocol (Fan et al., 2007, p.189-199) while polished, needle-like, disk-shaped nanoelectrodes were fabricated using a similar protocol to the procedures described. (Mauzeroll and LeSuer, 2007, p. 199-211) The fabrication procedure specifically produces disk shaped Pt microelectrode sealed in a quartz capillary and laser pulled until a dimensionless radius of glass (RG) inferior to 10 is obtained. In brief, 25 μm annealed Pt wires were pulled into quartz glass capillaries (length of 150 mm, an outer diameter of 1 mm, and an inner diameter of 0.3 mm) under vacuum with the help of a P-2000 laser pipet puller (Sutter Instruments, CA, USA). The pulling program results in the formation of a long and sharp microelectrode with a thin glass sheath, which facilitates membrane penetration. The effective radius was evaluated from steady-state voltammetry.

1.2.6.2 Electrochemical Measurements. Prior to analysis, the microelectrode is electrochemically cleaned using cyclic voltammetry in H_2SO_4 (0.5 M) between -0.3 V and 1.5 V during 20 cycles, rinsed and dried. For the measurements in ($[Ru(NH3)6]^{3+}$) (1 mM dissolved in PBS), a probe approach curve at a speed of 1 μm/s was acquired above the immobilized HeLa cells exposed to ($[Ru(NH_3)_6]^{3+}$). A -0.35 V *vs.* Ag/AgCl potential was applied at the microelectrode in order to obtain an electrochemical image of the ($[Ru(NH_3)_6]^{3+}$) (III) reduction to ($[Ru(NH_3)_6]^{3+}$) (II). For the $FcCH_2OH$ (1 mM dissolved in MEM^-), a probe approach curve was recorded at a speed of 1 μm/s above the cells using a 25 μm diameter Pt microelectrode following 70 min of exposure to $FcCH_2OH$. A 0.4 V *vs.* Ag/AgCl potential was applied at the electrode to obtain an electrochemical image of the

$FcCH_2OH$ oxidation to $[FcCH_2OH]^+$. Finally, probe approach curves of a Pt microelectrode biased at 0.4 V *vs.* Ag/AgCl were recorded across the cell membrane of single HeLa cells that had been exposed to $FcCH_2OH$ for 1h.

1.2.7 Statistical analysis. All values were measured in triplicates and subsequently statistically evaluated. Based on a student's t-distribution, errors were calculated applying a two-tailed test with n=3, $\alpha = 0.025$ and therefore a confidence level (CL) of 95% is given.

1.3. Results and Discussion

HeLa and HeLa-R were used to study the influence of redox mediators on the intracellular thiol redox state using a combination of electrochemical and fluorescent techniques. To adequately compare the results obtained from both techniques, it is first important to control the basic cell culture conditions that alter cell metabolism and affect the magnitude of the recorded electrochemical response.

1.3.1 Influence of cell environment. It is well known that the surrounding cell media influences the response of cells. As such, a careful control of media conditions during SECM measurements is an unavoidable first step towards multidrug resistance quantification, because the electrochemical measurements must be performed in a non-disrupting media. Moreover, the presence of serum in the media is problematic during electrochemical measurements because it leads to electrode fouling. For this reason, the influence of two culture media, which do not contain serum, have been studied: the classical electrochemical media, Phosphate Buffered Saline (PBS), and Dulbecco's Modified Eagle Medium without serum ($DMEM^-$).

The influence of culture media was studied on two cell lines having distinct morphologies and resistance phenotypes. The human cervical adenocarcinoma HeLa cells (HeLa) and human cervical adenocarcinoma multidrug-resistant HeLa cells (HeLa-R) exhibit intrinsically different morphologies when maintained under the same culture conditions.

Adherent HeLa cells present a triangular shape (Fig. 1.1a) while adherent HeLa-R cells present a reduction in cytoplasmic volume, are spherical and grow in colonies (Fig. 1.1b). (Puck, Marcus and Cieciura, 1956) HeLa and HeLa-R cells also differ in their expression level of MRP1 (190 kDa) as confirmed by western blotting followed by immunodetection using a specific MRP1 monoclonal antibody (Fig. 1.1c). The housekeeping gene, glyceraldehyde-3-phosphate dehydrogenase (GAPDH, 36 kDa), was used as control protein and was expressed in both cell lines. The observed expression level of resistant protein and housekeeping gene are consistent with literature. (Barber *et al.*, 2005; Kast and Gros, 1998)

By varying the culture media the cell morphology changes incurred were studied by optical microscopy and flow cytometry. As presented in Figure 1.1 (d-f, right panel), prolonged exposure to PBS affects the HeLa cell morphology since cells separate and become globular. Although clearly stressed, the exposed HeLa cells do not detach from the culture dish and cell staining with Trypan blue confirmed that no excessive cell death occurred after 4 hrs of incubation in PBS. Even though the cells are not dying, the observed cytoskeletal perturbations are among early events leading to major metabolic changes. (Bronaugh *et al.*, 1989; Kamisato and Nowakowski, 1988) In contrast, HeLa cells incubated in $DMEM^-$ show no external sign of stress (Fig. 1.1d-f, left panel).

The influence of culture media on morphology changes was further investigated and quantified by flow cytometry (Fig 1.2a-d). The dot plot displaying the forward scattering signal and the side scattering signals is showing a focused distribution in $DMEM^-$ after an incubation of 2 hrs (Fig. 1.2a). A broadening of distribution occurs with increasing incubation period (Fig. 1.2c) or incubation in PBS (Fig. 1.2b, d). By taking the focused morphology distribution in $DMEM^-$ at 2 hrs incubation as reference, the percentage of cells with a similar morphology is calculated for all conditions (see supporting figure S1.1). In $DMEM^-$ 77.49 % (67.87 % in PBS) of all cells belong to the focused distribution after 2 hrs incubation period. After 4 hrs 64.05 % (55.15 % in PBS) of cells still hold a similar morphology. A similar effect was observed in HeLa-R cells (see supporting figure S1.2). These results demonstrate that incubation in $DMEM^-$ media, contrary to PBS, maintain the standard HeLa and HeLa-R cell morphology for up to four hours.

The influence of culture media on the viability and metabolism of both cell lines was further studied by flow cytometric measurements that used propidium iodide (PI) and 5-chloromethylfluorescein diacetate (CMFDA) as fluorescent indicators of viability and intracellular thiol redox state (Fig. 1.2e). (Longobardi Givan, 2004) The influence of the media on the dose response of CMFDA revealed potential limitations of substituting the preferred media, $DMEM^-$, by PBS. When both cell lines were incubated in $DMEM^-$ or PBS for 30 minutes at 37 °C and 5% CO_2, the CMFDA dose response of the PBS incubated cells saturates as compared to that observed in $DMEM^-$ (Fig. 1.2e). This effect is likely due to a higher permeability of the cell membrane caused by the alteration of cell osmolarity by PBS. (Nakajima and Ikada, 1995) The cell viability remains nevertheless stable under both conditions and is in agreement with previous results (Fig. 1.1d-f).

The intracellular redox state of both cell lines is however significantly affected by PBS incubation. As such, incubation in $DMEM^-$ media is preferable to that in PBS because it sustains morphologically and metabolically representative HeLa and HeLa-R cells for up to four hours. During this period, electrochemical measurements such as those presented in a subsequent section are thus expected to be representative of the normal behavior of each cell line.

1.3.2. Differential response of HeLa-R and HeLa cell to the presence of redox mediators.

The differential behavior of HeLa-R and HeLa can first be studied by flow cytometry with CMFDA fluorescent staining. In the present study, CMFDA is employed as a fluorescent tag since it binds to thiol groups and allows monitoring of intracellular glutathione homeostasis. (Hedley and Chow, 1993; Voehringer *et al.*, 1998) Figure 1.3a shows a comparison of the dose response of the CMFDA fluorescence signal in HeLa and HeLa-R cell lines. The CMFDA dose response of the HeLa cells displays enhanced sensitivity as compared to that obtained with HeLa-R cells. This can be due to two major effects. First, it was previously shown that HeLa-R cells contain less intracellular glutathione as compared to HeLa cells. (Souslova and Averill-Bates, 2004) Second, a fraction of CMFDA gets pumped out of the cell by MRP1 before it can react with thiol groups inside the

cell. The dose response of both cell lines displays a wide linear range from zero to 2.5 μM CMFDA. Finally, no substantial cell death was observed in the presence of CMFDA over this range based on propidium iodide fluorescence intensity (Fig 1.3a). This result is in accordance with literature. (Mascotti, McCullough and Burger, 2000)

The interaction of two redox mediators: ferrocenemethanol ($FcCH_2OH$) and hexaammineruthenium(III) chloride ($[Ru(NH_3)_6]^{3+}$), was next assessed with HeLa and HeLa-R cells and their effect on the intracellular thiol redox state monitored by CMFDA fluorescence. The former is cell permeable (Sun *et al.*, 2008) but its effect on cell metabolism and intracellular redox state remains unclear. The latter is a highly charged redox mediator that is cell impermeable (Sun *et al.*, 2008) and serves as a negative control in Bio-SECM studies. (Bard, Li and Zhan, 2006; Li and Bard, 2009; Sun *et al.*, 2008; Amemiya *et al.*, 2006)

Under standard electrochemical conditions, no considerable cell death occurs in 1 mM $FcCH_2OH$/DMEM$^-$-treated cells (see supporting figure S1.3). HeLa cell incubation in $FcCH_2OH$ results in a statistically significant increase (confidence level (CL) 95%) in CMFDA fluorescence intensity (Fig. 1.3b). This indicates that the intracellular concentration of GSH is increased upon initial exposure to $FcCH_2OH$. In the HeLa-R cells, no statistically significant (CL 95%) fluorescence intensity shift is observed (Fig. 1.3c). This suggests that $FcCH_2OH$, like CMFDA, is pumped out of the cell by MRP1, an indication that this mechanism acts unspecifically and actively. Incubation of both cells lines in the cell impermeable redox mediator ($[Ru(NH_3)_6]^{3+}$) did not result in significant (CL 95%) CMFDA fluorescence intensity increase (Fig. 1.3d).

Importantly, the increase in CMFDA fluorescence in the presence of $FcCH_2OH$ is a transient effect that is subject to the equilibrium dynamics of the reduced and oxidized glutathione ratio. Upon 30 min incubation in $FcCH_2OH$, a statistically significant (CL 95%) CMFDA fluorescence intensity increase in HeLa cells is observed. For $FcCH_2OH$ incubation periods exceeding 60 min, it is expected that the backward enzyme assisted reaction, responsible for maintaining the cells' redox state homeostasis, prevails (Figure 1.4). (Schraufstatter *et al.*, 1985)

1.3.3. Differential response of Hela-R and Hela cells during SECM studies. To date, no efficient and reliable cell-based methods have been designed to effectively monitor the cell's GSH/GSSG redox state and potential capacity as a target for a given chemotherapeutic drug. The glutathione metabolism inside all cells of the human body is important for the cellular defense against reactive oxygen species (ROS). This major antioxidant tripeptide reacts non-enzymatically with radicals and acts as the electron donor for the reduction of peroxides. (Dringen, 2000) Moreover glutathione is essential for cell proliferation and maintains the thiol redox potential in cells keeping sulfhydryl groups of proteins in the reduced form. (Cotgreave and Gerdes, 1998) The detailed glutathione function, its metabolism and oxygen-reduction-pathways have been described previously. (Dringen, 2000; Lantz *et al.*, 2001; Markovic *et al.*, 2007; Meister, 1994a; Meister, 1994b; Wang and Ballatori, 1998) Our finding that the mediator couple ($FcCH_2OH/[FcCH_2OH]^+$) interacts with the oxidized and reduced form of glutathione suggests that the couple can be used intracellularly and extracellularly to evaluate the cell's redox state by electrochemistry.

The response of both cell lines in presence of the previously used electrochemical species, ($[Ru(NH_3)_6]^{3+}$) and $FcCH_2OH$, has been further studied using SECM. Starting with HeLa cells, an electrochemical image of the cell in presence of ($[Ru(NH_3)_6]^{3+}$) was acquired. In this configuration, a decrease in the recorded cathodic current was observed, when the microelectrode is scanned across the HeLa cells (Fig. 1.5a). Since ($[Ru(NH_3)_6]^{3+}$) is a cell impermeable redox mediator, its diffusion to the surface of the microelectrode is hindered in close proximity to the cells and a decrease in reduction current is observed. These results are consistent with similar SECM studies. (Sun *et al.*, 2008; Mauzeroll *et al.*, 2002) This experiment illustrates that although the cells are exposed to PBS and therefore the membrane integrity is not fully maintained, as discussed previously (Fig. 1.2e), during SECM mapping, we observe a decrease in current in the presence of ($[Ru(NH_3)_6]^{3+}$), proving that this redox mediator indeed does not interact with cells. In a second step, measurements with $FcCH_2OH$ have been performed. The electrochemical image obtained when $FcCH_2OH$ is used as the mediator is presented in Figure 1.5b. The observed response significantly differs from that obtained with $Ru(NH_3)_6]^{3+}$: an increase in anodic current is observed when the microelectrode is positioned above the cells. This current increase occurs because the microelectrode generates $[FcCH_2OH]^+$, which thereafter diffuses within the confined volume of the

microelectrode and cell surface, and is regenerated by a cell component back to $FcCH_2OH$. This aspect has further been investigated by performing an approach curve above a cell, as presented in Figure 1.5c. As the microelectrode approaches the cell, the current decreases due to the hindered diffusion of $FcCH_2OH$ to the microelectrode active surface. However this decrease in current does not correlate with negative feedback as shown in Figure 1.5c. Both curves would have been superimposed if no regeneration of mediator had occurred. We verified that a realistic uncertainty of the experimental parameter (microelectrode radius, surrounding glass thickness) does not influence the accordance to the data significantly. The discrepancy between the negative feedback and the approach curve in the presence of $FcCH_2OH$ confirms the significant regeneration of the mediator during electrochemical imaging. This observation is in accordance with what has been observed in SECM literature. (Li and Bard, 2009)

In the past, the $FcCH_2OH$ regeneration has not been consistently observed in cases where the cells die during the experiments. (Liu, Rotenberg and Mirkin, 2000) This indicates that the regeneration of $FcCH_2OH$ is related to an active process. The extent of $FcCH_2OH$ efflux is therefore potentially related to the resistant phenotype of the cells. To confirm this idea, electrochemical imaging in presence of $FcCH_2OH$ above Hela-R cells has been carried out (Fig. 1.5d). When the microelectrode is rastered across the HeLa-R cells the observed response is very different from that observed using HeLa (Fig. 1.5c). A slight decrease in current is recorded above cells.

The differential response between HeLa and Hela-R cells means that $FcCH_2OH$ glutathione efflux for resistant cells could be measured electrochemically using Bio-SECM leading to quantification of the extend of cell's resistance.

One has to underline that difference from negative feedback observed above HeLa cells (Figure 1.5b and 1.5c) cannot be due to $[FcCH_2OH]^+$ released from cells. Indeed, in contrast to $FcCH_2OH$, which diffuses into cells, $[FcCH_2OH]^+$ is cell impermeable. This aspect is demonstrated Figure 1.6, that presents results from fluorescence microscopy experiments with CMFDA and a solution of $[FcCH_2OH]^+$ obtained through classical bulk electrolysis. Figure 1.6 shows that there is no significant (CL 95%) difference between the fluorescence intensity of the HeLa cells exposed and unexposed to $[FcCH_2OH]^+$. If

$[FcCH_2OH]^+$ had entered the cell, it would have reacted with GSH, as determined electrochemically elsewhere. (Schreyer and Mikkelsen, 1999; Wring, Hart and Birch, 1991) This would have reduced the available intracellular concentration of GSH that would have otherwise reacted with the CMFDA and resulted in a reduction in the fluorescence intensity as compared to that observed in the unexposed cells. Based on the present results, it appears that the charged species $[FcCH_2OH]^+$ is cell impermeable, and that the difference from negative feedback observed Figure 5b and 5c cannot be explained by direct $[FcCH_2OH]^+$ cell release.

According to those results, it seems that differential response between Hela and Hela-R cells is likely to be related to the cell component, glutathione, responsible for the regeneration reaction using corroborating electrochemical and fluorescent experiments. Exact quantification of this differential response is however behind the scope of this preliminary study.

1.4. Conclusion

Establishing the relation between $FcCH_2OH/[FcCH_2OH]^+$, the efflux mediated by multidrug resistance proteins, and GSH/GSSG in a human cancer cell line is an important first step towards the quantification of multidrug resistance. Given the nature of Bio-SECM and its hyphenation with fluorescence microscopy, the intracellular flux of $FcCH_2OH$ and extent of regeneration reaction of $[FcCH_2OH]^+$ will be used to relate multidrug resistance to ubiquitous glutathione. This could lead to the establishment of a quantifiable indicator for multidrug resistance activity that can be used over cell life and across cell lines thereby enabling targeted drug screening and improving existing chemotherapeutical treatments.

Acknowledgment. JM and BA acknowledge the Natural Sciences and Engineering Research Council of Canada (NSERC) and the Canadian Foundation for Innovative (CFI) for their financial support. BA holds a Canada Research Chair in Molecular Oncology from the Canadian Institutes of Health Research (CIHR). The authors thank Dr. Philippe Gros (McGill

University, Montreal) for providing the MRP1 overexpressing variant of the HeLa cells and Matthias Geissler (Industrial Materials Institute, NRC, Boucherville) for providing Zeonor disks. SK thanks Pharmaqam for the award of the Pharmaqam Entrance Fellowship. The technical contributions of M. Marion and Dr. Charles Cougnon and Christian Kuss are also acknowledged.

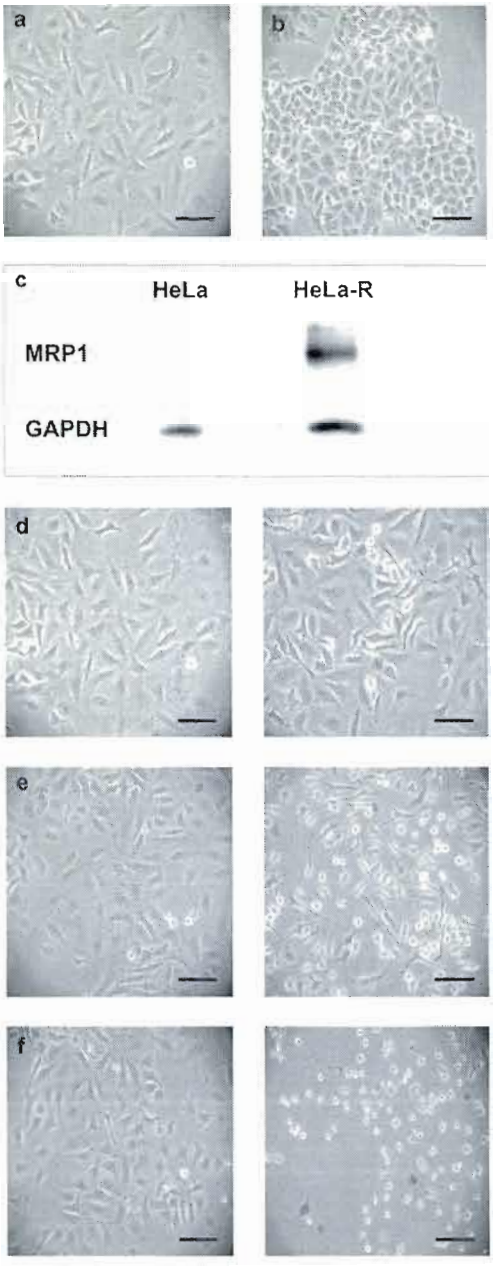

Figure 1.1 Optical micrographs and western blot comparing both strains of HeLa cells. (a) HeLa cells in complete medium ($DMEM^+$). (b) HeLa-R cells in $DMEM^+$. (c) Western blot showing the constitutive expression of MRP1 protein in the multidrug resistant HeLa cells. The housekeeping gene GAPDH was used as a control. (d-f) Comparison of HeLa cells exposed to medium devoid of serum ($DMEM^-$) (left panel) and PBS pH 7.4 (right panel). Images were acquired after 0 min (d), 30 min (e) and 240 min (f) incubation. Scale bar for all micrographs correspond to 100 μm.

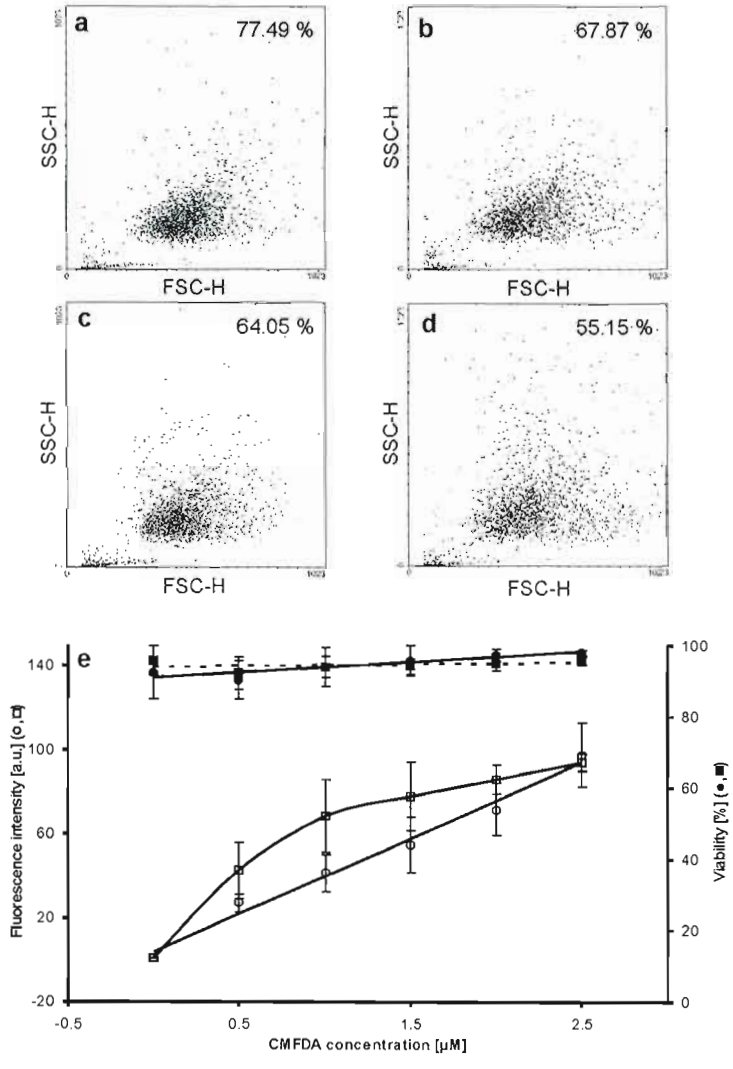

Figure 1.2 Statistical validation of morphological changes in HeLa cells. (a) The dot plot displaying the forward (FSC-H) and side scattering (SSC-H) signals shows a focused distribution after 2 hrs in DMEM$^-$. Distribution broadening can be seen when cells are exposed to DMEM$^-$ for 4 hrs (c) or to PBS pH 7.4 during 2 hrs (b) and 4 hrs (d). Cell viability and the dose-response relationship between CMFDA concentration and cell fluorescence intensity is shown for cells exposed to DMEM$^-$ or PBS. (e) HeLa cells were incubated for 30 min in DMEM$^-$ (PI ●, CMFDA ○) or and in PBS pH 7.4 (PI ■, CMFDA □).

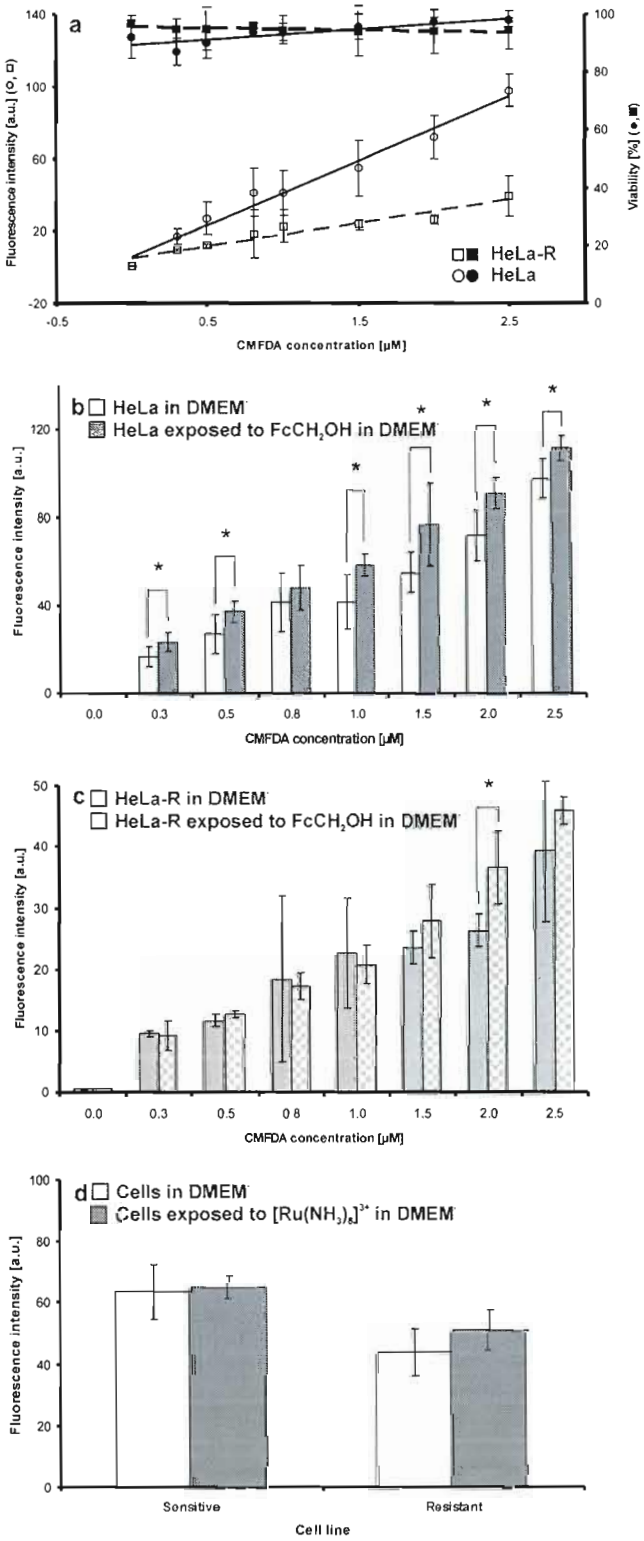
a
Fluorescence intensity [a.u.] (○, □)
Viability [%] (■, ●)
CMFDA concentration [µM]
HeLa-R
HeLa
b HeLa in DMEM
HeLa exposed to FcCH2OH in DMEM
Fluorescence intensity [a.u.]
CMFDA concentration [µM]
c HeLa-R in DMEM
HeLa-R exposed to FcCH2OH in DMEM
Fluorescence intensity [a.u.]
CMFDA concentration [µM]
d Cells in DMEM
Cells exposed to [Ru(NH3)6]3+ in DMEM
Fluorescence intensity [a.u.]
Sensitive
Resistant
Cell line

Figure 1.3 Cell viability and the dose-response relationship between CMFDA concentration and cell fluorescence intensity, obtained by flow cytometry, are shown for both cell strains exposed 30 min to $DMEM^-$. (a) HeLa (PI ●, CMFDA ○) and HeLa-R (PI ■, CMFDA □). (**b-c**) Dose-response relationship between different doses of CMFDA and its fluorescence intensity for the HeLa (**b**) and HeLa-R (**c**) HeLa cells incubated 30 min in either $DMEM^-$/1 mM $FcCH_2OH$ (dark grey, patterned) or in $DMEM^-$ only (white, light grey). The asterisks correspond to a significant increase of fluorescence intensity (n = 3; error bars representing the confidence interval of 95%) between groups exposed to $DMEM^-$/$FcCH_2OH$ and $DMEM^-$. (**d**) Flow cytometry fluorescence measurements in the presence of 2 μM CMFDA staining of both cell strains exposed 30 min to $DMEM^-$ containing or not 1 mM $[Ru(NH_3)_6]^{3+}$.

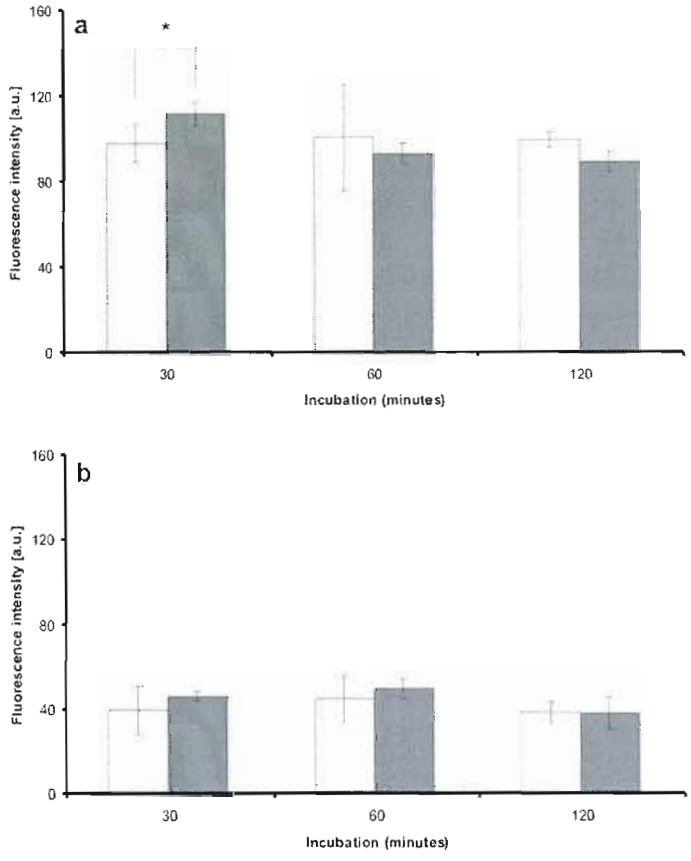

Figure 1.4 Influence of $FcCH_2OH$ incubation time on CMFDA fluorescence intensity. HeLa (**a**) and HeLa-R (**b**) HeLa cells were exposed to 1 mM $FcCH_2OH$ in $DMEM^-$ for 30, 60 and 120 min and compared to those only incubated in $DMEM^-$. Flow cytometry fluorescence measurements of CMFDA (2.5 μM) added to the medium after 15, 45 or 105 min of incubation. The asterisks correspond to a significant difference (n = 3; error bars representing the confidence interval of CL 95%) between indicated groups.

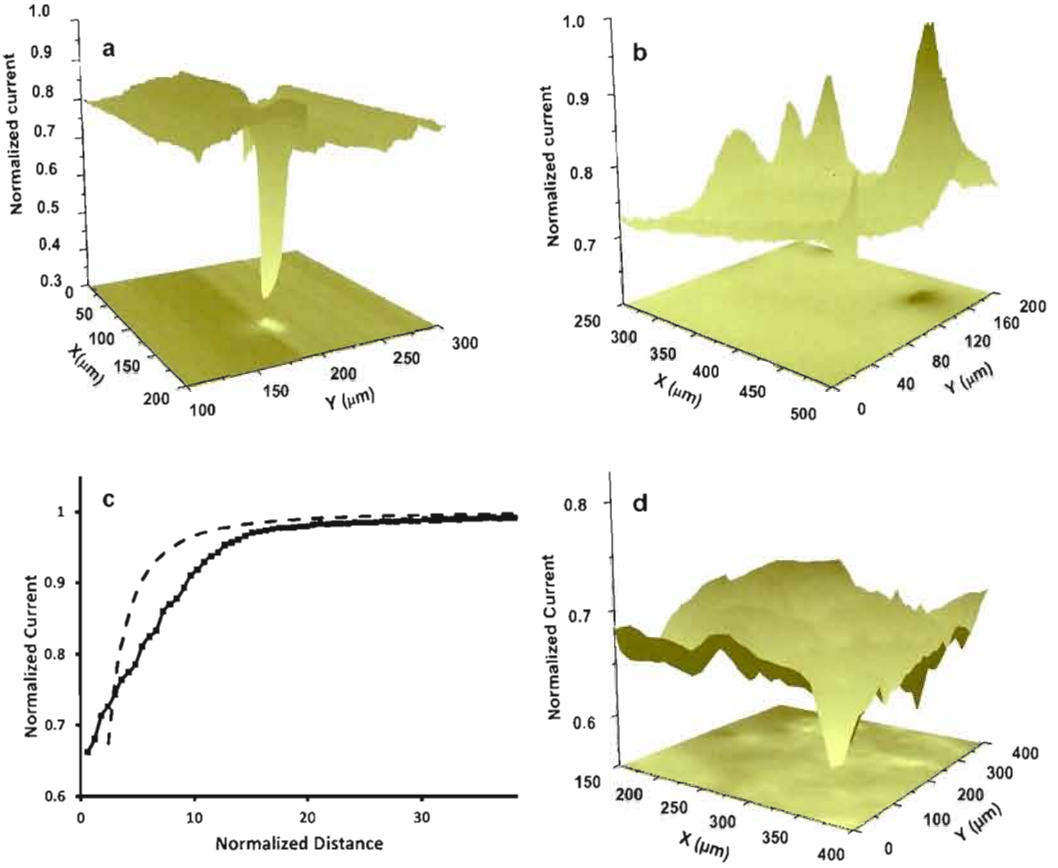

Figure 1.5 (**a**) SECM electrochemical image of $[Ru(NH_3)_6]^{3+}$ (III) 1 mM reduction above HeLa cells. A - 0.35 V *vs.* Ag/AgCl potential was applied at the 1 μm diameter Pt microelectrode to reduce the $[Ru(NH_3)_6]^{3+}$ (III). Normalized current (current divided by current measured far from substrate) is presented for all images. (**b**) SECM electrochemical image the $FcCH_2OH$ oxidation to $[FcCH_2OH]^+$. SECM electrochemical image of $FcCH_2OH$ 1 mM above HeLa cells is shown. A 0.4 V *vs.* Ag/AgCl potential was applied at the 25 μm diameter Pt microelectrode to oxidize $FcCH_2OH$. (**c**) Approach curve in $FcCH_2OH$ 0.75 mM from above a HeLa cell (full line). Negative feedback theoretical curve (expression taken from literature (Cornut and Lefrou, 2007) shows mismatch with experimental curve (see text). Pt microelectrode of about 340 nm diameter; applied potential more anodic than 0.4V *vs.* Ag/AgCl. (**d**) SECM electrochemical image of $FcCH_2OH$ 1 mM above HeLa-R cells. An 0.4 V *vs.* Ag/AgCl potential was applied at the 25 μm diameter Pt microelectrode to oxidize $FcCH_2OH$.

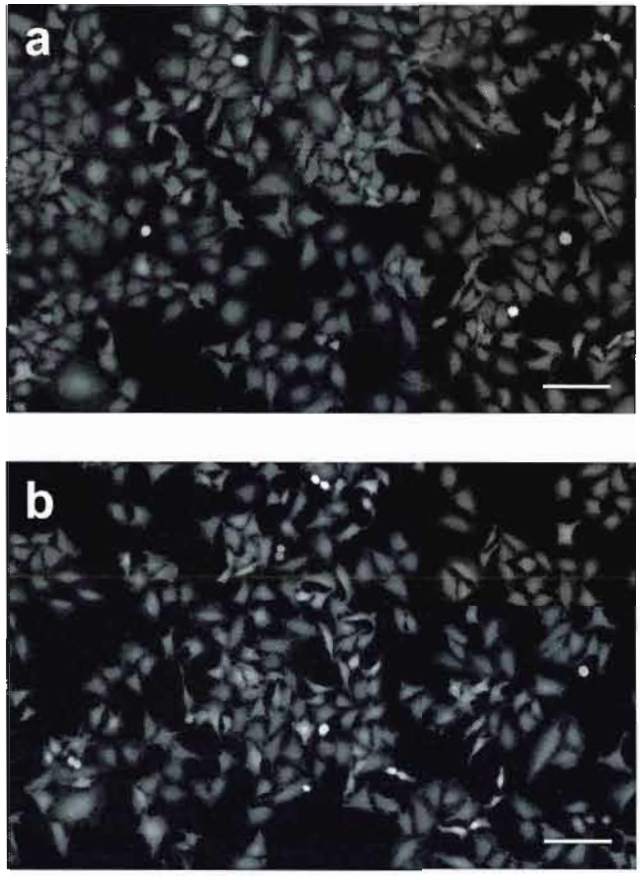

Figure 1.6 Fluorescence images of HeLa cells. The fluorescence intensity of the unexposed HeLa cells (in $DMEM^-$; **a**) is compared to cells exposed to $[FcCH_2OH]^+$ in MEM– for 30 min (**b**). There is no substantial difference in the fluorescence intensity of the CMFDA. Micrographs were acquired using a Nikon Eclipse TE2000-U inverted microscope and Nikon NIS-Element software (version 3.0). Scale bar for all micrographs correspond to 100 μm.

1.5. References

Amemiya, Shigeru, Jidong Guo, Hui Xiong and Darrick A. Gross. 2006. Biological applications of scanning electrochemical microscopy: chemical imaging of single living cells and beyond. *Analytical and Bioanalytical Chemistry,* vol. 386, no 3, p. 458-471.

Ascione Alessandro, Maurizio Cianfriglia, Maria L. Dupuis, Alessandra Mallano, Andrea Sau, Francesca Pellizzari Tregno, Silvia Pezzola and Anna M. Caccuri. 2009. The glutathione S-transferase inhibitor 6-(7-nitro-2,1,3-benzoxadiazol-4-ylthio)hexanol overcomes the MDR1-P-glycoprotein and MRP1-mediated multidrug resistance in acute myeloid leukemia cells. *Cancer Chemotherapy and Pharmacololgy,* vol. 64, p. 419-424.

Bakos Éva and László Homolya. Portrait of multifaceted transporter, the multidrug resistance-associated protein 1 (MRP1/ABCC1). *European Journal of Physiology,* vol. 453, p. 621-641.

Barber Robert D., Dan W. Harmer, Robert A. Coleman and Brian J. Clark. 2005. GAPDH as a housekeeping gene: analysis of GAPDH mRNA expression in a panel of 72 human tissues. *Physiological Genomics,* vol. 21, p. 389-395.

Bard, Allen J., Xiao Li and Wei Zhan. 2006. Chemical imaging living cells by scanning electrochemical microscopy. *Biosensors and Bioelectronics,* vol. 22, no. 4, p. 461-472.

Bard, Allen J. and Michael V. Mirkin. 2001. *Scanning Electrochemical Microscopy,* New York: Marcel Dekker, Inc, p. 650.

Bauermann, Luciana Pitta, Wolfgang Schuhmann and Albert Schulte. 2004. An Advanced Biological Scanning Electrochemical Microscope (Bio-SECM) for Studying Individual Living Cells. *Physical Chemistry Chemical Physics,* vol. 6, p. 4003-4008.

Beaulieu, Isabelle, Matthias Geissler and Janine Mauzeroll. 2009. Oxygen Plasma Treatment of Polystyrene and Zeonor: Substrates for Adhesion of Patterned Cells. *Langmuir,* vol. 25, p. 7169-7176.

Borst, Piet, Raymond Evers, Marcel Kool and Jan Wijnholds. 2000. A family of drug transporters: the multidrug resistance-associated proteins. *Journal of the National Cancer Institute,* vol. 92, no. 16, p. 1295-1302.

Bradford Marion M. 1976. A rapid and sensitive method for the quantitation of microgram quantities of protein utilizing the principle of protein-dye binding. *Analytical Biochemistry*, vol. 72, p. 248-254.

Bronaugh Robert L., Steven W. Collier, Jan E. Storm and Raymond F. Stewart. 1989. In vitro evaluation of skin absorption and metabolism. *Journal of Toxicology - Cutaneous and Ocular Toxicology,* vol. 8, p. 453-467.

Cornut Renaud and Christine Lefrou. 2007. A unified new analytical approximation for negative feedback currents with a microdisk SECM tip. *Journal of Electroanalytical Chemistry,* vol. 608, p. 59-66.

Cotgreave Ian A. and Robert G. Gerdes. 1998. Recent Trends in Glutathione Biochemistry—Glutathione–Protein Interactions: A Molecular Link between Oxidative Stress and Cell Proliferation? *Biochemical and Biophysical Research Communications,* vol. 242, p. 1-9.

Dringen Ralf. 2000. Metabolism and functions of glutathione in brain. *Progress in Neurobiology,* vol. 62, p. 649-671.

Fan, Fu-Ren F., Jose Fernandez, Biao Liu, Janine Mauzeroll and Cynthia G. Zoski. 2007. «Platinum and gold inlaid disks ≥ 5μm diameter». In *Handbook of Electrochemistry,* Cynthia G. Zoski, p. 189-199. Amsterdam: Elsevier B.V.

Goldstein, Lori J., Ira Pastan and Michael M. Gottesman. 1992. Multidrug resistance in human cancer. *Critical Reviews In Oncology/Hematology*, vol. 12, no. 3, p. 243-253.

Grant Caroline E., Gunnar Valdimarsson, David R. Hipfner, Kurt C. Almquist, Susan P. C. Cole and Roger G. Deeley. 1994. Overexpression of multidrug resistance-associated protein (MRP) increases resistance to natural product drugs. *Cancer Research,* vol. 54, p. 357-361.

Hedley, David W. and Sue Chow. 1993. Evaluation of Methods for Measuring Cellular Glutathione Content Using Flow Cytometry. *Cytometry,* vol. 15, p. 349-358.

Kamisato Javier K. and Maja Nowakowski. 1988. Morphological and biochemical alterations of macrophages produced by a glycan, PSK. *Immunopharmacology, vol.* 16, p. 89-96.

Kast, Christina and Philippe Gros. 1998. Epitope Insertion Favors a Six Transmembrane Domain Model for the Carboxy-Terminal Portion of the Multidrug Resistance-Associated Protein. *Biochemistry,* vol. 37, no. 8, p. 2305-2313.

Kaya, Takatoshi, Yu-suke Torisawa, Daisuke Oyamatsu, Matsuhiko Nishizawa and Tomokazu Matsue. 2003. Monitoring the Cellular Activity of a Cultured Single Cell by Scanning Electrochemical Microscopy (SECM). A Comparison with Fluorescence Viability Monitoring. *Biosensors and Bioelectronics,* vol. 18, p. 1379-1383.

Lantz R. Clark, Ranulfo Lemus, Robert W. Lange and Meryl H. Karol. 2001. Rapid reduction of intracellular glutathione in human bronchial epithelial cells exposed to

occupational levels of toluene diisocyanate. *Toxicological Science,* vol. 60, p. 348-355.

Li, Xiao and Allen J. Bard. 2009. Scanning electrochemical microscopy of HeLa cells–Effects of ferrocene methanol and silver ion. *Journal of Electroanalytical Chemistry,* vol. 628, no. 1-2, p. 35-42.

Liu, Biao, Susan A. Rotenberg, and Micheal V. Mirkin. 2000. Scanning electrochemical microscopy of living cells: Different redox activities of nonmetastatic and metastatic human breast cells. *Proceedings of the National Academy of Sciences,* vol. 97, no. 18, p. 9855-9860.

Longobardi Givan, Alice. 2004. *Flow cytometry: First principles.* New York: Wiley-Liss.

Markovic Jelena, Consuelo Borrás, Ángel Ortega, Juan Sastre, José Vina and Federico V. Pallardó. 2007. Glutathione is recruited into the nucleus in early phases of cell proliferation. *Journal of Biological Chemistry,* vol. 282, p. 20416-20424.

Mascotti Kristin, Jeffrey McCullough and Scott R. Burger. 2000. HPC viability measurement: trypan blue versus acridine orange and propidium iodide. *Transfusion,* vol. 40, p. 693-696.

Mauzeroll, Janine and Allen J. Bard. 2004. Scanning electrochemical microscopy of menadione-glutathione conjugate export from yeast cells. *Proceedings of the National Academy of Sciences,* vol. 101, no. 21, p. 7862-7867.

Mauzeroll Janine, Mihai Buda, Allen J. Bard, Francisco Prieto and Manuela Rueda. 2002. Detection of Tl (I) Transport through a Gramicidin- Dioleoylphosphatidylcholine Monolayer Using the Substrate Generation- Tip Collection Mode of Scanning Electrochemical Microscopy. *Langmuir,* vol. 18, p. 9453-9461.

Mauzeroll, Janine, Allen J. Bard, Omeed Owhadian and Terrence J. Monks. 2004. Menadione metabolism to thiodione in hepatoblastoma by scanning electrochemical microscopy. *Proceedings of the National Academy of Sciences,* vol. 101, no. 51, p. 17582-17587.

Mauzeroll, Janine and Robert J. LeSuer. 2007. «Laser-pulled ultramicroelectrodes». In *Handbook of Electrochemistry*, 2007, Cynthia G. Zoski, p. 199-211. Amsterdam: Elsevier B.V.

Meister Alton. 1994. Glutathione-ascorbic acid antioxidant system in animals. *Journal of Biologicl Chemistry,* vol. 269, p. 9397-9400.

Meister Alton. 1994. Glutathione, ascorbate, and cellular protection. *Cancer Research,* vol. 54, p. 1969-1969.

Morrow, Charles S. and Kenneth H. Cowan. 1990. Glutathione S-transferases and drug resistance. *Cancer cells,* vol. 2, no. 1, p. 15-22.

Nakajima Naoki and Yoshito Ikada. 1995. Effect of Solution Osmotic Pressure on Cell Fusion by Poly (Ethylene Glycol). *Journal of Bioactive and Compatible Polymers,* vol. 10, p. 14-27.

Persidis, Aris. 1999. Cancer multidrug resistance. *Nature Biotechnology,* vol. 17, p. 94-95.

Puck Theodore T., Philip I. Marcus and Steven J. Cieciura. 1956. Clonal growth of mammalian cells in vitro growth characteristics of colonies from single HeLa cells with and without a "feeder" layer. *Journal of Emperimental Medicine,* vol. 103, p. 273-284.

Ricci Giorgio, Francesca De Maria, Giovanni Antonini, Paola Turella, Angela Bullo, Lorenzo Stella, Giuseppe Filomeni, Giorgio Federici and Anna M. Caccuri. 2005. 7-Nitro-2,1,3-benzoxadiazole derivatives, a new class of suicide inhibitors for glutathione *S*-transferases. Mechanism of action of potential anticancer drugs. *Journal of Biological Chemistry,* vol. 280, p. 26397-26405.

Saito, Takeshi, Ching-Chou Wu, Hitoshi Shiku, Tomoyuki Yasukawa, Masaki Yokoo, Takashi Ito-Sasaki, Hiroyuki Abe, Hiroyoshi Hoshi and Totokazu Matsue. 2006. Oxygen consumption of cell suspension in a poly (dimethylsiloxane)(PDMS) microchannel estimated by scanning electrochemical microscopy. *The Analyst,* vol. 131, no. 9, p. 1006-1011.

Schraufstätter Ingrid U., Daniel B. Hinshaw, Paul A. Hyslop, Roger G. Spragg, Charles G. Cochrane. 1985. Glutathione cycle activity and pyridine nucleotide levels in oxidant-induced injury of cells. *Journal of Clinical Investigation,* vol. 76, p. 1131-1139.

Schreyer Suzanne K. and Susan R. Mikkelsen. 1999. A Synthetic Cysteine Oxidase Based on a Ferrocene−Cyclodextrin Conjugate. *Bioconjugate Chemistry,* vol. 10, p. 464-469.

Sina Asmaa, Simon Lord-Dufour and Borhane Annabi. 2009. Cell-based evidence for aminopeptidase N/CD13 inhibitor actinonin targeting of MT1-MMP-mediated proMMP-2 activation. *Cancer Letters,* vol. 279, p. 171-176.

Souslova, Tatiana and Diana A. Averill-Bates. 2004. Multidrug-resistant hela cells overexpressing MRP1 exhibit sensitivity to cell killing by hyperthermia: Interactions with etoposide. *International Journal of Radiation Oncology Biology Physics,* vol. 60, no. 5, p. 1538-1551.

Sun Peng, François O. Laforge, Thushara P. Abeyweera, Susan A. Rotenberg, James Carpino and Michael V. Mirkin. 2008. Nanoelectrochemistry of mammalian cells. *Proceedings of the National Academy of Sciences,* vol. 105, p. 443-448.

Voehringer, David W., David J. McConkey, Timothy J. McDonnell, Shawn M. Brisbay and Raymond E. Meyn. 1998. Bcl-2 expression causes redistribution of glutathione to the nucleus. *Proceedings of the National Academy of Sciences,* vol. 95, no. 6, p. 2956-2960.

Wang Wei and Nazzareno Ballatori. 1998. Endogenous glutathione conjugates: occurrence and biological functions. Pharmacological Reviews, vol. 50, p. 335-356.

Wring Stephen A., John P. Hart and Brian J. Birch. 1991. Voltammetric behaviour of screen–printed carbon electrodes, chemically modified with selected mediators, and their application as sensors for the determination of reduced glutathione. *The Analyst,* vol. 116, p. 123-129.

1.6. Supporting Information

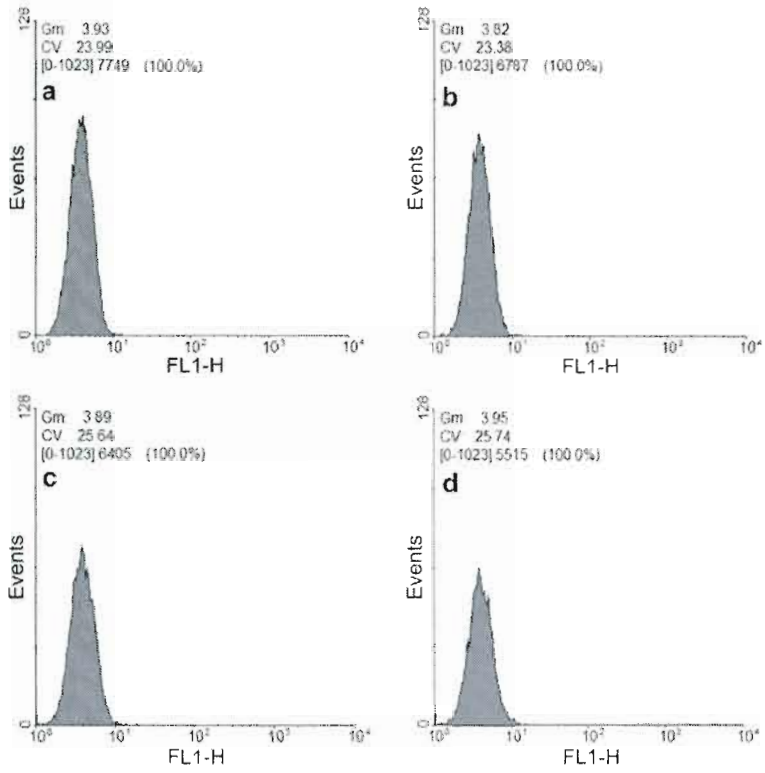

Supporting figure S1.1 Statistical validation of morphological changes in HeLa cells. Exposure for 2 hrs to $DMEM^-$ (**a**) and PBS (**b**). Exposure for 4 hrs to $DMEM^-$ (**c**) and PBS (**d**).

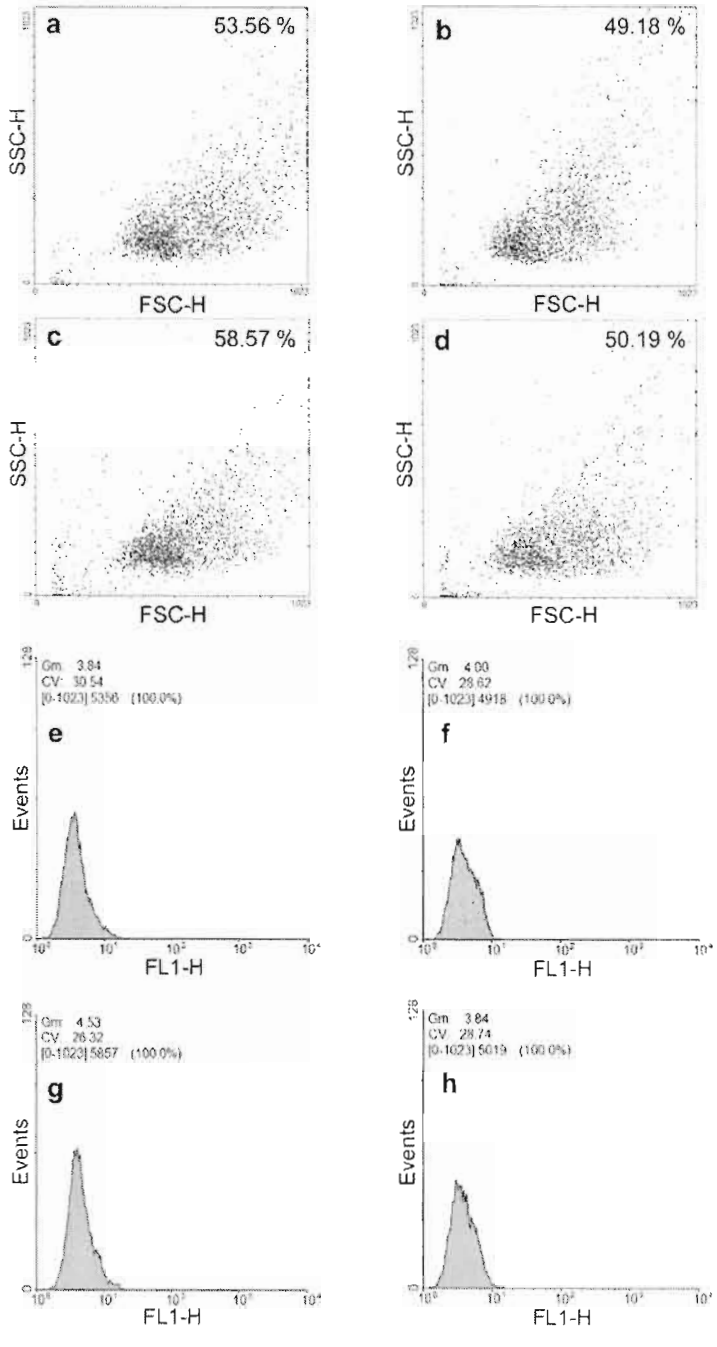

Supporting figure S1.2 Statistical validation of morphological changes in HeLa-R cells. Dot plots (**a-d**) as well as histograms (**e-h**) showing distribution broadening when the cells are exposed to $DMEM^-$ for 4 hrs (**c, g**) or PBS for 2 hrs (**b, f**) or 4 hrs (**d, h**).

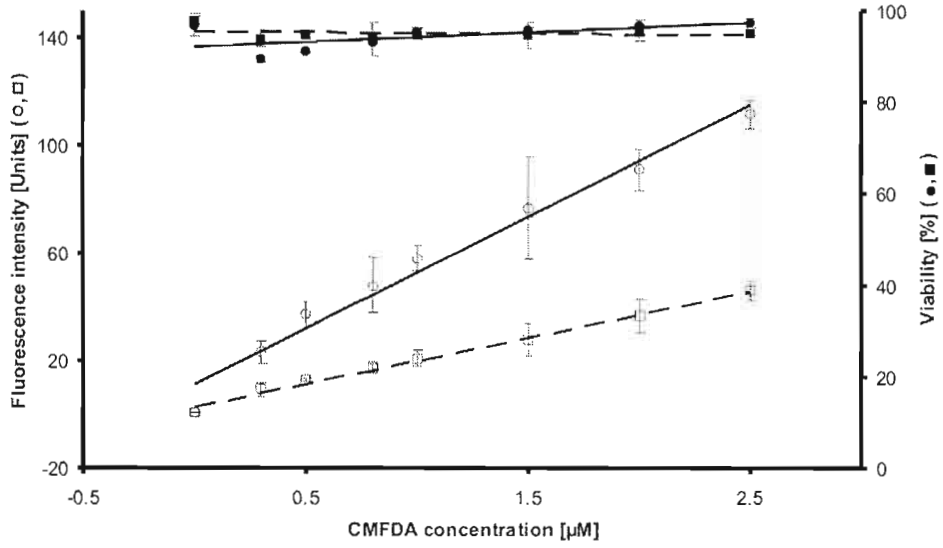

Supporting figure S1.3 Cell viability and the dose-response relationship between CMFDA concentration and cell fluorescence intensity. Cells exposed 30 min to $DMEM^-$ and $FcCH_2OH$.

Detailed information about membrane preparation and western blotting. MRP1 and a control protein, GAPDH (Immuno Chemical, CA, USA), were detected by western blot analysis. HeLa and HeLa-R cells were maintained as described previously and lysed in buffer containing 150 mM NaCl, NP-40 1 % v/v, deoxycholic acid 0.5 wt%, sodium dodecyl sulphate (SDS) 0.1 wt% and 50 mM Tris/HCl (pH 7.5 at 4 °C). Cell debris was removed by centrifugation at 1,000 *g* for 10 min. The Bradford method was used for protein quantification of the supernatant.

Immunodetection of MRP1 and GAPDH, 20 μg of proteins completed with 5 μL loading buffer (62.5 mM Tris/HCl (pH 6.8), glycerol 10 % v/v, SDS 2 wt%, bromophenol blue 0.00625 wt%) were separated on a 7.0 % SDS polyacrylamide gel. The electrophoresis buffer contained 19.2 mM glycine, 25 mM Tris/HCl and 0.1 wt% SDS. Electrophoresis was carried out at a constant voltage of 130 V. The proteins were transferred to a polyvinylidene fluoride (PVDF) membrane (Millipore, MA, USA) using a semidry blotting system (W.E.P Company, USA). The transfer buffer contained 96 mM glycine, 10 mM Tris/HCl, methanol 10 % v/v (pH 8.4). A constant current of 80 mA/gel was applied for 1.5 hrs. To block non specific and hydrophobic sites, membranes were incubated overnight at 4 °C in 3.0 wt% skim milk in Tris-buffered saline (Sigma-Aldrich, ON, Canada) containing 0.3 % v/v Tween 20 (Sigma-Aldrich, ON, Canada) (TBS-Tween 0.3 % v/v). Membranes were washed three times for 20 min in TBS-Tween 0.3 % v/v and incubated for 1 h at room temperature with TBS-Tween 0.3 % v/v containing the MRP1 specific monoclonal antibody QCRL (1:100) (Abcam Inc Cambridge, MA, USA). Following three 20 min washes in TBS-Tween 0.3 % v/v, the specific proteins on the PVDF membranes were detected using horseradish peroxidase anti-mouse antibody (1:1,000) (Amersham Pharmacia Biotech, Rainham, UK) in 1.0 wt% skim milk in TBS-Tween 0.3 % v/v. Membranes were washed and MRP1 was analyzed using ECL chemiluminescence plus kit (HyGlo, Denville Scientific Inc, NJ, USA). Revealed protein expression was detected and quantified using a film processor (Mini medical series, AFP imaging, USA). Given the intense QCRL response in the HeLa-R cells, the exposure time was optimized to 1 s. Present antibody bindings were removed by incubating PVDF membranes 1 hr in 0.2 M glycin in nanopure water purified using the Millipore Milli-Q Biocel Ultrapure water system (Fisher, ON, Canada). Membranes were washed three times in TBS-Tween 0.3 % for 20 min and the same membranes were used to detect GAPDH as control protein. Membrane blocking procedures were performed as described previously. The GAPDH specific monoclonal antibody (1:10,000) in TBS-Tween 0.1 % + 3 wt% bovine serum albumin (BSA) + 0.02 wt% NaN_3 was exposed to the membranes for 20 min and protein detection and analysis was performed as described before for MRP1-QCRL detection.

CHAPTER II

SCIENTIFIC ARTICLE: CREATING VERSATILE CELL PATTERNS FOR BIOLOGICAL SCANNING ELECTROCHEMICAL MICROSCOPY

The previous chapter describes the evaluation of the Redox couple $FcCH_2OH/[FcCH_2OH]^+$ as mediator during Biological Scanning Electrochemical Microscopy (Bio-SECM) measurements as well as the relation between $FcCH_2OH/[FcCH_2OH]^+$, GSH/GSSG and multidrug resistance in human cancer cells. First electrochemical studies on cancer cells have been performed showing the strong potential behind the technique of Bio-SECM for medical and bioanalytical applications. In order to use the described relations to quantify multidrug resistance, cells of different cell lines need to be aligned under the microscope under controlled conditions.

The following chapter presents a new cell patterning procedure in order to improve working conditions during Bio-SECM studies. Using elastomeric through-hole membranes (SEBS) and Zeonor® 1060R substrates, defined patterns of different cell types are to be achieved. Zeonor® 1060R substrates are biocompatible plastic surfaces that were treated with oxygen plasma and provide therefore an efficient basis for cell growth. The SEBS copolymer membranes, as processed at the Industrial Materials Institute, National Research Council of Canada, are to be evaluated as an alternative to the commonly used polydimethylsiloxane (PDMS) membranes to overcome previous disadvantages in cell patterning.

The presented results outline the usefulness of versatile cell patterns achieved following the presented protocol. The precise positioning of cells improves the

reproducibility of Bio-SECM studies, specifically enabling cell analysis in a shorter period of time and analysis of multiple cell types at the same time under the same conditions.

Article in preparation

Creating versatile Cell Patterns for Biological Scanning Electrochemical Microscopy

Sabine Kuss[1], *Daniel Brassard*[2], *Matthias Geissler*[2], *Janine Mauzeroll*[1*]

[1]Laboratory for Electrochemical Reactive Imaging and Detection for Biological Systems, Department of Chemistry, NanoQAM Research Centre, Université du Québec à Montréal, C.P. 8888, Succ. Centre-ville, Montréal, QC, Canada, H3C 3P8.

[2]Industrial Materials Institute, National Research Council of Canada, 75 de Mortagne Boulevard, Boucherville, QC, Canada, J4B 6Y4

* Corresponding author. E-mail: Mauzeroll.janine@uqam.ca.

Sabine Kuss performed all experiments treated all data and wrote the manuscript. Dr. Daniel Brassard and Dr. Matthias Geissler prepared polymer membranes and substrates, Dr. Geissler also participated in writing the manuscript. Prof. Janine Mauzeroll and Dr. Matthias Geissler directed the research.

Abstract

Biological Scanning Electrochemical Microscopy (Bio-SECM) is a promising technique that can quantify the flux of substances transported in and out of cells. To study cells using Bio-SECM, the target cell's growth and positioning underneath a micro-scale electrode needs to be controlled without interfering with their normal behavior and metabolism. Herein we describe a relatively simple and cost-efficient method based on the use of elastomeric through-hole membranes for producing cell patterns on plastic supports. Specifically, we demonstrate the patterning of cells in the form of islands on oxygen plasma treated Zeonor® for both single cell patterns and co-culture of two different cell lines. Resultant patterns have been characterized using Bio-SECM in conjunction with optical and fluorescence microscopy. The presented study will impact future bioanalytical research, because it allows more precise studies on cells in a variety of scientific fields, such as cell and developmental biology and endocrinology.

2.1 Introduction

In the last decade, a number of new techniques emerged focusing on more efficient and effective approaches of cancer treatment. One of those techniques is Biological Scanning Electrochemical Microscopy (Bio-SECM). Employing micro- or nano-scale electrodes, Bio-SECM can be used to quantify the flux of substances consumed by or released from a cell. In the past years, multiple cell types have been analyzed (Bard, Li and Zhan, 2006; Bauermann, Schuhmann and Schulte, 2004; Kaya *et al.*, 2003; Li and Bard, 2009; Liu, Rotenberg and Mirkin, 2000; Mauzeroll and Bard, 2004; Mauzeroll *et al.*, 2004; Saito *et al.*, 2006), successful imaging techniques have been developed (Kurulugama *et al.*, 2005) and analytical strategies have been proposed (Kuss *et al.*, 2011). So far, the possibilities of those techniques are not exclusively, but also limited by controlling the cellular environment to be able to study cell's characteristics on the micron level. One aspect is the proper arrangement of target cells underneath a micro- or nanoscale electrode and to control their growth and position during electrochemical measurements.

Protocols for cell patterning procedures exist since the 1960s (Carter, 1965; Carter, 1967a; Carter, 1967b) and have been developed and advanced since then. The advent of soft lithography is one of the major milestones in this field. (Kane *et al.*, 1999) Unlike photolithography (Kleinfeld, Kahler and Hockberger, 1988), soft lithography involves elastomeric polymers, such as polydimethylsiloxane (PDMS), to replicate and transfer structural information provided by a mask, mold or stamp in a functional material (Csucs *et al.*, 2003; Lahann *et al.*, 2001; Liu and Chen, 2005; Singhvi *et al.*, 1994; Tan *et al.*, 2004; Xia and Whitesides, 1998) Inspired by that, stencils emerged allowing patterning of cell or biomolecules through holes in those elastomeric masks. (Folch *et al.*, 2000; Tourovskaia *et al.*, 2003) Despite all the advantages of PDMS, such as its price compared to silicon, its flexibility, its conform nature and optical transparency, there are also disadvantages in using PDMS. Problems in adhesion, shrinking, capillary force stress and sagging of structures were observed, leading to defects in the created pattern. (Xia and Whitesides, 1998) The purpose of this study is therefore to investigate an alternative offering all the advantages of the PDMS, while overcoming the previously mentioned disadvantages. Furthermore, its effectiveness in preparation of Bio-SECM experiments is evaluated.

2.2 Experimental Section

2.2.1 Cell culture. All products were purchased from Sigma-Aldrich (ON, Canada) if not indicated differently. HeLa (CCL-2, American Type Culture Collection, VA, USA) were grown in Dulbecco's Modified Eagle's Medium (DMEM high glucose, HyClone, UT, USA) completed with 10 % v/v heat inactivated fetal bovine serum (Gibco/Invitrogen, ON, Canada), 2 mM glutamine, 25 mM 4-(2-Hydroxyethyl)piperazine-1-ethanesulfonic acid (HEPES), penicillin and streptomycin (50 units/ml) (HYQ HyClone, UT, USA), which was used as basic medium ($DMEM^+$). HeLa-R overexpress the Multidrug Resistance Protein 1 (MRP1) and are resistant to actinomycin D, etoposide, adriamycin and vincristine. (Kast and Gros, 1998) Cells were maintained in tissue culture flasks (Sarstedt Inc, QC, Canada) at 37 °C and 5 % CO_2 using a CO_2/Multi-gas incubator (Sanjo Scientific, Japan). The culture medium for the HeLa-R contained etoposide (VP-16, 250 ng/ml), which was removed prior to experiments. (Souslova and Averill-Bates, 2004) Both cell lines, ranging from 70 % to 90 % confluence, were washed with 37 °C phosphate-buffered saline (PBS) (pH 7.4 at 25 °C) and harvested with 37 °C 0.25 % v/v Trypsin-EDTA solution (10x, 2.0 g EDTA, in 0.9 wt% NaCl).

2.2.2 Fluorescent staining. Both cell lines were labelled either using the PKH2 (Green) or the PKH26 (Red) Fluorescent Cell Linker Kit (Sigma-Aldrich, ON, Canada). These fluorescent markers lable the cell membrane by incorporation into the lipid region of the biphospholipid layers. (Horan and Slezak, 1989) Cells were harvested with 37 °C 0.25 % v/v Trypsin-EDTA solution (10x, 2.0 g EDTA, in 0.9 wt% NaCl). 2 x 107 cells were transferred into a 15 ml falcon tube (Sarstedt Inc, Montreal, QC) and washed once with basic medium missing serum ($DMEM^-$). Cells were centrifuged at 400 x g for 5 minutes and the supernatant was removed. Cells were resuspended in 1 ml of Diluent C (supplied with the Cell Linker Kit). Cell suspension was added to 1 ml PKH2 or PKH26 dye (4 μM) and mixed immediately by pipetting. The suspension was incubated at 25 °C for 4 minutes whereas the tube was frequently inverted to assure homogeneous mixing. The staining reaction was stopped by adding 2 ml of 1 % Bovine Serum Albumin (BSA). Cell suspension was diluted adding 4 ml of $DMEM^+$ and centrifuged at 400 x g for 10 minutes at 25 °C to separate cells

from staining solution. The supernatant was removed and cells were transferred into a new 15 ml falcon tube. Three washes were performed using 8 ml of $DMEM^+$ each and centrifugation at 400 x g for 10 minutes. Cells were resuspended and suspension was used in appropriate dilutions during the cell patterning procedure.

2.2.3 Preparation of Plastic Substrates. Zeonor slides (25 × 75 mm^2 in area, 1 mm in thickness) were prepared by injection molding using a Boy 30A injection tool (Dr. Boy GmbH, Neustadt-Fernthal, Germany). Zeonor® 1060R (Zeon Chemicals, Louisville, KY) was molded at a temperature of 250 to 260 °C, an injection speed of 40 mm/s and a pressure of 132 bar. The mold (stainless steel, custom-fabricated) was cooled for 15 s before the slide was released. Disks (2.3 mm in diameter) were obtained by punching Zeonor slides in manual fashion followed by washing with methanol, ethanol and deionized (DI) water (18.2 MΩ cm), respectively, to clean the surface of monomers or residual plasticizing agents. Cell culture substrates were exposed to oxygen plasma (Plasmalab80Plus, Oxford Instruments, Bristol, UK) at a pressure of 50 mTorr and a power/gas flow ratio of 40 W/sccm for 4 min. (Beaulieu, Geissler and Mauzeroll, 2009)

2.2.4 Fabrication of Membranes. Elastomeric through-hole membranes (SEBS) were fabricated from Versaflex® CL30 (GLS Corp., McHenry, IL) using a mold that was prepared by photolithography using SU-8 (GM1040, Gersteltec, Pully, Switzerland) on a 4″ silicon wafer (Silicon Quest International, Inc., Santa Clara, CA). The wafer was first baked on a hot plate at 200 °C for 10 min; SU-8 resist was applied through spin coating, which was followed by a pre-bake at 65 and 95 °C for 5 and 15 min, respectively, using a temperature ramp of 2 °C min^{-1}. Resist was exposed to UV light with a wavelength of 365 nm (Hg i-line) at 280 μJ cm^{-2} through a transparency-based photomask (FineLineImaging, Colorado Springs, CO) using a 6200 mask aligner (EV Group, Schärding, Austria). Post-exposure bake was done using the same conditions as for the pre-bake. Resist features were developed in propylene glycol monomethyl ether acetate (Sigma-Aldrich Corp., St. Louis, MO) for 2 min; the wafer was rinsed with isopropanol (Anachemia, Montréal, QC) and dried with a stream of nitrogen gas. Resultant resist pattern was hard-baked at 130 °C for 2 hrs. Finally, the master was coated with a thin, anti-

adhesive layer formed from $^{1}H,^{1}H,^{2}H,^{2}H$-perfluorooctyl-trichlorosilane (Aldrich) using deposition from the vapor phase under reduced pressure. CL30 was received in the form of pellets; the material was extruded at 165 °C to yield a film of 150 μm in thickness, which was then imprinted with the master using an EVG 520 embossing tool (EV Group) operated at 160 °C, an applied force of 1×10^{4} N, and a pressure of 1×10^{-3} mbar. All fabrication steps were carried out in a clean room environment (class 1000). Planar PDMS slabs were prepared from Sylgard 184 (Dow Corning, Midland, MI) by curing the mixed prepolymers of PDMS (elastomer base/curing agent = 10/1, w/w) on a flat polystyrene surface (Corning, Petri dish, Sigma-Aldrich) in an oven at 60 °C for 12 hrs.

2.2.5 Cell Patterning. Cell culture substrates were placed in a 30-mm Petri dish and fixed using biocompatible high vacuum grease (Dow Corning, MI, USA). 3 ml of $DMEM^{+}$ was added and bubbles were removed in a desicator by applying vacuum pressure for 15 min. Remaining bubbles were finally eliminated by pipetting $DMEM^{+}$ directly on the membrane. When a first cell suspension (HeLa-R) was added, cells attached to the free oxygen plasma spots in the SEBS membrane or on the Zeonor® slide. The sample was incubated at 37 °C, 5 % CO_2 for 18 hrs before PDMS membrane was removed. A second cell suspension (HeLa) was added and sample was incubated for 5-24 hrs at 37 °C, 5 % CO_2. In case oxygen plasma treatment of the Zeonor® slide was applied before the SEBS membrane was placed, the SEBS membrane is now removed, revealing defined cell patterns.

2.2.6 Optical and Fluorescent Imaging. Optical micrographs of platted cultured cells were acquired using an inverted microscope (Nikon Eclipse TS100, Nikon, Montreal, QC) equipped with a camera (Olympus CAMEDIA C-500 ZOOM, using Gimp 2.6). Fluorescence images were acquired using a confocal microscope.

2.2.7 Electrochemical measurements.

2.2.7.1 Electrodes. A three-electrode setup was used for voltammetry and Bio-SECM experiments with 25 μm Pt diameter laser pulled Pt working electrodes, a commercial

Ag/AgCl reference and 0.5 mm Pt auxillary. The preparation of conventional 25 μm Pt microelectrodes followed a well established fabrication protocol (Fan *et al.*, 2007, p. 189-199) while polished, needle-like microelectrodes were fabricated similar to procedures described earlier. (Mauzeroll and LeSuer, 2007, p. 199-211) The fabrication procedure specifically produces disk shaped Pt microelectrode sealed in a quartz capillary and laser pulled until a dimensionless radius of glass (RG) inferior to 10 is obtained. The RG value is defined as the isolator radius to conductor radius ratio at the tip of the microelectrode. In brief, 25 μm annealed Pt wires were pulled into quartz glass capillaries (length of 150 mm, an outer diameter of 1 mm, and an inner diameter of 0.3 mm) under vacuum with the help of a P-2000 laser pipette puller (Sutter Instruments, CA, USA). The pulling program results in the formation of a long and sharp microelectrode with a thin glass sheath, which facilitates membrane penetration. The effective radius was evaluated from steady-state voltammetry.

2.2.7.2 Electrochemical Measurements. For the measurements in $FcCH_2OH$ (1 mM dissolved in $DMEM^-$), a cyclic voltammogram was acquired by applying a potential at the microelectrode ranging from zero to 0.5 V *vs.* Ag/AgCl. A stationary current at 0.45 V *vs.* Ag/AgCl was recorded. An approach curve at a speed of 1 μm/s above plastic using a 25 μm diameter Pt microelectrode was acquired biasing the working electrode at 0.45 V *vs.* Ag/AgCl. The same potential was applied at the electrode to obtain an electrochemical image of the $FcCH_2OH$ oxidation to $[FcCH_2OH]^+$ while scanning across an area containing three patterned HeLa cells, when cells were exposed 10 minutes to $FcCH_2OH$. Finally the microelectrode was rastered across a 200 x 300 μm area applying a 0.45 V *vs.* Ag/AgCl potential to record an electrochemical image of patterned HeLa cells.

2.3 Results and Discussion

In order to study multiple cell types using Biological Scanning Electrochemical Microscopy (Bio-SECM), a novel protocol was developed enabling cell patterning in a variety of shapes.

Figure 2.1 describes a newly established cell patterning procedure that allows controlling cancer cell growth *in vitro* and thus making single cell studies much easier and more precise. This novel technique employs a new kind of polymer membrane (SEBS membrane) as well as Zeonor® slides treated in oxygen plasma, whereby the introduction of oxygen surface functionalities promote cell attachment. (Beaulieu, Geissler and Mauzeroll, 2009) The SEBS membrane is made from Versaflex CL30, a styrenic ethylene/butylene block-copolymer, which has recently been introduced for microfabrication and patterning. (Geissler *et al.*, 2009a; Geissler *et al.*, 2009b) This elastomer provides a convenient and low-cost alternative to PDMS that is commonly used in cell patterning procedures. (Goubko and Cao, 2009) For example, its thermoplastic nature makes it possible to produce thin-film membranes that can support small-scale openings while retaining mechanical stability, promoting release from the mold without damage as well as convenient handling and manipulation. Furthermore the SEBS membrane adheres better than PDMS to a plastic substrate or to other membranes as used in the co-culturing protocol. The SEBS membrane contains circular openings, ranging from 500 to 50 μm in diameter to produce cell islands in different sizes resulting from holes in the membrane. The presented protocol has to be adjusted to each cell line according to their morphology and growth nature. For example, HeLa cells are more efficiently patterned using a SEBS membrane that is not treated with oxygen plasma and placed on the treated Zeonor® slide (Fig 2.1 a). A better choice, in case of the HeLa-R cells, is a SEBS membrane that was treated together with the Zeonor® slide (Fig 2.1 b), because of their tendency to grow in colonies.

Following the described protocol, HeLa cells (Fig 2.2 a) as well as HeLa-R cells (2.2 b) can be successfully patterned in different dimensions. Membrane holes ranging from 500 to 200 μm diameter allow cell growth in defined islands whereas holes of 50 μm diameter result in single cell patterning or groups of 2 to 6 cells. This defined physical separation of cells gives rise to new controllable experimental parameters for studies, such as cell communication or cell signalling, but also observation of cell death and the cell's response to drugs or other medical treatments. Patterning of cancer cells in such an effective way is currently unique and will open new possibilities in developmental and cell biology as well as in cancer research. This procedure is also applicable for other cancer cell lines than HeLa, such as the Gliablastoma cancer cells U87 (Fig 2.3). In this case, it is recommended to use a

SEBS membrane that was treated together with the Zeonor® slide and removed before exposing it to the cell suspension (Fig 2.1, b). As shown in Figure 2.4, the patterns, obtained using a treated membrane, are stable at least 48 hrs, due to the sharp boarders of the substrate treated or untreated with oxygen plasma. Cells are moving (Fig 2.4 a, white arrow) and dividing (Fig 2.4 b, black arrow) within the oxygen plasma treated spots. Outside of the pattern area cells have to hold on to each other to be able to survive (Fig. 2.4 c, orange arrow). If a cell is too far from an island, it is not able to grow and detaches from the surface (Fig. 2.4 c, green arrow).

The presented results already display how defined the newly established material and protocol can be applied. Another important feature of this protocol is the ability to pattern co-cultures. In the past other patterning techniques had been developed allowing co-culturing (Goubko and Cao, 2009); single cell patterning, however, remains inefficient, not well defined or the unnatural morphology of the patterned cells suggests altered development or metabolism of the cells. Additionally no co-pattern of single cells has been achieved. (Cheng, Li and Komvopoulos, 2009; Hu *et al.*, 2010; Irimia and Karlsson, 2003; Ishizaki, Saito and Takai, 2010; Jin *et al.*, 2009; Mercey *et al.*, 2010) In order to pattern HeLa and Hela-R cells on the same substrate, a SEBS membrane was used, treated with oxygen plasma together with the Zeonor® slide and without removing the SEBS membrane after the plasma treatment. PDMS membranes were used to cover spots partially or completely before adding a suspension of HeLa-R cells. Cells attached to the free oxygen plasma spots in the SEBS membrane during incubation. When HeLa-R cells reached a sufficient confluence the PDMS membrane was removed. A HeLa cell suspension was added and after another incubation period co-pattern could be observed. As shown in Figure 2.5 a, HeLa (red) and HeLa-R (green) can be co-cultured in separate islands or even in divided islands (Fig 2.5 b). This technique will allow the precise comparison of cells of different types using electrochemical techniques, such as Bio-SECM, since different cells can now be studied at the same time and under the same conditions.

Bio-SECM is a promising technique to allow studies of living cells by their characteristics, such as multidrug resistance. (Kuss *et al.*, 2011) A variety of cell lines has been analyzed by Bio-SECM (Bard, Li and Zhan, 2006; Bauermann, Schuhmann and Schulte, 2004; Kaya *et al.*, 2003; Li and Bard, 2009; Liu, Rotenberg and Mirkin, 2000;

Mauzeroll and Bard, 2004; Mauzeroll *et al.*, 2004; Saito *et al.*, 2006) and a defined patterning of target cells, such as single cell patterns, will open the door for analytical studies using Bio-SECM even wider. To perform first measurements on patterned HeLa cells a cyclic voltammogram was generated to characterize the working electrode and to obtain the stationary current depending on the electrode and involved redox mediator, here ferrocenemethanol ($FcCH_2OH$) (Fig 2.6 a). Therefore a potential ramp of zero to 0.5 V *vs.* Ag/AgCl was applied at the 25 µm diameter Pt microelectrode, oxidizing $FcCH_2OH$ to its cation $[FcCH_2OH]^+$. The current as a measure of the oxidation rate is recorded showing a stationary current at about 0.45 V *vs.* Ag/AgCl (Fig 2.6 a). To further position the electrode, the Zeonor® slide was approached at a speed of 0.5 µm/sec (Fig 2.6 b). During this approach $FcCH_2OH$ continuously reacts at the tip of the microelectrode, while the reaction rate is determined by the flux of $FcCH_2OH$ to the active surface of the tip. By approaching the Zeonor® slide the current decreases, since the diffusion process is hindered by the presence of the substrate (Fig 2.6 b, scheme). Once the microelectrode is positioned above a sample an electrochemical image can be created, by rastering in constant height mode across an area, showing the reactivity depending on the nature of the substrate as shown in Figure 2.7. The 25 µm diameter Pt microelectrode was scanned across a patterned area containing three HeLa cells with an initial tip to substrate distance of 20 µm (Fig 2.7 a). A 0.45 V *vs.* Ag/AgCl potential was applied and the electrode was positioned next to the cells. The response in current is shown in Figure 2.7 b when the cells were exposed to $FcCH_2OH$ for 10 min (blue). A decrease in current is observed every time the microelectrode passes over a cell. This decrease in current is not considered as pure negative feedback, which is defined as the approach of an insulator, nor is it considered as real positive feedback, described as the approach of a conductor. In this case an intermediate situation is presented. The current decreases, because of the hindered diffusion of the $FcCH_2OH$, but it was also shown that cells are able to regenerate $FcCH_2OH$ within the first 30 min of exposure to this redox mediator, resulting in an increase in current. (Kuss *et al.*, 2011) In the presented experiment (Fig 2.7 b, blue) both events seem to take place concurrently. If it was pure negative feedback, the decrease in current was expected to be the same at 10 min of cell's exposure to $FcCH_2OH$ as at 90 min. Figure 2.7 b, red shows a less intense decrease when the electrode was scanned above the same sample after 90 min cell's exposure to $FcCH_2OH$. This decrease in response

is observed although the initial tip to substrate distance was reduced to 12 µm, affirming the contribution of the regeneration reaction in the observed signal.

Demonstrating the imaging capabilities of Bio-SECM, an electrochemical image of patterned HeLa cells in presence of $FcCH_2OH$ was acquired (Fig 2.8). In the above mentioned configuration, the microelectrode is rastered across the HeLa cells (Fig. 2.8 a and b). As shown in the 2D-Contour-Plot (Fig 2.8 c) and in the 3D-Plot (Fig 2.8 d) of the Bio-SECM electrochemical image of the $FcCH_2OH$ oxidation, a decrease in the recorded current was observed, when the microelectrode passes a HeLa cell. These images illustrate the usefulness of cell patterning for Bio-SECM measurements. The obtained patterning strategies lower the risk to interfere with the cell's normal metabolism severely, since the instrumental set up and validation process of the experiment requires less time.

One has to underline that the use of constant height mode in Bio-SECM studies constitutes one major disadvantage. The presence of a slope of the substrate, although possible to be corrected computationally to some extent, cannot be avoided experimentally. That means, as shown in Figure 2.7 b, a consistent loss of signal intensity is obtained due to the increasing distance between microelectrode tip and substrate. This problem can be approached performing measurements using Constant Distance Mode during Bio-SECM studies. At Constant Distance Mode the electrode keeps the same distance from the surface when rastered across a sample. This technique allows coupling of information about topography and reactivity of the sample depending on the nature of the substrate and will therefore be most meaningful in future bioanalytical research. This technique is currently under development and first studies on living cells emerged. (Kurulugama *et al.*, 2005; Etienne *et al.*, 2006; Katemann, Schulte and Schuhmann, 2003; Katemann, Schulte and Schuhmann, 2004; Lee, Ding and Bard, 2002)

2.4 Conclusion

The establishment of the presented cell patterning protocol is a major step towards precise Bio-SECM measurements on cancer cells, since it allows the controlled growth of different cell lines for several days. Multiple cell lines have been successfully patterned in

different sizes and shapes. The patterning of single cells has a great potential to impact future research in developmental and cell biology as well as in cancer research, since it allows studies on a single cell basis that might lead to analyzes of a variety of cancer cell's characteristics, such as multidrug resistance. Even more importantly, the resulting co-cultures allow the direct comparison of cell lines and use of one cell line as standard during experiments. The invasion capacity of one cancer type or the comparison of cell lines by their response to stress, drugs or other medical treatments are just a few examples how the presented study could be used in future bioanalytical research.

Acknowledgement. The authors acknowledge the Natural Sciences and Engineering Research Council of Canada (NSERC) and the Canadian Foundation for Innovation (CFI) for their financial support. We thank Dr. Philippe Gros (McGill University, Montreal) for providing the MRP1 overexpressing variant of the HeLa cells. The technical contribution of Denis Flipo and Chistian Kuss is also acknowledged.

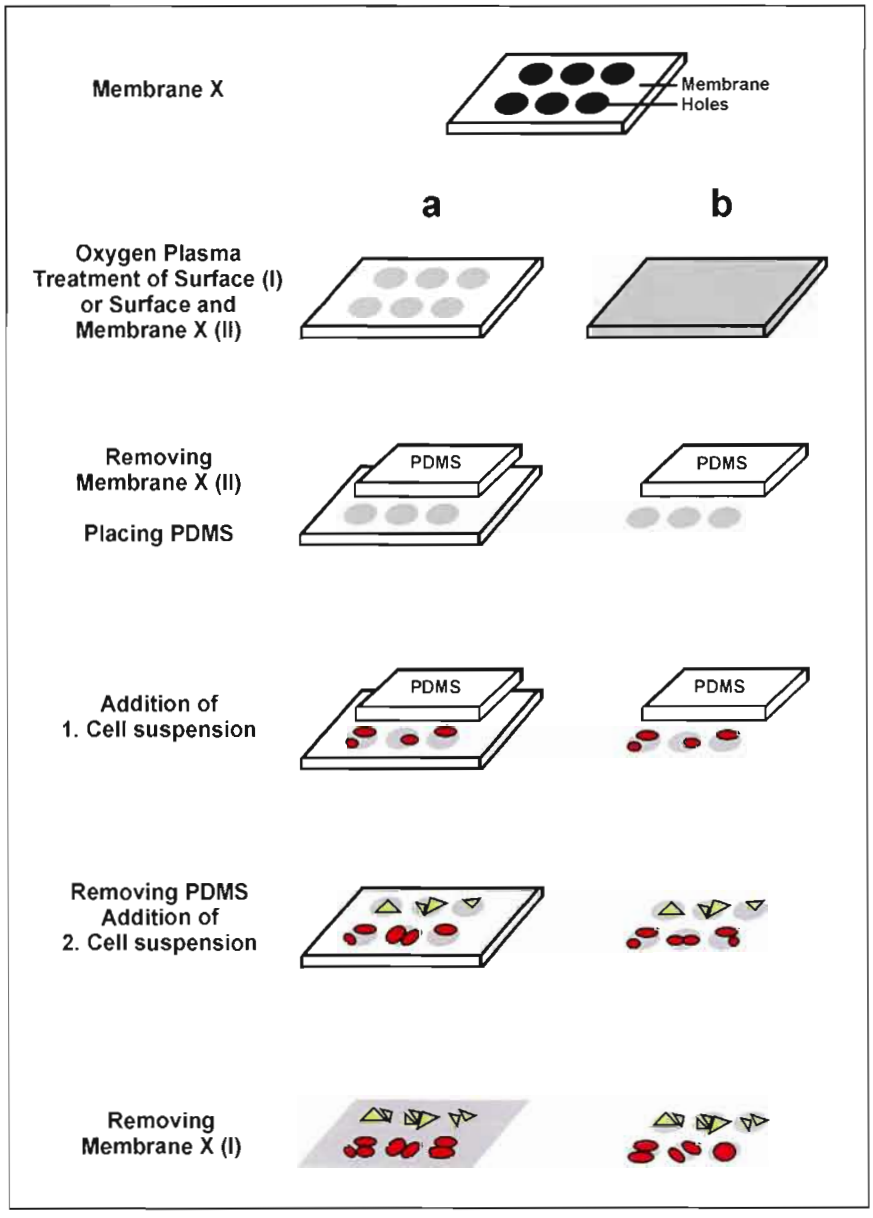

Figure 2.1 Schematic representation of two cell patterning procedures. A Zeonor® slide is treated with oxygen plasma before (b) or after (a) the SEBS membrane is placed. Using a PDMS membrane, holes (a) or plasma spots (b) are covered. A first cell suspension is added and incubated for at least 12 hrs. After removing PDMS a second cell suspension can be added and is incubated for 12 to 24 hrs. The SEBS membrane is removed (a) and cell patterns are revealed.

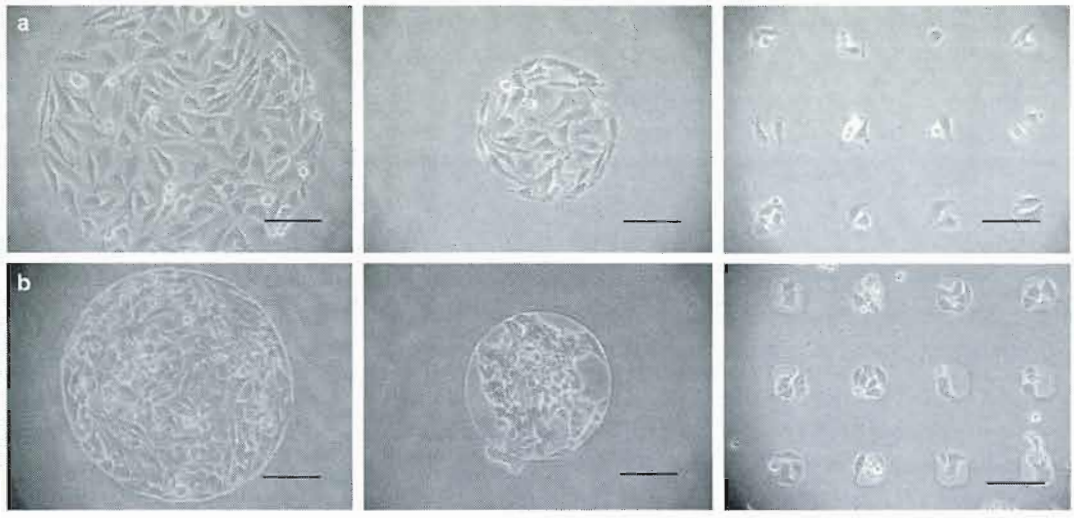

Figure 2.2 Optical micrographs of cell patterns. (a) HeLa and (b) HeLa-R in 500 μm islands (left panels), in 200 μm islands (middle panels) and 50 μm islands (right panels). Scale bar in all micrographs corresponds to 100 μm.

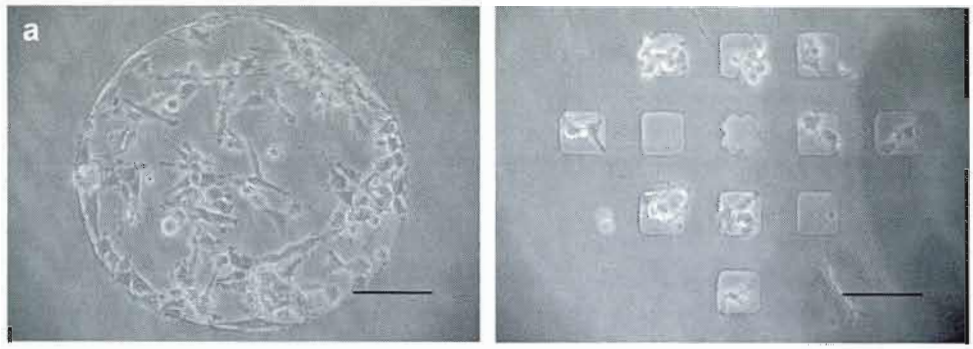

Figure 2.3 Optical micrographs of U87 cell patterns. Scale bar in all micrographs corresponds to 100 μm.

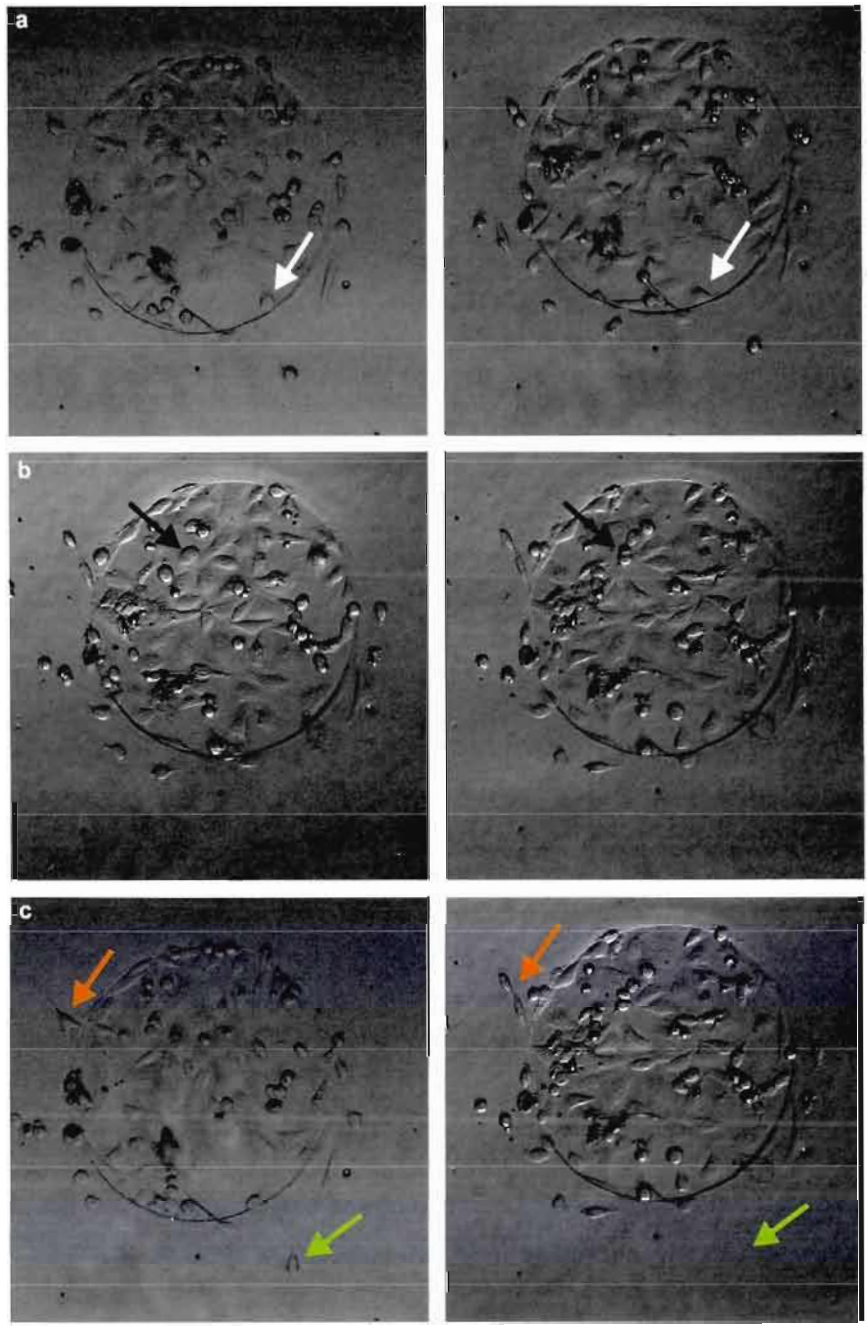

Figure 2.4 Optical micrographs of HeLa cells patterned in an oxygen plasma spot. Images were taken from a time lap video of 48 hrs. Arrows indicate one example of each characteristic. (a) Cells are moving and (b) dividing within the pattern. (c) Outside of the oxygen plasma treated area cells have to hold on to each other (orange arrow), otherwise they detach from the surface (green arrow).

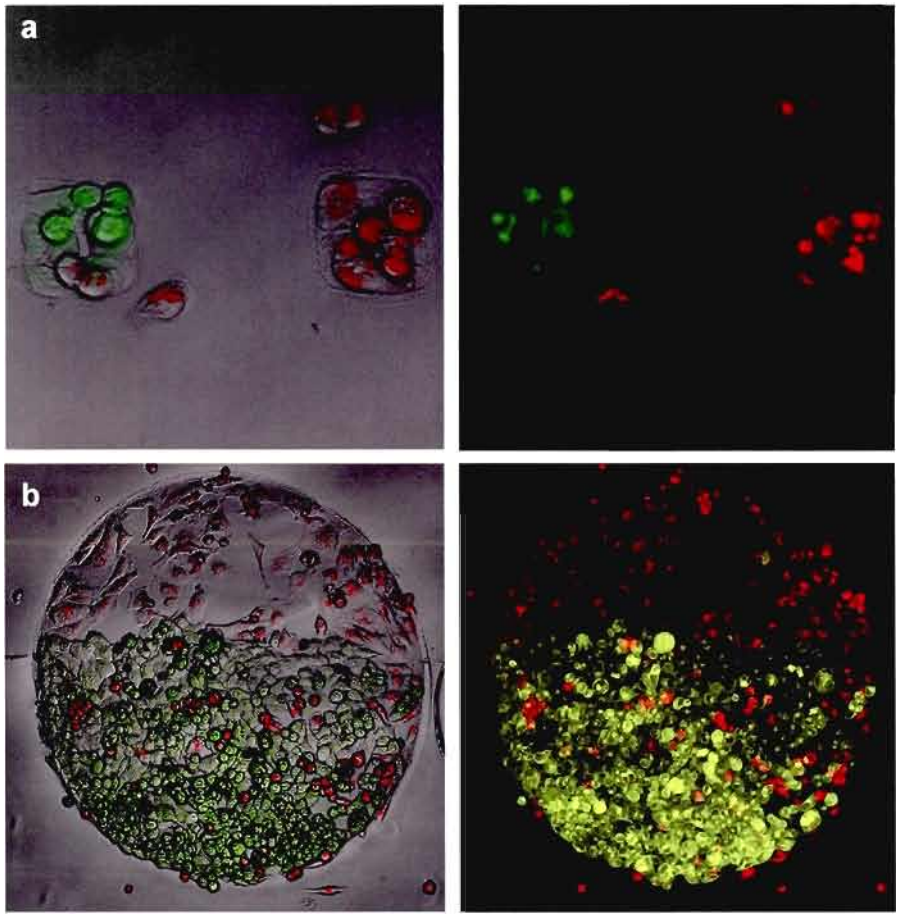

Figure 2.5 Optical micrographs of Hela and HeLa-R cell patterns in co-culture obtained by confocal microscopy. Cell lines were stained with PKH2 (green, HeLa-R) and PKH26 (red, HeLa) respectively. (a) 50 μm and (b) 500 μm oxygen plasma spots containing both cell lines.

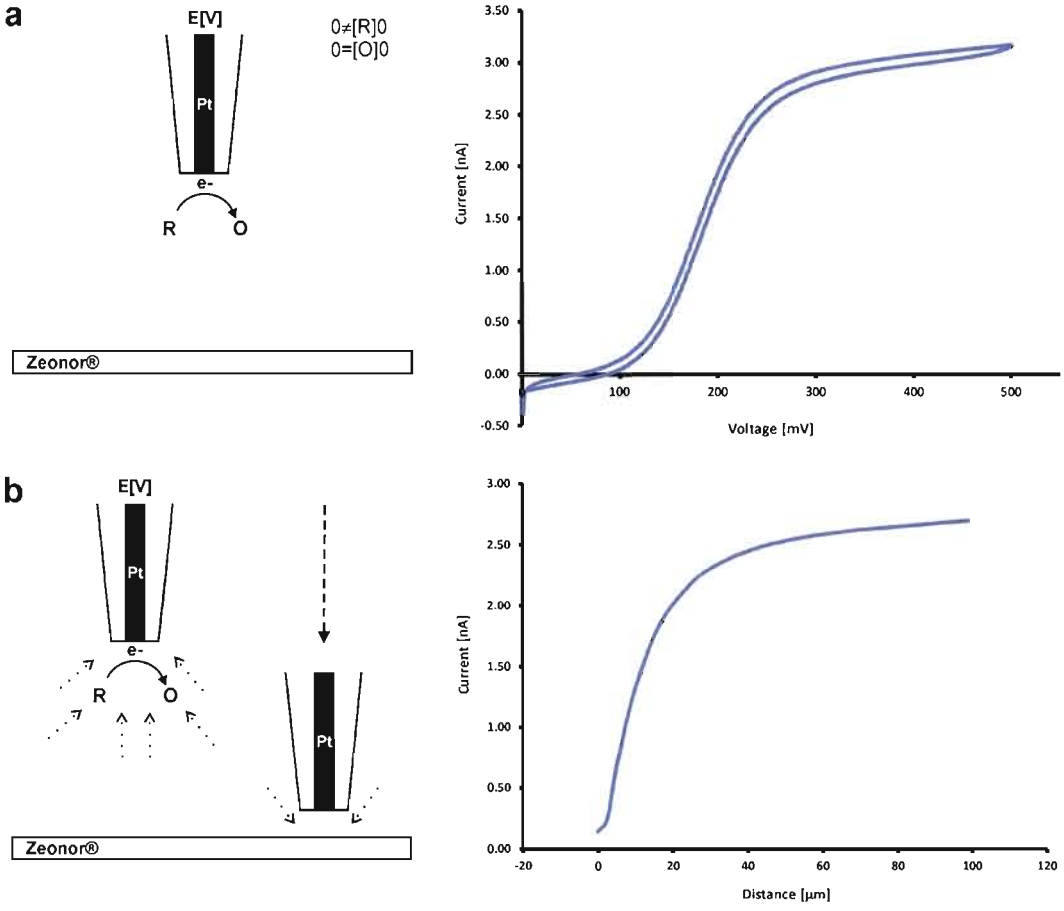

Figure 2.6 Preparation of SECM measurements of patterned cells. (a) Cyclic voltammogram showing the oxidation of $FcCH_2OH$ to $[FcCH_2OH]^+$ at a 25 µm diameter Pt microelectrode by applying a potential of zero to 0.5 V *vs.* Ag/AgCl. (b) Approach curve in $FcCH_2OH$ 1 mM above plastic. A decrease in current is observed due to the lowered diffusion (dotted arrows) of $FcCH_2OH$ to the electrode when approaching the substrate.

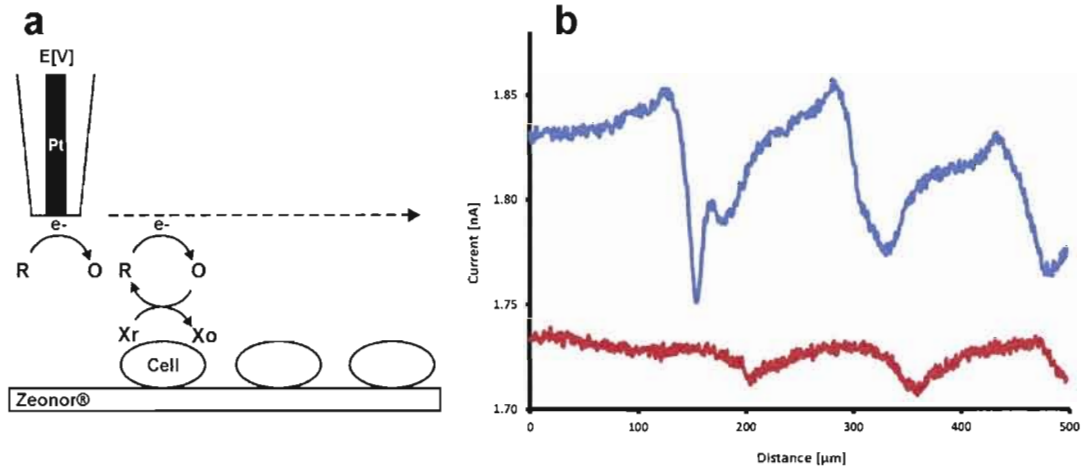

Figure 2.7 Bio-SECM line scan above three HeLa cells. (a) Schematic representation of electrochemical measurement. A potential of 0.45 V *vs.* Ag/AgCl was applied at the 25 µm diameter Pt microelectrode to oxidize $FcCH_2OH$ to $[FcCH_2OH]^+$ above the cells. (b) Diagram showing response in current 20 µm above substrate when cells were exposed for 10 min to $FcCH_2OH$ (blue) and 12 µm above substrate when cells were exposed for 90 min to $FcCH_2OH$ (red).

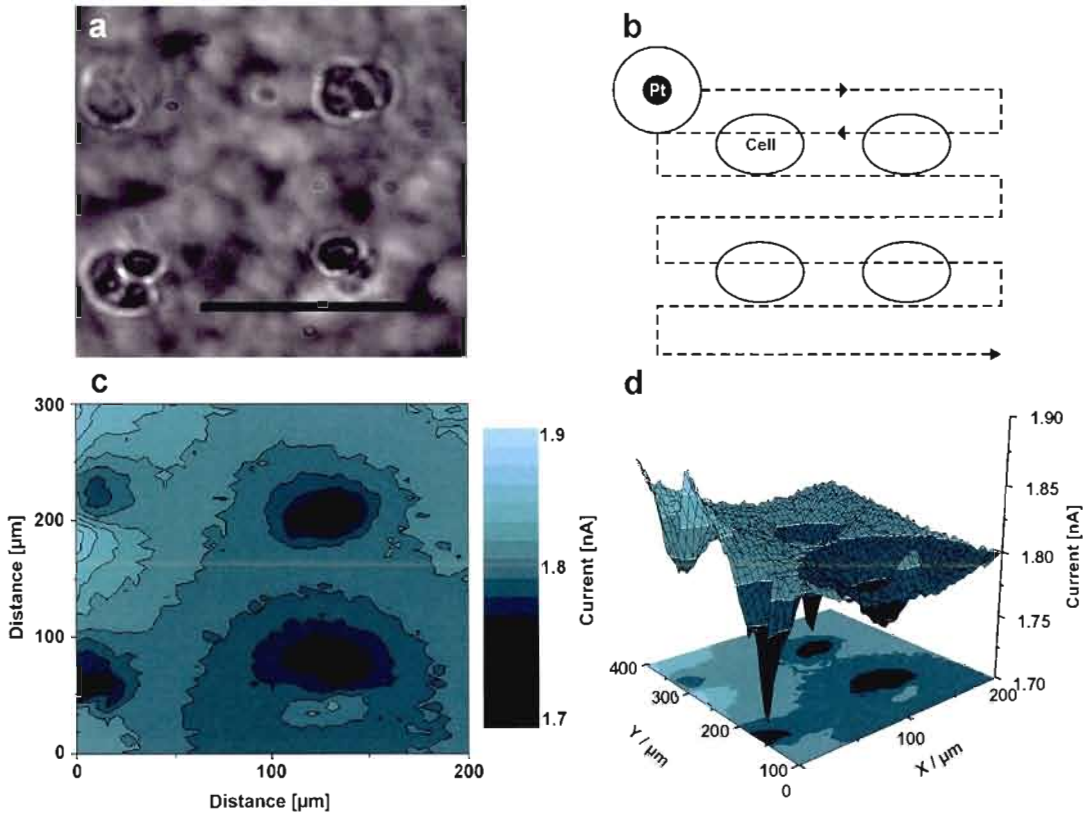

Figure 2.8 Bio-SECM electrochemical image of a HeLa cell pattern. (a) Optical micrograph 2 hrs after electrochemical measurements of the analyzed patterned region. Scale bar corresponds to 100 µm. (b) Schematic representation in top view of Bio-SECM measurement. (c) 2D Contour-Plot and (d) 3D-Plot of Bio-SECM electrochemical image of $FcCH_2OH$ 1 mM oxidation above HeLa cells. A potential of 0.45 V *vs.* Ag/AgCl was applied at the 25 µm diameter Pt microelectrode to oxidize $FcCH_2OH$ to $[FcCH_2OH]^+$.

2.5 References

Bard, Allen J., Xiao Li and Wei Zhan. 2006. Chemical imaging living cells by scanning electrochemical microscopy. *Biosensors and Bioelectronics,* vol. 22, no. 4, p. 461-472.

Bauermann, Luciana Pitta, Wolfgang Schuhmann and Albert Schulte. 2004. An Advanced Biological Scanning Electrochemical Microscope (Bio-SECM) for Studying Individual Living Cells. *Physical Chemistry Chemical Physics,* vol. 6, p. 4003-4008.

Beaulieu, Isabelle, Matthias Geissler and Janine Mauzeroll. 2009. Oxygen Plasma Treatment of Polystyrene and Zeonor: Substrates for Adhesion of Patterned Cells. *Langmuir,* vol. 25, p. 7169-7176.

Carter, Stephen B. 1965. Principles of cell motility: The direction of cell movement and cancer invasion. *Nature,* vol. 208, no. 5016, p. 1183-1187.

Carter, Stephen B. 1967. Haptotaxis and the mechanism of cell motility. *Nature,* vol. 213, no. 5073, p. 256-260.

Carter, Stephen B. 1967. Haptotactic islands. A method of confining single cells to study individual cell reactions and clone formation. *Experimental Cell Research,* vol. 48, no. 1, p. 189-193.

Cheng, Qian, Song Li and Kyriakos Komvopoulos. 2009. Plasma-assisted surface chemical patterning for single-cell culture. *Biomaterials,* vol. 30, no. 25, p. 4203-4210.

Csucs, Gabor, Roger Michel, Jost W. Lussi, Marcus Textor and Gaudenz Danuser. 2003. Microcontact printing of novel co-polymers in combination with proteins for cell-biological applications. *Biomaterials,* vol. 24, no. 10, p. 1713-1720.

Etienne, Mathieu, Emily C. Anderson, Stephanie R. Evans, Wolfgang Schuhmann and Ingrid Fritsch. 2006. Feedback-Independent Pt Nanoelectrodes for Shear Force-Based Constant-distance Mode Scanning Electrochemical Microscopy. *Analytical Chemistry,* vol. 78, no. 20, p. 7317-7324.

Fan, Fu-Ren F., Jose Fernandez, Biao Liu, Janine Mauzeroll and Cynthia G. Zoski. 2007. «Platinum and gold inlaid disks ≥ 5μm diameter». In *Handbook of Electrochemistry,* Cynthia G. Zoski, p. 189-199. Amsterdam: Elsevier B.V.

Folch, Albert, Byung-Ho Jo, Octavio Hurtado, David J Beebe and Mehmet Toner. 2000. Microfabricated elastomeric stencils for micropatterning cell cultures. *Journal of biomedical materials research,* vol. 52, no. 2, p. 346-353.

Geissler, Matthias, Emmanuel Roy, Gerardo A. Diaz-Quijada, Jean-Christophe Galas and Teodor Veres. 2009. Microfluidic Patterning of Miniaturized DNA Arrays on Plastic Substrates. *ACS Applied Materials & Interfaces,* vol. 1, no. 7, p. 1387-1395.

Geissler, Matthias, Emmanuel Roy, Jean-Sebastien Deneault, Melanie Arbour, Gerardo A. Diaz-Quijada, Andre Nantel and Teodor Veres. 2009. Stretching the Stamp: A Flexible Approach to the Patterning of Miniaturized DNA Arrays. *Small,* vol. 5, no. 22, p. 2514-2518.

Goubko, Catherine A. and Xudong Cao. 2009. Patterning multiple cell types in co-cultures: A review. *Materials Science and Engineering: C,* vol. 29, no. 6, p. 1855-1868.

Horan, Paul K. and Sue E. Slezak. 1989. Stable cell membrane labelling. *Nature,* 1989. 340: p. 167-168.

Hu, Jie, Jian Shi, Fan Zhang, Lei Lei, Xin Li, Li Wang, Li Liu and Yong Chen. 2010. High resolution and hybrid patterning for single cell attachment. *Microelectronic Engineering,* vol. 87, no. 5-8, p. 726-729.

Irimia, Daniel and Jens O. M. Karlsson. 2003. Development of a cell patterning technique using poly(ethylene glycol) disilane. *Biomedical Microdevices,* vol. 5, no. 3, p. 185-194.

Ishizaki, Takahiro, Nagahiro Saito and Osamu Takai. 2010. Correlation of cell adhesive behaviors on superhydrophobic, superhydrophilic, and micropatterned superhydrophobic/superhydrophilic surfaces to their surface chemistry. *Langmuir,* vol. 26, no. 11, p. 8147-8154.

Jin, Li H., Bing Y. Yang, Li Zhang, Pei L. Lin, Chen Cui and Jing Tang. 2009. Patterning of HeLa cells on a microfabricated au-coated ITO substrate. *Langmuir,* vol. 25, no. 9, p. 5380-5383.

Kane, Ravi S., Shuichi Takayama, Emanuele Ostuni, Donald E. Ingber and George M. Whitesides. 1999. Patterning proteins and cells using soft lithography. *Biomaterials,* vol. 20, p. 2363-2376.

Kast, Christina and Philippe Gros. 1998. Epitope Insertion Favors a Six Transmembrane Domain Model for the Carboxy-Terminal Portion of the Multidrug Resistance-Associated Protein. *Biochemistry,* vol. 37, no. 8, p. 2305-2313.

Katemann, Bernardo B., Albert Schulte and Wolfgang Schuhmann. 2003. Constant-Distance Mode Scanning Electrochemical Microscopy (SECM) - Part I: Adaptation of a non-Optical Shear-Force-Based Positionning mode for SECM Tips. *Chemistry: A European Journal,* vol. 9, p. 2025-2033.

Katemann, Bernardo B., Albert Schulte and Wolfgang Schuhmann. 2004. Constant-Distance Mode Scanning Electrochemical Microscopy. Part II: High-Resolution SECM Imaging Employing Pt Nanoelectrodes as Miniaturized Scanning Probes. *Electroanalysis,* vol. 16, no. 1-2, p. 60-65.

Kaya, Takatoshi, Yu-suke Torisawa, Daisuke Oyamatsu, Matsuhiko Nishizawa and Tomokazu Matsue. 2003. Monitoring the Cellular Activity of a Cultured Single Cell by Scanning Electrochemical Microscopy (SECM). A Comparison with Fluorescence Viability Monitoring. *Biosensors and Bioelectronics,* vol. 18, p. 1379-1383.

Kleinfeld, David, Kristian H. Kahler and Philip E. Hockberger. 1988. Controlled outgrowth of dissociated neurons on patterned substrates. *Journal of Neuroscience,* vol. 8, no. 11, p. 4098-4120.

Kurulugama, Ruwan T., David O. Wipf, Sara A. Takacs, Sirinun Pongmayteegul, Paul A. Garris and John E. Baur. 2005. Scanning electrochemical microscopy of model neurons: Constant distance imaging. *Analytical Chemistry,* vol. 77, no. 4, p. 1111-1117.

Kuss, Sabine, Isabelle Beaulieu, Mohammed A. Mezour, Borhane Annabi and Janine Mauzeroll. 2011. Multidrug Resistance Assessment using Biological Scanning Electrochemical Microscopy. *Submitted to Bioelectrochemistry*. BIOELECHEM-D-10-00231R1

Lahann, Jörg, Insung S. Choi, Jinwook Lee, Klavs F. Jensen and Robert Langer. 2001. A new method toward microengineered surfaces based on reactive coating. *Angewandte Chemie - International Edition,* vol. 40, no. 17, p. 3166-3169.

Lee, Youngmi, Zhifeng Ding and Allen J. Bard. 2002. Combined Scanning Electrochemical/Optical Microscopy with Shear Force and Current Feedback. *Analytical Chemistry,* vol. 74, no. 15, p. 3634-3643.

Li, Xiao and Allen J. Bard. 2009. Scanning electrochemical microscopy of HeLa cells–Effects of ferrocene methanol and silver ion. *Journal of Electroanalytical Chemistry,* vol. 628, no. 1-2, p. 35-42.

Liu, Biao, Susan A. Rotenberg, and Micheal V. Mirkin. 2000. Scanning electrochemical microscopy of living cells: Different redox activities of nonmetastatic and metastatic human breast cells. *Proceedings of the National Academy of Sciences,* vol. 97, no. 18, p. 9855-9860.

Liu, Wendy F. and Christopher S. Chen. 2005. Engineering biomaterials to control cell function. *Materials Today,* vol. 8, no. 12, p. 28-35.

Mauzeroll, Janine and Allen J. Bard. 2004. Scanning electrochemical microscopy of menadione-glutathione conjugate export from yeast cells. *Proceedings of the National Academy of Sciences,* vol. 101, no. 21, p. 7862-7867.

Mauzeroll, Janine, Allen J. Bard, Omeed Owhadian and Terrence J. Monks. 2004. Menadione metabolism to thiodione in hepatoblastoma by scanning electrochemical microscopy. *Proceedings of the National Academy of Sciences,* vol. 101, no. 51, p. 17582-17587.

Mauzeroll, Janine and Robert J. LeSuer. 2007. «Laser-pulled ultramicroelectrodes». In *Handbook of Electrochemistry,* 2007, Cynthia G. Zoski, p. 199-211. Amsterdam: Elsevier B.V.

Mercey, Emilie, Patricia Obeïd, Denise Glaise, Maria-Luisa Galvo-Munoz, Christiane Guguen-Guillouzo and Brigitte Fouqué. 2010. The application of 3D micropatterning of agarose substrate for cell culture and in situ comet assays. *Biomaterials,* vol. 31, no. 12, p. 3156-3165.

Saito, Takeshi, Ching-Chou Wu, Hitoshi Shiku, Tomoyuki Yasukawa, Masaki Yokoo, Takashi Ito-Sasaki, Hiroyuki Abe, Hiroyoshi Hoshi and Totokazu Matsue. 2006. Oxygen consumption of cell suspension in a poly (dimethylsiloxane)(PDMS) microchannel estimated by scanning electrochemical microscopy. *The Analyst,* vol. 131, no. 9, p. 1006-1011.

Singhvi, Rahul, Amit Kumar, Gabriel P. Lopez, Gregory N. Stephanopoulos, Daniel I. C. Wang, George M. Whitesides and Donald E. Ingber. 1994. Engineering cell shape and function. *Science,* vol. 264, no. 5159, p. 696-698.

Souslova, Tatiana and Diana A. Averill-Bates. 2004. Multidrug-resistant hela cells overexpressing MRP1 exhibit sensitivity to cell killing by hyperthermia: Interactions with etoposide. *International Journal of Radiation Oncology Biology Physics,* vol. 60, no. 5, p. 1538-1551.

Tan, John L., Wendy Liu, Celeste M. Nelson, Srivatsan Raghavan and Christopher S. Chen. 2004. Simple approach to micropattern cells on common culture substrates by tuning substrate wettability. *Tissue engineering,* vol. 10, no. 5-6, p. 865-872.

Tourovskaia, Anna, Thomas Barber, Bronwyn T. Wickes, Danny Hirdes, Boris Grin, David G. Castner, Kevin E. Healy and Albert Folch. 2003. Micropatterns of chemisorbed cell adhesion-repellent films using oxygen plasma etching and elastomeric masks. *Langmuir,* vol. 19, no. 11, p. 4754-4764.

Xia, Younan and George M. Whitesides. 1998. Soft lithography. *Annual Review of Materials Science,* vol. 28, no. 1, p. 153-184.

CHAPTER III

PROSPECT: TOWARDS A CONSTANT DISTANCE MODE USING A TAPPING APPROACH

The previous chapter describes the patterning of different cell types in order to improve electrochemical studies on biological samples, such as cancer cells, using the technique of Biological Scanning Electrochemical Microscopy. Successful positioning of cells in islands, small groups or even single cells have been performed, furthermore allowing co-pattern of multiple cell lines on the same substrate. However, positioning of cells under the microscope is not the only challenge, also the electrode positioning during scanning can be improved.

The following chapter presents preliminary studies for another approach to make Bio-SECM analysis more precise and efficient by controlling the substrate to electrode tip distance. Therefore a constant distance mode is adapted using a vibrating microelectrode that is scanned over a sample in a tapping manner. The vibration modulation close to the substrate, due to the increased viscosity of the medium is therefore monitored. The established constant distance mode is tested on different substrates, including soft samples, such as cells.

The presented results indicate the usefulness of the constant distance mode in Bio-SECM studies, since it overcomes the disadvantage of the constant height mode by gathering topography information, including the inevitable slope of the substrate. The coupling of information about topography and reactivity of the substrate will therefore lead to a reliable procedure for quantifying reactivity measurements on cells.

3.1 Introduction

3.1.1 Principle of shear force distance control

Biological Scanning Electrochemical Microscopy (Bio-SECM) has a great potential to impact future medical and bioanalytical research. (Amemiya *et al.*, 2006; Bard, Li, Zhan, 2006; Bauermann, Schuhmann and Schulte, 2004; Kaya *et al.*, 2003; Li and Bard, 2009; Liu, Rotenberg and Mirkin, 2000; Kuss *et al.*, 2011) The accuracy and precision of this electrochemical technique, however, is limited depending on the abilities of the executing machine and software. To overcome disadvantages of the well known and applied constant height mode during Bio-SECM measurements, a shear force based constant distance mode was introduced to the field of Scanning Electrochemical Microscopy (SECM) in 2000 (Hengstenberg, Kranz and Schuhmann, 2000) and shortly after combined with functional electrodes in SECM. (Lee, Ding and Bard, 2002) This constant distance method was adopted from near field scanning optical microscopy (NSOM), where it was first introduced in 1992 to control the probe to sample distance. While the underlying principles of NSOM and SECM are very different, they both are scanning probe microscopy techniques and the use of this type of probe to sample distance control can be used in a very similar manner. In the shear force technique the increasing shear force acting between the medium and the probe in close proximity to the sample surface is used as a feedback signal to control the probe to sample distance. (Dunn, 1999) The probe is always stimulated to a vibration but the detection of the vibration dampening varies, including the use of a tuning fork or a focused laser beam. (Beaulieu *et al.*, 2010) In the presented work the electrode is stimulated to a vibration by a dither piezo, while a receiver piezo records the electrodes vibration. Although in the first SECM studies a group of algae was successfully imaged using constant-current mode, (Lee, Ding and Bard, 2002) the topographic imaging in constant distance mode remains a challenge.

In the following years more and more adaptations of the shear force based constant distance emerged. (Etienne *et al.*, 2006; Katemann, Schulte and Schuhmann, 2003; Katemann, Schulte and Schuhmann, 2004; Kurulugama *et al.*, 2005) A significant

improvement in SECM imaging was achieved by Kurulugama and colleages (Kurulugama *et al.*, 2005) by imaging neuron cells by regulating the distance using either constant-current mode or constant-impedance mode. In both approaches no shear force is detected but the response of the ions in solution. The main disadvantage of the constant-current mode is the need for a redox mediator that can be detected independently from the other species in the solution and that does not interact or pass into the cell. Constant-impedance mode shows promising results, however here, too, topological and reactivity information is collected electrochemically. Resulting high-resolution images of neurons display and underline the potential of Bio-SECM studies in the future. In order to decouple information about topography from non-electrochemical measurements with the electrochemical reactivity of a biological substrate the shear force constant distance mode was adapted in the presented study. Our goal is the specific analysis of different cell lines in the future.

3.1.2 Tapping approach

Figure 3.1 shows a schematic representation of the constant distance mode for Bio-SECM studies using a tapping approach. Therefore a 5 µm diameter Pt microelectrode is positioned 10 µm above the plastic surface, vibrating in response to stimulation by a dither piezo. The microelectrode is rastered horizontally at a speed of 0.5 µm/sec above a sample, tapping down in a chosen resolution, ranging from 0.1 to 5 µm (Fig. 3.1 dotted line). Thereby the tip always stops at the same distance above the surface, due to a change of the electrode vibration, recorded by a receiver piezo. Those measurement points are collected by software that generates an image as if the microelectrode is scanned over a sample always keeping the same distance to the surface (Fig. 3.1 dashed line). This technique allows decoupling of information about topography and reactivity of the sample depending on the nature of the substrate.

3.2 Experimental Section

3.2.1 Cell culture. All products were purchased from Sigma-Aldrich (ON, Canada) if not indicated differently. HeLa (CCL-2, American Type Culture Collection, VA, USA) were grown in Dulbecco's Modified Eagle's Medium (DMEM high glucose, HyClone, UT, USA)

completed with 10 % v/v heat inactivated fetal bovine serum (Gibco/Invitrogen, ON, Canada), 2 mM glutamine, 25 mM 4-(2-Hydroxyethyl)piperazine-1-ethanesulfonic acid (HEPES), penicillin and streptomycin (50 units/ml) (HYQ HyClone, UT, USA), which was used as basic medium ($DMEM^+$). Cells were maintained in tissue culture flasks (Sarstedt Inc, QC, Canada) at 37 °C and 5 % CO_2 using a CO_2/Multi-gas incubator (Sanjo Scientific, Japan). Cells, ranging from 70 % to 90 % confluence, were washed with 37 °C phosphate-buffered saline (PBS) (pH 7.4 at 25 °C) and harvested with 37 °C 0.25 % v/v Trypsin-EDTA solution (10x, 2.0 g EDTA, in 0.9 wt% NaCl). 500.000 cells were seeded into a 30-mm Petri dish containing a plastic substrate, fixed using biocompatible high vacuum grease (Dow Corning, MI, USA). For the electrochemical measurements, the plastic substrate was removed and placed into the electrochemical cell.

3.2.2 Preparation of plastic substrates. Zeonor slides (25 × 75 mm2 in area, 1 mm in thickness) were prepared by injection molding using a Boy 30A injection tool (Dr. Boy GmbH, Neustadt-Fernthal, Germany). Zeonor® 1060R (Zeon Chemicals, Louisville, KY) was molded at a temperature of 250 to 260 °C, an injection speed of 40 mm/s and a pressure of 132 bar. The mold (stainless steel, custom-fabricated) was cooled for 15 s before the slide was released. Disks (2.3 mm in diameter) were obtained by punching Zeonor slides in manual fashion followed by washing with methanol, ethanol and deionized (DI) water (18.2 MΩ cm), respectively, to clean the surface of monomers or residual plasticizing agents. Cell culture substrates were exposed to oxygen plasma (Plasmalab80Plus, Oxford Instruments, Bristol, UK) at a pressure of 50 mTorr and a power/gas flow ratio of 40 W/sccm for 4 min. (Beaulieu, Geissler and Mauzeroll, 2009)

3.2.3 Electrochemical measurements.

3.2.3.1 Electrodes. A three-electrode setup was used for voltammetry and Bio-SECM experiments with 25 µm Pt diameter laser pulled Pt working electrodes, a commercial Ag/AgCl reference and 0.5 mm Pt auxillary. The preparation of conventional 25 µm Pt microelectrodes followed a well established fabrication protocol (Fan *et al.*, 2007, p. 189-

199) while polished, needle-like microelectrodes were fabricated similar to procedures described earlier. (Mauzeroll and LeSuer, 2007, p. 199-211) The fabrication procedure specifically produces disk shaped Pt microelectrode sealed in a quartz capillary and laser pulled until a RG inferior to 10 is obtained. In brief, 25 µm annealed Pt wires were pulled into quartz glass capillaries (length of 150 mm, an outer diameter of 1 mm, and an inner diameter of 0.3 mm) under vacuum with the help of a P-2000 laser pipette puller (Sutter Instruments, CA, USA). The pulling program results in the formation of a long and sharp microelectrode with a thin glass sheath, which facilitates membrane penetration. The effective radius was evaluated from steady-state voltammetry.

3.2.3.2 Imaging in constant distance mode. A cyclic voltammogram was acquired by applying a potential at the microelectrode ranging from zero to 0.4 V *vs.* Ag/AgCl. A stationary current at 0.35 V *vs.* Ag/AgCl was recorded. A full frequency scan was acquired, showing a high resonance of the Pt microelectrode at a frequency of 175 kHz. An approach curve at a speed of 0.5 µm/s above plastic and at a frequency of 175 kHz using a 5 µm diameter Pt microelectrode was acquired recording amplitude or phase with a stop level of 10 %. Another full frequency scan was recorded in contact with the substrate. Both spectra were subtracted revealing a phase change as well as an amplitude damping at a frequency of 350 kHz. This frequency was applied at the electrode to obtain an electrochemical image of the topography of the substrate while scanning in constant distance mode across an area containing solid structures, HeLa cells, or none of the previous. Finally the microelectrode was rastered in constant distance mode across the mentioned areas monitoring the phase with a break after a change of the response signal of 6 °. An approach maximum of 10,000 nm indicates the maximal distance in Z-direction, whereas the piezo moves down at a step size of 10 nm first, followed by the Z-motor. The pull up distance indicates the retraction height to recover the initial signal.

3.3 Topographical imaging of different samples

In order to study cells using Biological Scanning Electrochemical Microscopy (Bio-SECM), the constant distance mode is adapted for the purpose of overcoming the disadvantages of constant height mode in previous Bio-SECM studies (see chapter 2).

3.3.1 Experimental preparation

In order to find a frequency that gives a sufficient shear force response a full frequency spectrum is recorded (Fig. 3.2 a) and a region of interest, here 100 to 600 kHz, is magnified for better analysis (Fig. 3.2 b). Seven resonance frequencies could be identified in the scanned area by observing the amplitude as a function of the stimulated frequency. A cyclic voltammogram was generated to characterize the working electrode (Fig.3.3 a) and an approach curve above plastic was recorded at a frequency of 175 kHz to position the electrode in a defined distance to the surface. A decrease in amplitude and phase signal is observed due to the increased viscosity of the medium (Fig. 3.3 b). By comparing the amplitude and phase signal during the approach it becomes clear that the change in phase is much more sensitive and therefore the better choice during Bio-SECM measurements. The signal of the amplitude in contrast seems unstable and is much more affected by background noise. To identify a frequency with the most efficient shear force response a frequency spectra from 250 kHz to 600 kHz was recorded on target as well as 10 μm above the substrate. The subtraction spectrum reveals a phase change as well as an amplitude damping at a frequency of 350 kHz (Fig. 3.4). This frequency was chosen for the imaging of different samples.

3.3.2 Imaging of solid substrates and a biological sample

Figure 3.5 shows preliminary results of the validation experiments for constant distance mode in order to study biological samples. It is important to note that these experiments are of preliminary nature and no reactivity information has been recorded. The potential of this approach is illustrated in Figure 3.5 a when an image was acquired of a solid substrate containing scratches. Deepening as small as 1.75 μm could be displayed precisely. As mentioned in chapter 2, a slope of the substrate cannot be avoided experimentally, reducing the accuracy of quantifying measurements. Using the constant distance mode this

slope can be observed in the topography information gathered during the experiment (Fig. 3.5 b) while the reactivity information remain unaffected by the slope. A comparison with an experiment on cells shows the challenges remaining using this method (Fig. 3.5 c). Due to the softness of the sample acquiring an image of cells requires an adjustment of the electrode as well as software related parameters. Although the presence of another scratch could be monitored, cells could be detected, but not displayed in their topography or shape. Once the microelectrode approached a cell, the targets detached from the surface, stuck to the electrode or were not identified as substrate. Therefore the size and material of the microelectrode need to be reconsidered as well as the approach parameters inserted into the executing software.

3.4 Conclusion

The adaption of the presented constant distance mode using a tapping approach is another important step towards precise Bio-SECM measurements on cancer cells, since it clearly overcomes the disadvantage of the constant height mode by recognizing the slope in the topography information gathered during the experiment. Thereby the reactivity information remains unaffected by the slope of the substrate. Preliminary studies and analysis of different substrates have been performed, showing successful imaging of a solid surface. Topographical imaging of HeLa cells remains a challenge and optimization of the experimental conditions is necessary. The coupling of information about topography and reactivity of the substrate in the future will lead to a reliable procedure for quantifying reactivity measurements on cells.

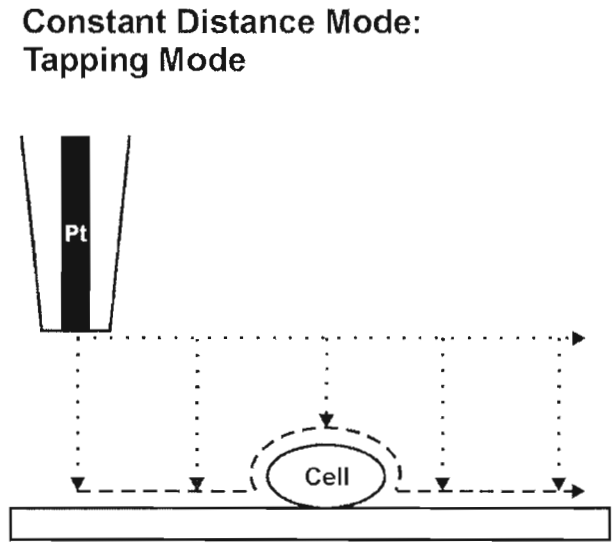

Figure 3.1 Schematic Representation of Constant Distance Mode using a tapping approach. Electrochemical measurement is performed by keeping the same tip to substrate distance when rastered across a sample. The electrode scans in X direction while approaching the surface in a chosen resolution (dotted line). This technique allows coupling of information about topography and reactivity of the sample depending on the nature of the substrate and creates an image as if scanning performed completely in close proximity to the surface (dashed line).

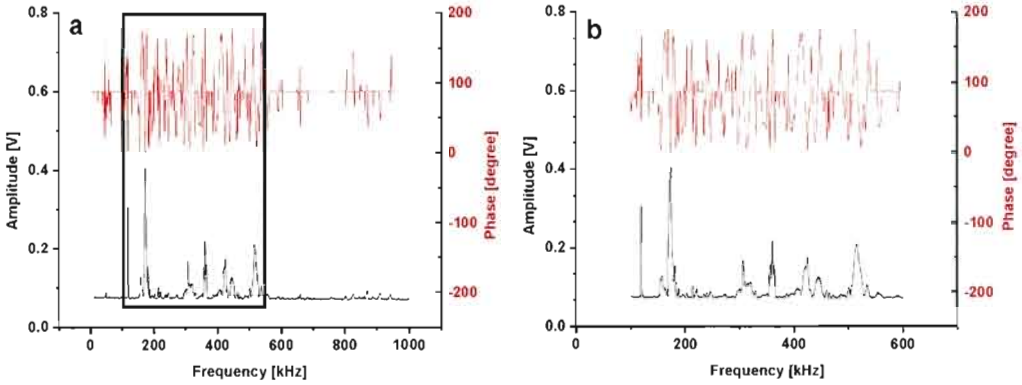

Figure 3.2 Electrode resonance measurement for Bio-SECM studies in Constant Distance Mode. (a) Full frequency scan using a 5 μm diameter Pt microelectrode. (b) Frequency scan of area indicated by box in (a).

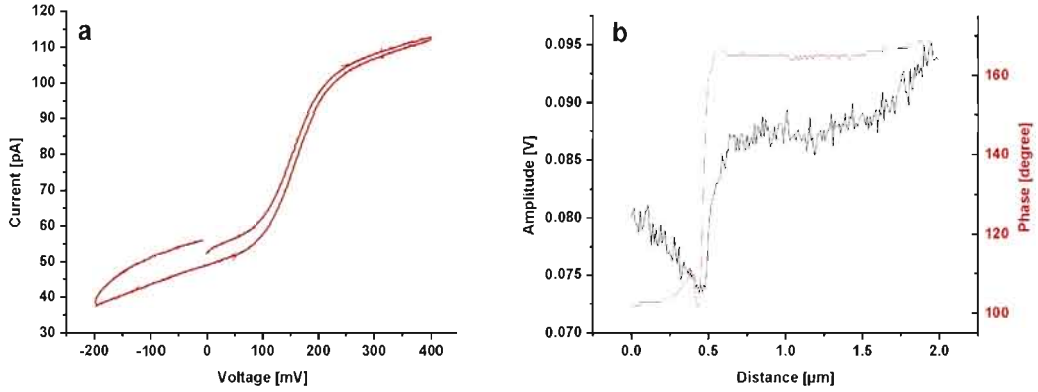

Figure 3.3 Preparation of Bio-SECM measurements in Constant Distance Mode. (a) Cyclic voltammogram showing the oxidation of $FcCH_2OH$ to $[FcCH_2OH]^+$ at a 5 µm diameter Pt microelectrode by applying a potential of zero to 0.4 V *vs.* Ag/AgCl. (b) Approach curve above plastic at a frequency of 350 kHz. Amplitude damping as well as a change in phase is observed due to the increased viscosity of the medium.

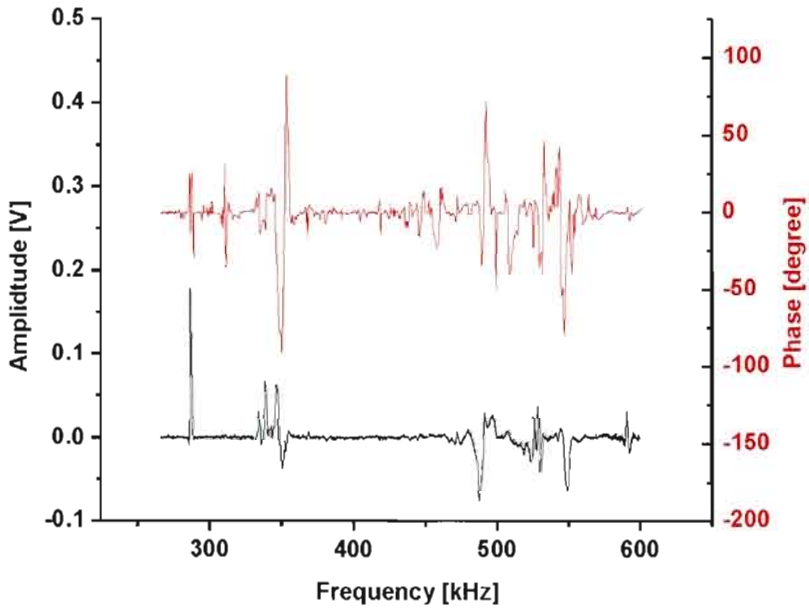

Figure 3.4 Subtraction spectrum of frequency scans in solution and on target. At a frequency of 350 kHz a phase change as well as an amplitude damping is observed.

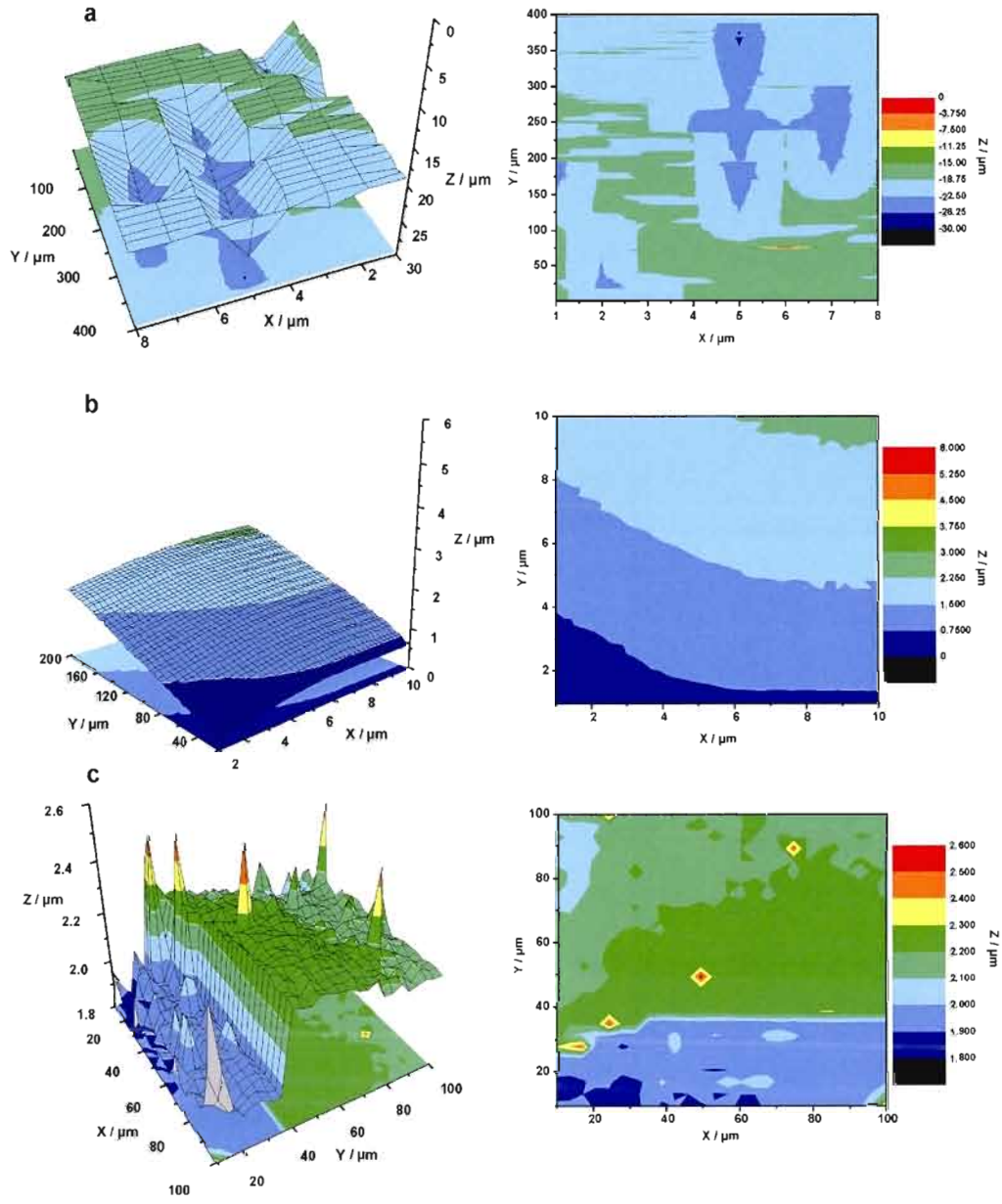

Figure 3.5 Bio-SECM measurements using constant distance mode. (a) 3D-Plot of the topography of a solid substrate. (b) 3D-Plot image of the topography of an empty plastic slide and (c) a plastic surface containing HeLa cells.

CONCLUSION

The presented work is a thesis in partial fulfillment of the requirements for the degree of Master of Science. The presented work is written as thesis by article and presents three chapters that each put emphasis on different aspects of this Master studies topic.

The goal of the presented work is to evaluate and advance the applicability of Bio-SECM to biological systems. SECM is an interesting technique and in principle its application to study living cells can provide much new information that is unreachable with any other technique. However, little research has been connecting SECM and Biology so far. Bio-SECM is a new technique exploring this connection. It is developed mainly in electrochemical laboratories. The very promising features of SECM for biological and biochemical research are brought into conjunction with routinely used optical microscopy. Regarding the progress in the last decade, Bio-SECM is now developed to a point where application of the technique has to lead to further development. Much more involvement of biochemists and biologists is therefore a very important requirement for successful implementation of Bio-SECM in biochemical and biological laboratories.

Bio-SECM can be advanced on two different levels: First, on the chemical theoretical level, interactions that can be probed by Bio-SECM have to be identified. These interactions need to be understood well in order to achieve meaningful results. Second, on a practical level, the instrument can be improved to allow constant distance measurements. Furthermore current Bio-SECM measurements often only lead to qualitative results, while reproducibility is lacking for quantitative conclusions. Evaluation of the experimental procedure and the effect of environmental parameters on the results are necessary to find key disturbing factors during Bio-SECM measurements. Smart engineering can then improve these experiments and allow for more accurate results.

To bring Bio-SECM forward towards a reliable standard technique to study living matter a number of objectives have to be achieved. The main objectives include the determination of an interaction partner for the redox mediator $FcCH_2OH$, the reproducibility of Bio-SECM measurements and the application of constant distance methods to biological samples. These objectives were approached using a combination of electrochemical and bioanalytical techniques. GSH as physiological redox active substance was proposed as possible interaction partner of $FcCH_2OH$. This interaction was evaluated with fluorescence microscopy and flow cytometry, before first constant height Bio-SECM imaging was applied to investigate glutathione levels and to assess multidrug resistance in human HeLa cells. Therefore the applicability of different media during SECM experiments was evaluated in order to guarantee accurate and representative results (Chapter 1). To allow easier, faster and more reproducible measurements, furthermore a new cell patterning method was developed allowing precise positioning of target cells in small groups and even co-cultures (Chapter 2). Constant distance measurements were performed modifying a published and developed method (Chapter 3).

Not only has the interaction between Glutathione and $FcCH_2OH$ been found but also a possible application of this interaction for multidrug resistance quantification has been proposed. Although this interaction is not fully evaluated yet, it provides a basis for further development and catapults Bio-SECM a huge way towards application in bioanalytical research and even diagnostics. One step has been taken in the presented work by evaluating cell viability under SECM conditions in the first chapter. Bio-SECM studies so far have often been conducted under non-physiological conditions leading to the involuntary measurement of dead cells. Furthermore cell positioning is improved using the proposed cell patterning techniques in the second chapter allowing evaluation of cell characteristics across cell lines under defined experimental conditions.

However, routine application remains a long term goal. Research is underway on all levels in the laboratory for Electrochemical Reactive Imaging and Detection for Biological Systems at the Université du Québec à Montréal to improve the technique of Bio-SECM. To

advance the constant distance performance the electrodes need to be optimized to detect even small changes in solvent viscosity near soft surfaces. Therefore different electrode materials need to be tested. Strategies to avoid cross contamination during co-culturing are followed currently. The effect of $FcCH_2OH$ on other model systems and the possible reaction cascade inside the cell must be elucidated and the timely response of the cell towards $FcCH_2OH$ has to be considered in further studies. Physical modeling of the electrode environment during measurements on cells can improve the understanding of the underlying processes. The development of ring micro electrodes may allow the measurement of the cells response to exposition to a substance, which is introduced through a central opening in the electrode during the measurement. Given the potential for high impact experimental research of Bio-SECM, focus has to be given to more pertinent cell lines in present cancer research, such as human lung cancer cells H69 and H69AR, which are also multidrug resistant.

To conclude, $FcCH_2OH$ was identified to interact with living cells and can therefore be used as mediator, making biological information accessible to Bio-SECM measurements. The improved experimental procedures and increased understanding of experimental necessities can serve to improve the accuracy and reproducibility of any Bio-SECM study. The presented work brings Bio-SECM a big step forward and should serve as a basis for further research.

APPENDIX A

REFERENCES OF INTRODUCTION AND CHAPTER III

Alberts, Bruce, Alexander Johnson, Julian Lewis, Martin Raff, Keith Roberts and Peter Walter. 2004. *Molekularbiologie der Zelle,* 4th ed., Weinheim: Wiley-VCH, p. 908-922.

Amemiya, Shigeru, Jidong Guo, Hui Xiong and Darrick A. Gross. 2006. Biological applications of scanning electrochemical microscopy: chemical imaging of single living cells and beyond. *Analytical and Bioanalytical Chemistry,* vol. 386, no 3, p. 458-471.

American Cancer Society. 2010. *Cancer Facts & Figures 2010.* Atlanta: American Cancer Society.

Atkins, Peter William. 2001. *Physikalische Chemie,* 3rd ed., Weinheim: Wiley-VCH.

Bard, Allen J. and Michael V. Mirkin. 2001. *Scanning Electrochemical Microscopy,* New York: Marcel Dekker, Inc, p. 650.

Bard, Allen J., Xiao Li and Wei Zhan. 2006. Chemical imaging living cells by scanning electrochemical microscopy. *Biosensors and Bioelectronics,* vol. 22, no. 4, p. 461-472.

Bauermann, Luciana Pitta, Wolfgang Schuhmann and Albert Schulte. 2004. An Advanced Biological Scanning Electrochemical Microscope (Bio-SECM) for Studying Individual Living Cells. *Physical Chemistry Chemical Physics,* vol. 6, p. 4003-4008.

Beaulieu, Isabelle, Matthias Geissler, Sabine Kuss and Janine Mauzeroll. 2010. Biological Scanning Electrochemical Microscopy. Accepted in *Analytical Chemistry.*

Beaulieu, Isabelle, Matthias Geissler and Janine Mauzeroll. 2009. Oxygen Plasma Treatment of Polystyrene and Zeonor: Substrates for Adhesion of Patterned Cells. *Langmuir,* vol. 25, p. 7169-7176.

Boquest, Andrew C., Billy N. Day and Randall S. Prather. 1999. Flow cytometric cell cycle analysis of cultured porcine fetal fibroblast cells. *Biology of reproduction,* vol. 60, no. 4, p. 1013-1019.

Borst, Piet, Raymond Evers, Marcel Kool and Jan Wijnholds. 2000. A family of drug transporters: the multidrug resistance-associated proteins. *Journal of the National Cancer Institute,* vol. 92, no. 16, p. 1295-1302.

Bourguignon, Lilly Y. W., Weiliang Xia and Gabriel Wong. 2009. Hyaluronan-mediated CD44 Interaction with p300 and SIRT1 Regulates beta-Catenin Signaling and NFkappaB-specific Transcription Activity Leading to MDR1 and Bcl-xL Gene Expression and Chemoresistance in Breast Tumor Cells. *Journal of Biological Chemistry,* vol. 284, no. 5, p. 2657-2671.

Carrano, Anthony V., Joe Gray, Richard Langlois, Karolyn Burkhart-Schultz and Marvin A. Van Dilla. 1979. Measurement and purification of human chromosomes by flow cytometry and sorting. *Proceedings of the National Academy of Sciences.* vol. 76, no. 3, p. 1382-1384.

Cosa, Gonzalo. 2002. Mechanism of Degradation of Pharmaceutical Products and Analogues, and Development of a Novel Fluorescence Technique for DNA-damage Detection. Dissertation.

Dunn, Robert C. 1999. Near-Field Scanning Optical Microscope. *Chemical Reviews,* vol. 99, no. 10, p. 2891-2927.

Etienne, Mathieu, Emily C. Anderson, Stephanie R. Evans, Wolfgang Schuhmann and Ingrid Fritsch. 2006. Feedback-Independent Pt Nanoelectrodes for Shear Force-Based Constant-distance Mode Scanning Electrochemical Microscopy. *Analytical Chemistry,* vol. 78, no. 20, p. 7317-7324.

Fan, Fu-Ren F., Jose Fernandez, Biao Liu, Janine Mauzeroll and Cynthia G. Zoski. 2007. «Platinum and gold inlaid disks ≥ 5μm diameter». In *Handbook of Electrochemistry,* Cynthia G. Zoski, p. 189-199. Amsterdam: Elsevier B.V.

Goldstein, Lori J., Ira Pastan and Michael M. Gottesman. 1992. Multidrug resistance in human cancer. *Critical Reviews In Oncology/Hematology*, vol. 12, no. 3, p. 243-253.

Goldys, Ewa M., Krystyna Drozdowicz-Tomsia, Guang Zhu, Hong Yu, Sun Jinjun, Motlan Motlan, Marek Godlewski. 2006. Fluorescence labelling. *Optica Applicata,* vol. 16, p. 217-224.

Gottesman, Michael M., Tito Fojo and Susan E. Bates. 2002. Multidrug resistance in cancer: role of ATP-dependent transporters. *Nature Reviews Cancer,* vol. 2, no. 1, p. 48-58.

Haberkorn, Uwe, Ludwig Strauss, Christoph Reisser, Dietrich Haag, Antonia Dimitrakopoulou, Sibylle Ziegler, Franz Oberdorfer, Volker Rudat and Gerhard van Kaick. 1991. Glucose uptake, perfusion, and cell proliferation in head and neck tumors: relation of positron emission tomography to flow cytometry. *The Journal of Nuclear Medicine,* vol. 32, no. 8, p. 1548-1555.

Hedley, David W. and Sue Chow. 1993. Evaluation of Methods for Measuring Cellular Glutathione Content Using Flow Cytometry. *Cytometry,* vol. 15, p. 349-358.

Hengstenberg, Andreas, Christine Kranz and Wolfgang Schuhmann. 2000. Facilitated Tip-Positioning and Applications of Non-Electrode Tips in Scanning Electrochemical Microscopy Using a Shear Force Based Constant-distant Mode. *Chemistry: A European Journal,* vol. 6, no. 9, p. 1547-1554.

Horan, Paul K. and Sue E. Slezak. 1989. Stable cell membrane labelling. *Nature,* 1989. 340: p. 167-168.

Katemann, Bernardo B., Albert Schulte and Wolfgang Schuhmann. 2003. Constant-Distance Mode Scanning Electrochemical Microscopy (SECM) - Part I: Adaptation of a non-Optical Shear-Force-Based Positionning mode for SECM Tips. *Chemistry: A European Journal,* vol. 9, p. 2025-2033.

Katemann, Bernardo B., Albert Schulte and Wolfgang Schuhmann. 2004. Constant-Distance Mode Scanning Electrochemical Microscopy. Part II: High-Resolution SECM Imaging Employing Pt Nanoelectrodes as Miniaturized Scanning Probes. *Electroanalysis,* vol. 16, no. 1-2, p. 60-65.

Kaya, Takatoshi, Yu-suke Torisawa, Daisuke Oyamatsu, Matsuhiko Nishizawa and Tomokazu Matsue. 2003. Monitoring the Cellular Activity of a Cultured Single Cell by Scanning Electrochemical Microscopy (SECM). A Comparison with Fluorescence Viability Monitoring. *Biosensors and Bioelectronics,* vol. 18, p. 1379-1383.

Kurulugama, Ruwan T., David O. Wipf, Sara A. Takacs, Sirinun Pongmayteegul, Paul A. Garris and John E. Baur. 2005. Scanning electrochemical microscopy of model neurons: Constant distance imaging. *Analytical Chemistry,* vol. 77, no. 4, p. 1111-1117.

Kuss, Sabine, Isabelle Beaulieu, Mohammed A. Mezour, Borhane Annabi and Janine Mauzeroll. 2011. Multidrug Resistance Assessment using Biological Scanning

Electrochemical Microscopy. *Submitted to Bioelectrochemistry*. BIOELECHEM-D-10-00231R1

Leith, Catherine P., I-Ming Chen, Kenneth J. Kopecky, Frederick R. Appelbaum, David R. Head, John E. Godwin, James K. Weick and Cheryl L.Willman. 1995. Correlation of multidrug resistance (MDR1) protein expression with functional dye/drug efflux in acute myeloid leukemia by multiparameter flow cytometry: identification of discordant MDR-/efflux+ and MDR1+/efflux-cases. *Blood,* vol. 86, no. 6, p. 2329-2342.

Li, Xiao and Allen J. Bard. 2009. Scanning electrochemical microscopy of HeLa cells–Effects of ferrocene methanol and silver ion. *Journal of Electroanalytical Chemistry,* vol. 628, no. 1-2, p. 35-42.

Liu, Biao, Susan A. Rotenberg, and Micheal V. Mirkin. 2000. Scanning electrochemical microscopy of living cells: Different redox activities of nonmetastatic and metastatic human breast cells. *Proceedings of the National Academy of Sciences,* vol. 97, no. 18, p. 9855-9860.

Lee, Youngmi, Zhifeng Ding and Allen J. Bard. 2002. Combined Scanning Electrochemical/Optical Microscopy with Shear Force and Current Feedback. *Analytical Chemistry,* vol. 74, no. 15, p. 3634-3643.

Longobardi Givan, Alice. 2004. *Flow cytometry: First principles.* New York: Wiley-Liss.

Marchetti, Carole, Guillaume Obert, Andre Deffosez, Pierre Formstecher and Philippe Marchetti. 2002. Study of mitochondrial membrane potential, reactive oxygen species, DNA fragmentation and cell viability by flow cytometry in human sperm. *Human Reproduction,* vol. 17, no. 5, p. 1257-1265.

Mauzeroll, Janine and Allen J. Bard. 2004. Scanning electrochemical microscopy of menadione-glutathione conjugate export from yeast cells. *Proceedings of the National Academy of Sciences,* vol. 101, no. 21, p. 7862-7867.

Mauzeroll, Janine, Allen J. Bard, Omeed Owhadian and Terrence J. Monks. 2004. Menadione metabolism to thiodione in hepatoblastoma by scanning electrochemical microscopy. *Proceedings of the National Academy of Sciences,* vol. 101, no. 51, p. 17582-17587.

Mauzeroll, Janine and Robert J. LeSuer. 2007. «Laser-pulled ultramicroelectrodes». In *Handbook of Electrochemistry*, 2007, Cynthia G. Zoski, p. 199-211. Amsterdam: Elsevier B.V.

Morrow, Charles S. and Kenneth H. Cowan. 1990. Glutathione S-transferases and drug resistance. *Cancer cells,* vol. 2, no. 1, p. 15-22.

Müller, Michiel. 2006. *Introduction to confocal fluorescence microscopy,* 2nd ed., Bellingham: SPIE.

Persidis, Aris. 1999. Cancer multidrug resistance. *Nature Biotechnology,* vol. 17, p. 94-95.

Saito, Takeshi, Ching-Chou Wu, Hitoshi Shiku, Tomoyuki Yasukawa, Masaki Yokoo, Takashi Ito-Sasaki, Hiroyuki Abe, Hiroyoshi Hoshi and Totokazu Matsue. 2006. Oxygen consumption of cell suspension in a poly (dimethylsiloxane)(PDMS) microchannel estimated by scanning electrochemical microscopy. *The Analyst,* vol. 131, no. 9, p. 1006-1011.

Voehringer, David W., David J. McConkey, Timothy J. McDonnell, Shawn M. Brisbay and Raymond E. Meyn. 1998. Bcl-2 expression causes redistribution of glutathione to the nucleus. *Proceedings of the National Academy of Sciences,* vol. 95, no. 6, p. 2956-2960.

Waggoner, Alan. 2006. Fluorescent labels for proteomics and genomics. *Current Opinion in Chemical Biology,* vol. 10, no. 1, p. 62-66.

Watson, James V. 1980. Enzyme kinetic studies in cell populations using fluorogenic substrates and flow cytometric techniques. *Cytometry Part A,* vol. 1, no. 2, p. 143-151.

Zaman, Guido J. R., Marcel J. Flens, Manuel R. van Leusden, Marcel de Haas, H. Sipko Mülder, Jan Lankelma, Herbert M. Pinedo, Rik J. Scheper, Frank Baas, Henricus J. Broxterman and Piet Borst. 1994. The human multidrug resistance-associated protein MRP is a plasma membrane drug-efflux pump. *Proceedings of the National Academy of Sciences,* vol. 91, no. 19, p. 8822-8826.